

United States  
Environmental Protection  
Agency

Environmental Monitoring  
Systems Laboratory  
P O Box 15027  
Las Vegas NV 89114

EPA-600/4-79-066  
October 1979

Research and Development

*Library Copy*



# Modeling Wind Distributions Over Complex Terrain

PROPERTY OF  
DIVISION  
OF  
METEOROLOGY



## RESEARCH REPORTING SERIES

Research reports of the Office of Research and Development, U.S. Environmental Protection Agency, have been grouped into nine series. These nine broad categories were established to facilitate further development and application of environmental technology. Elimination of traditional grouping was consciously planned to foster technology transfer and a maximum interface in related fields. The nine series are

1. Environmental Health Effects Research
2. Environmental Protection Technology
3. Ecological Research
4. Environmental Monitoring
5. Socioeconomic Environmental Studies
6. Scientific and Technical Assessment Reports (STAR)
7. Interagency Energy-Environment Research and Development
8. "Special" Reports
9. Miscellaneous Reports

This report has been assigned to the ENVIRONMENTAL MONITORING series. This series describes research conducted to develop new or improved methods and instrumentation for the identification and quantification of environmental pollutants at the lowest conceivably significant concentrations. It also includes studies to determine the ambient concentrations of pollutants in the environment and/or the variance of pollutants as a function of time or meteorological factors.

EPA-600/4-79-066  
October 1979

MODELING WIND DISTRIBUTIONS  
OVER COMPLEX TERRAIN

by

Mark A. Yocke  
Mei-Kao Liu

Systems Applications, Incorporated  
950 Northgate Drive  
San Rafael, California 94903

Contract No. 68-02-2446

Project Officer

James L. McElroy

Monitoring Systems Research and Development Division  
Environmental Monitoring Systems Laboratory  
U.S. Environmental Protection Agency  
Las Vegas, Nevada 89114

ENVIRONMENTAL MONITORING SYSTEMS LABORATORY  
OFFICE OF RESEARCH AND DEVELOPMENT  
U.S. ENVIRONMENTAL PROTECTION AGENCY  
LAS VEGAS, NEVADA 89114

## DISCLAIMER


This report has been reviewed by the Environmental Monitoring Systems Laboratory-Las Vegas, U.S. Environmental Protection Agency, and approved for publication. Approval does not signify that the contents necessarily reflect the views and policies of the U.S. Environmental Protection Agency, nor does mention of trade names or commercial products constitute endorsement or recommendation for use.

## FOREWORD

Protection of the environment requires effective regulatory actions that are based on sound technical and scientific data. This information must include the quantitative description and linking of pollutant sources, transport mechanisms, interactions, and resulting effects on man and his environment. Because of the complexities involved, assessment of specific pollutants in the environment requires a total systems approach that transcends the media of air, water, and land. The Environmental Monitoring Systems Laboratory-Las Vegas contributes to the formation and enhancement of a sound monitoring data base for exposure assessment through programs designed to:

- develop and optimize systems and strategies for monitoring pollutants and their impact on the environment
- demonstrate new monitoring systems and technologies by applying them to fulfill special monitoring needs of the Agency's operating programs

This report discusses the development of an air flow model for urban areas in complex terrain and the application of the model in Phoenix, Arizona. The model will be incorporated into an existing method for the design of ambient air quality monitoring networks (see EPA-600/4-77-019 and EPA-600/4-78-053). The method may be useful for regional or local agencies who have a need to plan new or modify existing networks. The Monitoring Systems Design and Analysis Staff may be contacted for further information on this subject.



George B. Morgan  
Director

Environmental Monitoring Systems Laboratory  
Las Vegas

## ABSTRACT

Accurate determination of wind fields is a prerequisite for successful air quality modeling. Thus, there is an increasing demand for objective techniques for analyzing and predicting wind distributions, particularly over rugged terrain, where the wind patterns are not only more complex, but also more difficult to characterize experimentally. This report describes the development of a three-dimensional wind model for rugged terrain based on mass continuity. The model is composed of several horizontal layers of variable thicknesses. For each layer, a Poisson equation is written with the wind convergence as the forcing function. Many types of wind perturbations over rugged terrain are considered in this model, including diversion of the flow due to topographic effects, modification of wind profiles due to frictional effects in the planetary boundary layer, convergence of the flow due to urban heat island effects, and mountain and valley winds due to thermal effects. Wind data collected during a comprehensive field measurement program at Phoenix, Arizona, were used to test the model. The model was shown both qualitatively and quantitatively to perform reasonably well in the application to Phoenix, and its utility was demonstrated by the relatively modest computing and data requirements in this application.

# CONTENTS

FOREWORD . . . . .	iii
ABSTRACT . . . . .	iv
LIST OF ILLUSTRATIONS . . . . .	vii
LIST OF TABLES . . . . .	viii
LIST OF ABBREVIATIONS AND SYMBOLS . . . . .	ix
ACKNOWLEDGEMENT . . . . .	xi
I INTRODUCTION . . . . .	1
II WIND FLOWS OVER CITIES LOCATED IN COMPLEX TERRAIN . . . . .	3
A. Geostrophic Flow and Its Modifications . . . . .	3
B. Thermally Induced Local Circulations . . . . .	4
C. Modification of Wind Flows Over Mountains . . . . .	5
1. Airflow Over a Mountain Range . . . . .	5
2. Airflow Over a Solitary Hill . . . . .	8
III REVIEW OF PREVIOUS MODELING STUDIES . . . . .	11
A. General Classification of Wind Models . . . . .	11
1. Interpolation Techniques . . . . .	11
2. Objective Techniques . . . . .	12
3. Diagnostic Models . . . . .	13
4. Dynamic Models . . . . .	13
B. Pertinent Existing Models . . . . .	14
1. Objective Techniques Based on Variational Principles . . . . .	15
2. Diagnostic Models Based on Mass Continuity . . . . .	16
IV DEVELOPMENT OF A WIND MODEL FOR COMPLEX TERRAIN . . . . .	18
A. The Model Equation . . . . .	18
B. Parameterization of the Vertical Fluxes . . . . .	22
1. Topographic Effects . . . . .	22
2. Boundary Layer Effects . . . . .	23
3. Thermal Effects . . . . .	27
C. Numerical Solution Procedure . . . . .	30

V	APPLICATION OF THE MODEL TO THE PHOENIX AREA . . . . .	34
A.	Data Base . . . . .	34
B.	Discussion of the Results . . . . .	39
C.	Statistical Analysis of the Results . . . . .	41
VI	CONCLUSIONS AND RECOMMENDATIONS . . . . .	47
APPENDIX A:	DECOMPOSITION OF A VELOCITY VECTOR . . . . .	48
APPENDIX B:	COMPARISON OF PREDICTED AND MEASURED SURFACE WINDS IN PHOENIX . . . . .	51
REFERENCES	. . . . .	105



## ILLUSTRATIONS

1	Formation of the Up-Valley Mountain Wind . . . . .	6
2	Formation of the Down-Valley Mountain Wind . . . . .	7
3	Classification of Types of Airflow Over Ridges with Typically Associated Wind Speed Profiles and Streamlines . . .	9
4	General Classification of Types of Airflow Over a Solitary Hill . . . . .	10
5	Cross-Sectional View of the Intersection of a Hypothetical Terrain with a Three-Dimensional Modeling Grid . . . . .	20
6	Schematic Diagram of a Flow Contacting the Slope of a Hill . .	23
7	Parameters Used in Defining the Diversion Effect . . . . .	24
8	Sketch Showing a Grid Cell Along the Left Boundary of the Modeling Region . . . . .	32
9	Modeling Grid Indicated on a Topographic Map of the Phoenix Area . . . . .	37
10	Frequency Distributions of Wind Speed and Wind Direction Deviations for 15 February 1977 . . . . .	42
11	Frequency Distributions of Wind Speed and Wind Direction Deviations for 16 February 1977 . . . . .	43
12	Frequency Distributions of Wind Speed and Wind Direction Deviations for 7 March 1977 . . . . .	44
13	Frequency Distributions of Wind Speed and Wind Direction Deviations for 10 March 1977 . . . . .	45

## TABLES

1	Phoenix Area Wind Measurement Station Names and Coordinates . . . . .	36
2	Mean Flow Imposed at Model Boundaries and Mountain- Valley Wind Coefficients Used for Phoenix Wind Simulations . .	38

## LIST OF ABBREVIATIONS AND SYMBOLS

### ABBREVIATIONS

km	kilometer(s)
m	meter(s)
m/sec	meter(s) per second
MST	mountain standard time
UTM	Universal Transverse Mercator

### SYMBOLS

$A$	slope vector	$H_{\max}$	highest terrain elevation
$a$	slope scalar	$h(x,y)$	terrain height as a function of location
$\bar{A}$	potential velocity vector	$i,j$	grid cell position indexes
$B$	multiplicative factor	$k$	von Karman's constant
$b$	intercept	$L$	Monin-Obukhov length
$\bar{B}$	solenoidal velocity vector	$\ln$	natural logarithm
$\tilde{B}$	solenoidal potential function	$M(x,y)$	"equivalent mountain" function
$c$	cutoff coefficient	$N$	number of measurements; number of vertical layers
$C_D$	drag coefficient	$n$	number of parameterized fluxes
$d$	derivative symbol	$r$	distance
$e$	base of natural logarithm	$Re$	Reynolds number
$f$	weighting function; dimensionless velocity	$r_i^{(k)}$	current residual of the $i$ -th equation
$F_r$	Froude number	$T_\infty$	free-stream (unperturbed) temperature
$f(x,y)$	forcing function		
$g$	gravitation constant		
$H$	average surface elevation in the grid cell; depth of model region		

# SYMBOLS (concluded)

$T_C$	temperature of the current	$\Delta$	difference operator
$T_E$	temperature of the environment	$\varepsilon^2$	mean square error
$T(x,y)$	spatial distribution of surface temperature	$\eta_i$	dimensionless parameter defined as
$U$	wind speed		$\frac{\Delta z_i}{\Delta x} \sqrt{\frac{Re}{2}}$
$U_\infty$	free-stream (unperturbed) velocity	$\theta$	arctan ( $\nabla h$ )
$u,v,w$	wind components corresponding to orthogonal Cartesian coordinates	$\phi$	potential function
$u_*$	frictional velocity	$\chi, \psi$	scalar functions
$\hat{u}$	interpolated wind speed in x-direction	$\Omega$	wind divergence
$\hat{v}$	interpolated wind speed in y-direction	$\omega$	vorticity of flow; component of total divergence
$\bar{v}$	vector velocity	$\partial$	partial derivative
$w$	weighting function; vertical velocity	$\nabla$	divergence operator
$\bar{x}$	position vector		
$x,y,z$	orthogonal Cartesian coordinates		
$z_0$	aerodynamic surface roughness length		
$\alpha$	empirical coefficient		
$\Gamma$	adiabatic lapse rate		
$\gamma$	environmental temperature lapse rate		
$\gamma'_i$	dimensionless parameter defined as $u(z_i)/U_\infty$		

## ACKNOWLEDGMENT

We wish to express our sincere gratitude to Dr. Thomas W. Tesche, who has made significant contributions to the formulation of the complex-terrain wind model discussed in this report.

## I INTRODUCTION

Efforts to establish air quality monitoring networks for urban areas have led investigators to develop various objective methods for selecting optimum measurement sites. One promising approach developed by Systems Applications, Incorporated (SAI) and the Las Vegas Environmental Monitoring Systems Laboratory (EMSL-LV) of the U.S. Environmental Protection Agency (EPA) entails the use of an air quality simulation model for the prediction of pollutant concentration distributions (Liu et al., 1977 and McElroy et al., 1978). When this method was applied to the metropolitan Las Vegas area, the wind speed and direction were found to be the environmental parameters that potentially can most significantly affect the network configurations (McElroy et al., 1978). *In general, the pollutant concentration is approximately proportional to the inverse of the wind speed.* Although a wind direction that is invariable during the averaging period of the pollutant measurements cannot change pollutant concentration levels, it can shift the locations of concentration maxima and thus affect the selection of monitoring sites.

In the past, meteorological stations have been deployed to measure wind distributions, and the data have subsequently been interpreted to provide the necessary input to an air quality simulation model. This approach suffers from several deficiencies. First, characterizing the spatial variations for a large urban complex may require many meteorological stations and, thus, great expense. Second, reliable and objective interpolation schemes are not available for reproducing acceptable wind fields from a finite number of measurements, especially in complex terrain. Third, the historical data used for monitor siting purposes generally lack detailed wind measurements, except for synoptic-scale climatological information. For these reasons, further studies on the modeling of wind fields were recommended.

The objective of this project was to develop physically based wind models that can be coupled with an air quality simulation model. The ultimate goal was to apply the coupled wind-air quality model in the design of air quality monitoring networks (McElroy et al., 1978). It was hoped that injecting atmospheric dynamics into the wind analysis would improve the accuracy of the wind predictions. Two types of special situations were specifically considered. These were (1) a coastal city and (2) an inland city in complex terrain. Whereas wind flows in coastal cities are typically dominated by land and sea breezes, particularly those in the low-latitude areas, the meteorological settings of inland cities are often characterized by the presence of complex terrain. Since coastal areas will be addressed in a separate document, this report focuses only on the problem of modeling the wind fields over an inland city located in complex terrain.

The next chapter describes the general features of the wind patterns over complex terrain. Chapter III discusses previous modeling studies. Chapter IV proposes a modeling approach capable of predicting three-dimensional wind distributions. Application of the model to the Phoenix, Arizona area is described in Chapter V. Finally, conclusions and recommendations are given in Chapter VI.

## II WIND FLOWS OVER CITIES LOCATED IN COMPLEX TERRAIN

Several excellent reviews on wind flows over mountainous regions have been made (Alaka, 1960; Reiter and Rasmussen, 1967; Flohn, 1969; Nicholls, 1973). They cover a wide range of topics related to the low-level airflows over complex terrain and provide an extensive list of references on the subject. Therefore, only a cursory description of the wind flows to be modeled is included here.

The distribution of winds in the atmospheric boundary layer is affected by air motions on all scales, ranging from the large-scale Rossby waves to the smallest turbulent eddies. Depending on a variety of factors and conditions, they all contribute in varying degrees of importance to the resultant wind observed at any geographical location. Because of the large spread in the spatial scales and the widely different mechanisms responsible for their occurrences, the following discussion is limited to those wind phenomena with spatial and temporal scales of interest to the dispersion of air pollutants from an urban area.

### A. GEOSTROPHIC FLOW AND ITS MODIFICATIONS

Above the surface boundary layer, air motion in the lower atmosphere, particularly in mid latitudes, is generally determined by a balance between the horizontal gradient of atmospheric pressure and the Coriolis force. The resulting flow, which is parallel to the constant pressure contours or isobars, has been termed the geostrophic wind. For situations where the isobars are curved, the wind flow is further modified by the centrifugal force and is known as the gradient flow. Deviations from the geostrophic motion can also be caused by the frictional force and horizontal temperature gradients. For example, modification of the geostrophic flow by the



frictional force near the earth's surface leads to the well-known Ekman spiral in the planetary boundary layer--the decrease in wind speed and the counterclockwise turning (in the Northern Hemisphere) of the wind direction as it approaches the surface.

On the other hand, if a significant horizontal gradient is present in the mean air temperature, the geostrophic wind is further altered, with the resultant flow called the thermal wind. The thermal wind is generally directed along the tangent to the isotherms in such a way that the area of lower temperatures is to the left in the Northern Hemisphere. Over mountainous terrain, the horizontal temperature gradient may be generated by the uneven heating of the slope.

#### B. THERMALLY INDUCED LOCAL CIRCULATIONS

Convective circulations in the atmospheric boundary layer are induced by buoyancy as a result of inhomogeneities in the surface temperatures. These thermal anomalies are, in turn, generated by differential heating and cooling of the land and water masses, the mountains, and the valleys. These diurnally varying flows, which include the land and sea breezes, the valley winds, and the slope winds, can extend over areas of tens of kilometers in extent. The inertial interaction between these local winds and the synoptic-scale flow is, therefore, one of the most influential factors in determining the near-surface flow pattern in low-altitude coastal areas and in mountainous regions. For example, in Los Angeles, the land and sea breezes are typically the dominating winds near the surface during the summer, when a strong, clockwise-turning sea breeze occurs during the day and a weak, counterclockwise-turning land breeze arises during the night. As solar heating is weakened in the winter, the interaction between the sea breeze and the synoptic-scale flow becomes more apparent.

The thermally-induced flow of greatest consequence to mountainous regions is the mountain-valley wind, which is also a result of uneven cooling and heating. In the evening, radiational cooling of the upper mountain slopes results in a thin wedge of cool air that descends the

slopes and begins to move down the canyons. This valley or canyon flow generally persists all night. After sunrise, the upper slopes heat up more rapidly than the valley floor, which is shielded by the overlying cool air mass. Gradually, the canyon wind changes direction and begins to move up the canyon and over the heated upper slopes. The gross aspects of the mountain-valley winds are now reasonably well understood. The formation of up-valley and down-valley (drainage) mountain winds is illustrated in Figures 1 and 2.

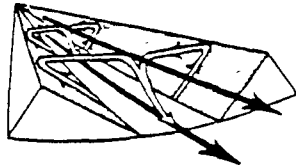
### C. MODIFICATION OF WIND FLOWS OVER MOUNTAINS

The presence of natural obstructions, such as mountains, obviously alters the wind distribution near the surface. As discussed earlier, changes in the atmospheric momentum and heat budgets also affect the air-flow over mountainous regions.

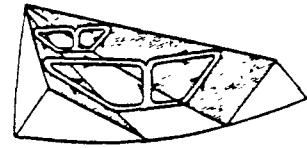
#### 1. Airflow Over a Mountain Range

According to Förrchtgott's classification scheme (Förrchtgott, 1949), four types of airflows over a two-dimensional mountain range can be identified:

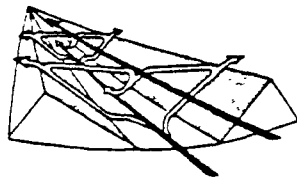
- > Laminar flow. Under light winds, flow over the ridges forms a smooth, shallow wave; close to the surface, vertical currents exist as a result of orographic lifting, and downstream phenomena do not occur.
- > Standing eddy. With stronger winds, a large, semi-permanent eddy forms to the lee of the mountain, creating a larger effective shape of the mountain with respect to the flow aloft.
- > Lee wave. With stable stratification and even stronger winds increasing with height, a lee wave system develops downwind of the mountain ridge. The amplitude of the waves is primarily determined by the shape of the mountain,



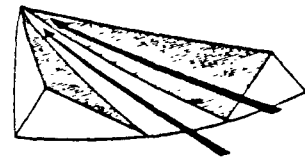
(a) Formation of up-slope winds shortly after sunrise when the down-valley wind is still blowing



(b) Predominance of up-slope winds as the down-valley wind dies in mid-morning



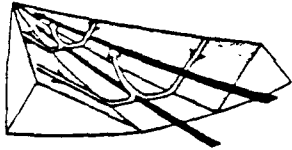
(c) Enhancement of up-slope winds by the onset of up-valley winds toward midday



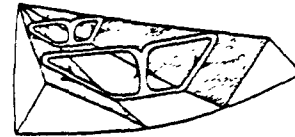
(d) Maintenance of up-valley winds as the up-slope winds cease in late afternoon

Source: Defant (1951).

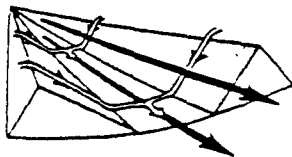
Figure 1. Formation of the up-valley mountain wind



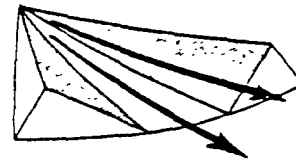
(a) Beginning of down-slope wind shortly after sunset before up-valley mountain wind dies



(b) Down-slope wind and return flow at center of valley after up-valley wind dies in late afternoon



(c) Down-valley mountain wind as return flow at center of valley ceases



(d) Down-valley mountain wind as the down-slope wind ceases at night

Source: Defant (1951).

Figure 2. Formation of the down-valley mountain wind

but the wavelength depends on the atmospheric stratification and the wind profile.

- > Rotor flow. Under very strong winds limited to a restricted vertical depth (on the order of the mountain's height), severe turbulence and quasi-stationary rotary vortices occur in the lee of the mountain ridge.

These flow patterns are presented schematically in Figure 3.

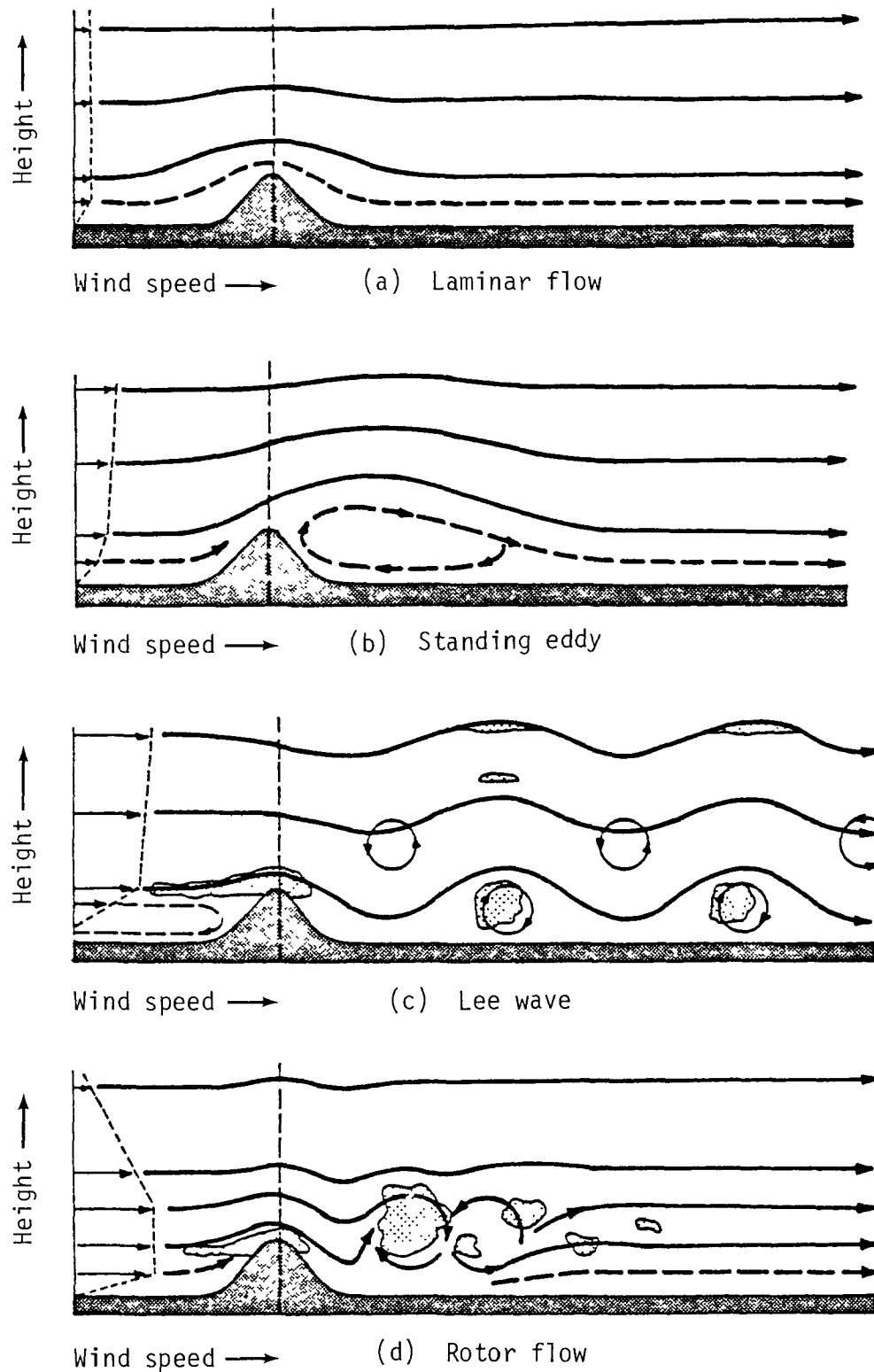
## 2. Airflow Over a Solitary Hill

Like wind flows over two-dimensional mountain ranges, those over a single, isolated, round hill can be classified into four types:

- > Bifurcation flow. Under light winds and stable stratifications, the airflow simply bifurcates at the base of the hill. No vertical currents exist; the flow is strictly horizontal.
- > Laminar flow. Under moderate winds and neutral or unstable stratifications, the airstream follows the geometric shape of the hill.
- > Lee wave. With stable stratifications and strong winds, three-dimensional lee waves form.
- > Turbulent flow. With very strong winds, turbulent motions prevail.

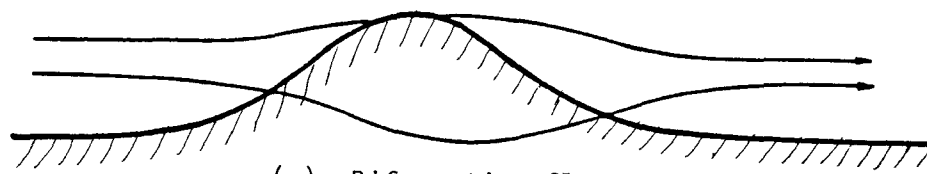
These flow patterns are illustrated in Figure 4.

As commented by many previous investigators, such an ideal mountain or valley probably does not exist in nature. Under most circumstances, the terrain to be modeled is complex or featureless. In these situations, the eventual wind field may be the result of superpositions of several of the flow patterns discussed above.

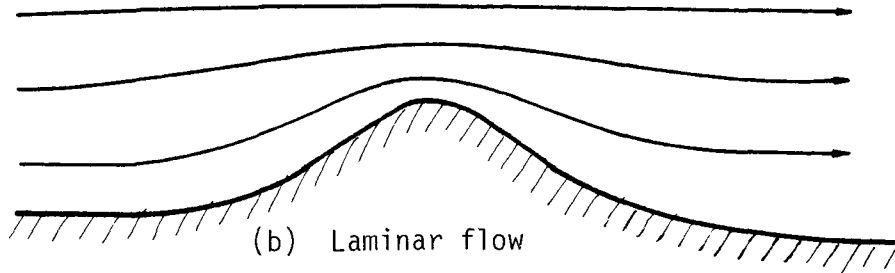


Source: Förchtgott (1949).

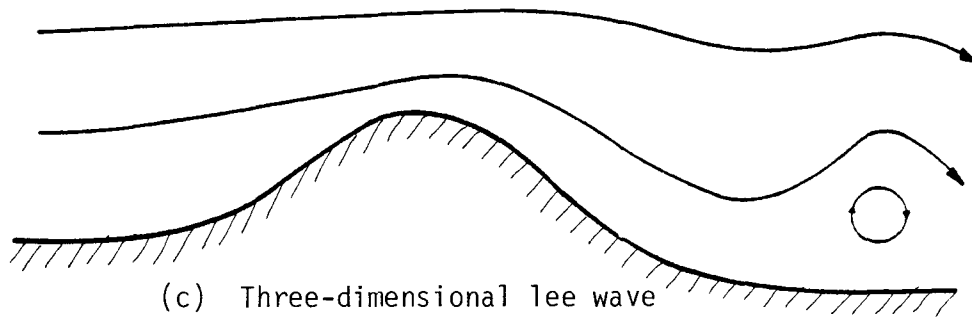
Figure 3. Classification of types of airflow over ridges with typically associated wind speed profiles and streamlines



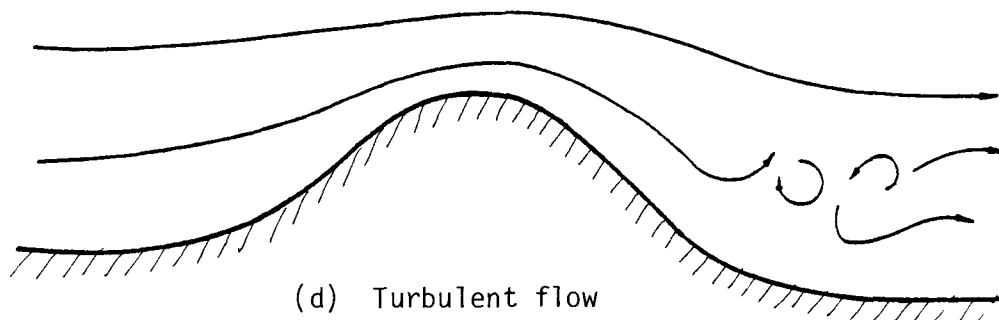
(a) Bifurcation flow



(b) Laminar flow



(c) Three-dimensional lee wave



(d) Turbulent flow

Figure 4. General classification of types of airflow over a solitary hill

### III REVIEW OF PREVIOUS MODELING STUDIES

A variety of wind models of interest to the present project have been developed. They range from simple, straightforward interpolations of wind measurements to complex, sophisticated, dynamic models. In the first section of this chapter, general classifications of these models are described, and advantages and limitations associated with each class are discussed. The second section focuses on those recently developed models that are particularly attractive and pertinent to the goal of this study.

#### A. GENERAL CLASSIFICATION OF WIND MODELS

The objective of any wind modeling effort is to develop a capability for either forecasting or projecting the wind distributions as a function of time or space. These models can be generally divided into four categories: interpolation techniques, objective techniques, diagnostic models, and dynamic models. Each is discussed below.

##### 1. Interpolation Techniques

The simplest interpolation scheme conceivable is the weighting of measurements by an influence factor. For example, in the spatial interpolation of wind speed, the interpolated value at location  $j$  can be written as

$$\hat{v}_j = \frac{\sum_i f(r_{ij}) v_i}{\sum_i f(r_{ij})}, \quad (1)$$



where  $v_i$  and  $\hat{v}_j$  are the observed wind speed at location  $i$  and the interpolated wind velocity at location  $j$ , respectively, and  $r_{ij}$  is the distance between locations  $i$  and  $j$ . The weighting function,  $f$ , for obvious reasons, has generally been assumed to be a function of  $r_{ij}$ . The inverse of the distance squared was the value chosen by Wendell (1970), Strand (1971), and Weisburd, Wayne, and Kokin (1972), whereas the inverse of the distance was selected by Eschenroeder and Martinez (1972) and Liu et al. (1973). Despite its simplicity, at least conceptually, this approach has been plagued by many fundamental difficulties. Among the problems associated with the use of this simple interpolation technique are:

- > The interpolated wind field is very sensitive to the choice of the weighting function and other similar artificial parameters.
- > The interpolated wind field is also sensitive to the number of wind measurement stations and the network configurations.
- > The interpolation scheme obviously lacks any basis in physics, and does not take into account the presence of the terrain unless reflected in the wind measurements.

As a result of these deficiencies, it was found that applications of this simple interpolation scheme are almost always less than acceptable (Liu et al., 1973).

## 2. Objective Techniques

Ideally, the ultimate goal of interpolation is to obtain a "best" fit of the observational data. A logical approach, based on mathematical optimization theory, is to minimize the deviations between the interpolated value and the real value at a grid point.

Assume that observational data of a scalar quantity  $u$  are available at  $N$  locations. The best fit,  $\hat{u}(\bar{x})$ , can be constructed from a linear combination of the observed data,  $u(\bar{x}_j)$ ,  $j = 1, 2, \dots, N$  using

$$\hat{u}(\bar{x}) = \sum_{j=1}^N w(\bar{x}, \bar{x}_j) u(\bar{x}_j) \quad . \quad (2)$$

The weighting functions,  $w(\bar{x}, \bar{x}_j)$ , are determined by minimizing the mean square error:

$$\epsilon^2 = [\hat{u}(\bar{x}) - u(x)]^2 \quad (3)$$

The mathematical basis for this approach has been developed by Gandin in the U.S.S.R. (Gandin, 1965) and by Panofsky (1949) and Sasaki (1970) in this country. The success of this method hinges on the assumption that the density of the meteorological stations is adequate for deriving the degree of details desired in the wind analysis. In other words, all necessary information to describe the variation of the interpolated quantity must be contained in the observational data. Unfortunately, this condition is seldom if ever met in air pollution studies. Models falling into this category are discussed in more detail in Section B.

### 3. Diagnostic Models

A common feature of diagnostic models is that they do not invoke the full set of equations describing the continuity of mass, heat, and momentum. In most cases, they are based simply on the equation of mass conservation. Important dynamic processes that govern the distribution of the winds are often parameterized using relationships established either theoretically or empirically. A distinct advantage of this approach is that it bypasses the need for numerically solving the dynamic equations, thus drastically reducing the computational burden. The success of this approach depends on the ingenuity in devising the model and the parameterization schemes. Such models are discussed in Section B.

### 4. Dynamic Models

Dynamic models are generally based on the numerical solutions of all pertinent equations expressing the conservation laws. Thus, these models

can simulate in a predictive mode the complicated, nonlinear interactions between the large-scale synoptic air motions and local circulations induced by topographic and/or thermal perturbations. The selection of suitable numerical techniques, the parameterization of the subgrid processes, and the initialization of the model are the major problems confronting the application of dynamic models. The use of dynamic models is further plagued by the requirement of a comprehensive data base for the exercise and verification of the model as well as the need for a potentially large computing budget to implement and operate the model in an explicit fashion.

Many dynamic models have been developed to simulate mesoscale atmospheric flows. They range from relatively simple one-dimensional models to complex three-dimensional ones. Examples of these models include:

- > Land and sea breeze models--Estoque (1963), Pielke (1973).
- > Urban heat island models--Myrup (1969), McElroy (1971).
- > Planetary boundary layer models--Estoque (1963), Deardorff (1970).
- > Mountain and valley wind models--Orville (1965), Hovermale (1965), Thyer (1966).

## B. PERTINENT EXISTING MODELS

Of the four general categories of wind models discussed above, the following two approaches appear to offer the most promise to the present study:

- > Objective techniques based on the variational principle
- > Diagnostic models based on mass continuity.

These two approaches seem to be particularly attractive because:

- > They invoke certain first principles such as mass continuity to supplement the wind measurements.

- > They are relatively simple to use and inexpensive to apply.

Considerable work relevant to these two modeling approaches has been carried out. These studies are summarized below.

## 1. Objective Techniques Based on Variational Principles

Dickerson (1973) appears to have been the first to apply this well-known technique from synoptic-scale meteorological analysis to air pollution problems. In an attempt to adjust the wind field in the San Francisco Bay Area using sparse and irregularly spaced measurements, he adopted a variational formalism similar to that of Sasaki (1970). Simply stated, his algorithm, using an iterative procedure, allows the measured wind field to be adjusted in such a way that the difference between the divergence of the adjusted wind field and that of the measured wind field is minimized in a least-squares sense. The requirement that the adjusted wind field be divergence-free was called the "strong constraint" by Sasaki (1970).<sup>\*</sup> As a result, Dickerson's model can provide a smooth, mass-consistent, two-dimensional wind field if enough wind measurements are available.

Dickerson's approach was extended to three-dimensional wind flows by Sherman (1975) in a model known as MATHEW. Although the overall conservation of mass is strictly imposed in this model, Sherman introduced different Gauss precision moduli for the horizontal and vertical directions. When the lower boundary conditions were properly adjusted according to local topography, significant improvements were reported in the computed wind field (Sherman, 1978).

More recently, Liu and Goodin (1976) examined three different methods for objective analysis, comparing the characteristics of each in the reduction of wind divergence and the rate of convergence of the iterative scheme. Each of the three methods is characterized by one of the following constraints:

---

<sup>\*</sup> In contrast, the requirement that the difference in the divergence, as measured by the residue in the continuity equation be only approximately equal to zero, is called the "weak constraint."

- > The divergence is minimized
- > The vorticity is fixed
- > The station measurements are fixed.

Liu and Goodin concluded that the most suitable method is the one in which the measured winds are held fixed while wind vectors at adjacent points are adjusted in order to reduce the divergence.

## 2. Diagnostic Models Based on Mass Continuity

To simulate the wind field over irregular terrain characterized by inhomogeneous surface temperatures, Anderson (1971) devised a simple diagnostic model that was essentially based on the vertically integrated mass conservation equation in steady state. The resulting model equation is a two-dimensional Poisson expression in which the forcing terms are perturbations of the free stream due to topographical and thermal anomalies. In this model, topographical and thermal perturbations are parameterized in terms of the slopes of the local topography and the temperature differences at the ground, respectively. The parameterization scheme contains empirical coefficients that must be determined through the use of observational data. Anderson applied his model to the State of Connecticut (Anderson, 1971) and to the Los Angeles air basin (Anderson, 1972). For both cases, he reported reasonable success.

Liu, Mundkur, and Yocke (1974) applied this technique to the San Bernardino Mountains to determine the feasibility of modeling the surface wind fields for simulating the spread of wind-driven brush fires. The predicted flow pattern reproduced the expected behavior of topographic and thermal perturbations. The computed wind distributions compared reasonably well with observational data collected by the Forest Fire Laboratory of the U.S. Forest Service and with values for the empirical coefficients chosen from a sensitivity analysis of the model.

In a similar study carried out in Norway, Grønskei (1972) also used the same procedures to compute the wind field in Oslo. The only difference between his model and Anderson's model is that Grønskei parameterized the thermal anomalies in terms of the sulfur dioxide emissions over the center of the city and the temperature differences between air and water over the open Oslo fjord. The sulfur dioxide emissions are presumably related to the strength of the urban heat island. More recently, Basso, Robinson, and Thuillier (1974) applied Anderson's model to study the flow patterns in the San Francisco Bay Area. The results of this effort also appear to show reasonably accurate comparisons of simulations with observations.

A slightly more sophisticated version of this approach is a model proposed by Fosberg and his colleagues (Fosberg, Marlatt, and Krupnak, 1976). In their model, equations governing the changes of divergence and vorticity were derived from the primitive equations. They assumed in the derivation that the inertial terms can be neglected and that dynamic changes in the flow field due to disturbances are transmitted by impulses. The first assumption should work fairly well when applied to the surface layer; the second is equivalent to the quasi-steady-state assumption. Under these assumptions, the divergence and vorticity equations are reduced to two-dimensional Poisson formulations. Fosberg, Marlatt, and Krupnak (1976) applied this model to the rugged area in northwest Oregon, and the resultant predicted wind field was deemed to be reasonable when compared with the observed surface winds.

## IV DEVELOPMENT OF A WIND MODEL FOR COMPLEX TERRAIN

Of the four wind modeling approaches identified in the previous chapter, the interpolation techniques, which are grossly simple and therefore often produce unacceptable results, were dismissed outright. At the other extreme, the application of the dynamic modeling approach to complex terrain did not appear to be feasible at this time because of many fundamental problems related to model formulation and excessive computation burden. As mentioned in the previous chapter, both the objective techniques and the diagnostic models appear to offer suitable alternatives for computing three-dimensional wind fields over complex terrain.

In an exploratory study carried out for the U.S. Forest Service, a two-dimensional wind model of the diagnostic type was developed for application to complex terrain (Liu, Mundkur and Yocke, 1974). This model was based on the solution of a two-dimensional Poisson equation expressing the conservation of mass. Perturbations in the prevailing wind field due to local topographic or thermal variations were treated as forcing functions. This model was applied to the Devil Canyon in the San Bernardino Mountains. The predicted winds compared favorably with the observational data collected by the Forest Fire Laboratory. The success of this undertaking has encouraged us to continue further development of this modeling approach.

### A. THE MODEL EQUATION

Modeling the wind field in the lower atmosphere is essentially tantamount to simulating the interactions between the free atmosphere and the surface boundary layer of the atmosphere. Depending on the characteristic spatial and temporal scales and other environmental parameters, such as the prevailing wind, the thermal stability, and the topography, these interactions take place at different levels of significance. For example, for a

region with a characteristic horizontal dimension on the order of  $10^3$  km or larger and a characteristic time scale on the order of days, the surface layer can be viewed as a layer feeding energy to the free atmosphere. As a result, any successful model on this scale must include the dynamic changes in the large-scale motion that are due to the surface layer. In contrast, on the scale of interest to the present project, with a horizontal dimension of  $10^2$  km and a time scale of a few hours, the synoptic-scale air motion can be viewed as nearly steady state. Consequently, the surface layer can be regarded as a passive system driven by the synoptic-scale flow and surface perturbations. This is the approach adopted in the present study.

The model equation is based on the three-dimensional steady-state equation expressing the conservation of mass for an incompressible fluid:

$$\frac{\partial u}{\partial x} + \frac{\partial v}{\partial y} + \frac{\partial w}{\partial z} = 0 \quad , \quad (4)$$

where  $x$ ,  $y$ , and  $z$  are the orthogonal Cartesian coordinates and  $u$ ,  $v$ , and  $w$  are the corresponding wind components. As shown in Figure 5, the modeling region is first divided into vertical layers. Note that the terrain is allowed to intersect the modeling region; consequently, portions of the modeling region (shaded in Figure 5) must be excluded in the calculations. Note also that it is not necessary to assume that the vertical layers are equally divided. By integrating Eq. (4) over each vertical slab, one can obtain the following set of equations:

$$\frac{\partial \bar{u}_i}{\partial x} + \frac{\partial \bar{v}_i}{\partial y} = -\bar{\omega}_i(x,y) \quad , \quad i = 1, 2, \dots, N \quad , \quad (5)$$

where  $N$  is the total number of vertical layers and  $\bar{u}_i$  and  $\bar{v}_i$  are the vertically averaged wind in the  $i$ -th layer, defined as follows:



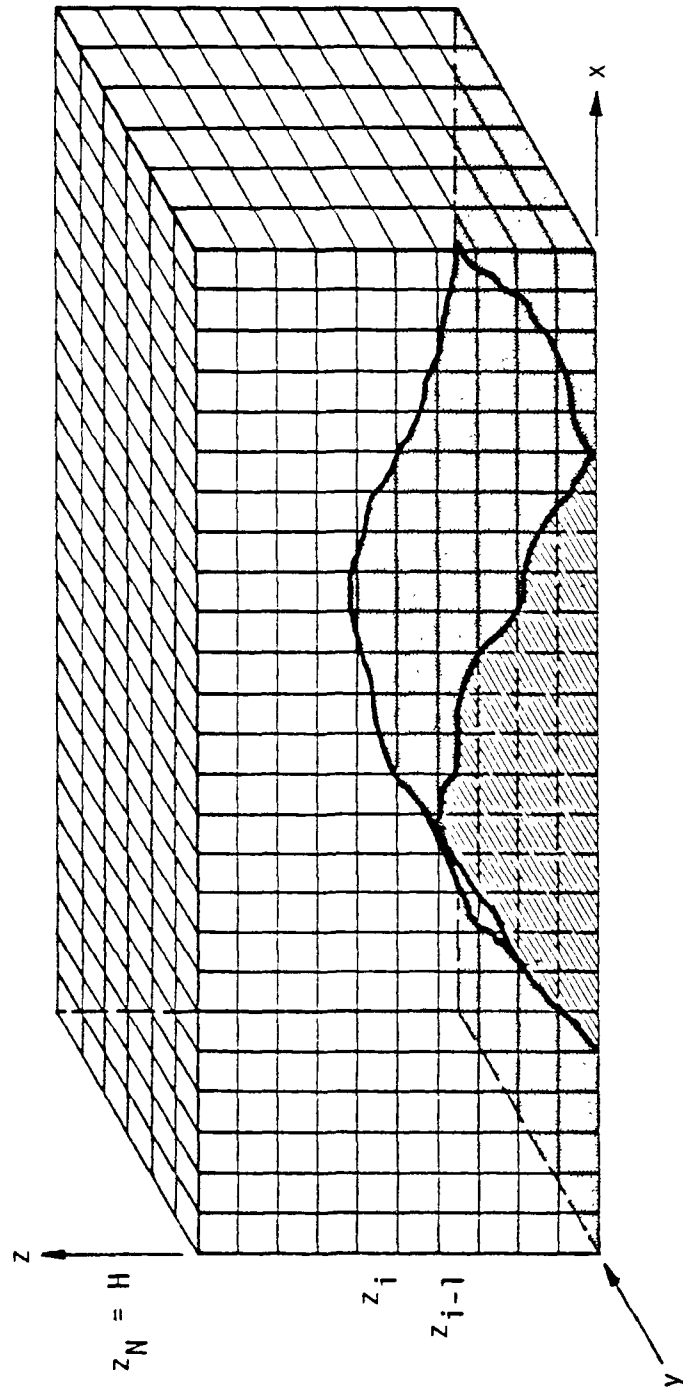


Figure 5. Cross-sectional view of the intersection (shown as shaded, dashed grid) of a hypothetical terrain with a three-dimensional modeling grid

$$\bar{u}_i = \frac{1}{\Delta z_i} \int_{z_{i-1}}^{z_i} u \, dz \quad , \quad (6)$$

$$\bar{v}_i = \frac{1}{\Delta z_i} \int_{z_{i-1}}^{z_i} v \, dz \quad , \quad (7)$$

$$\Delta z_i = z_i - z_{i-1} \quad ,$$

and  $\Omega_i$  is the wind divergence in the  $i$ -th layer:

$$\Omega_i(x,y) = \frac{w(z_i) - w(z_{i-1})}{\Delta z_i} \quad . \quad (8)$$

By defining the following two-dimensional potential functions\* for each of the vertical layers,

$$\bar{u}_i = \frac{\partial \phi_i}{\partial x} \quad , \quad (9)$$

$$\bar{v}_i = \frac{\partial \phi_i}{\partial y} \quad , \quad (10)$$

Eq. (5) can be cast into the conventional Poisson form:

$$\nabla^2 \phi_i = \frac{\partial^2 \phi_i}{\partial x^2} + \frac{\partial^2 \phi_i}{\partial y^2} = -\Omega_i \quad . \quad (11)$$

Once the distribution of the wind convergence is specified, solutions to these equations with appropriate boundary conditions can be computed readily using numerical techniques.

---

\* The question regarding the possibility of expressing a velocity vector as a potential function is addressed in Appendix A.

## B. PARAMETERIZATION OF THE VERTICAL FLUXES

The specification of wind convergence is the key feature of this model. It is proposed that the overall wind convergence is the sum of many components,  $\omega_{ij}$ , as weighted by empirically determined coefficients,  $\alpha_j$ ,

$$\Omega_i = \sum_{j=1}^n \alpha_j \omega_{ij} \quad . \quad (12)$$

In Chapter II, a discussion of the major physical processes that affect the wind distributions in the planetary boundary layer was presented. Only the following perturbations to the wind field over rugged terrain are, however, considered in the model:

- > Lifting and diversion of the flow due to topographic effects.
- > Wind profile modification due to frictional effects in the planetary boundary layer.
- > Convergence of the flow due to thermal effects.
  - Urban heat island
  - Mountain and valley winds.

These perturbations are treated through parameterization of the pertinent processes as follows.

### 1. Topographic Effects

Because the terrain is part of the modeling region in the present model formulation, certain aspects of the topographic effects are included indirectly as boundary conditions. For example, the no-slip condition is imposed whenever the flow encounters a solid surface. The often-observed lifting and diversion of the flow is, however, handled by parameterizing the vertical fluxes.

For high wind speeds and neutral and unstable conditions, it is perhaps logical to view an airflow contacting the slope of a hill to be perfectly elastic. Based on kinematic considerations, the vertical velocity can be expressed as (see Figure 6):

$$w = U \cdot \sin (\arctan \nabla h) \cdot e^{-k_1 z} \quad , \quad (13)$$

where  $h(x,y)$  is the terrain height as a function of location. The exponential term has been added to allow for the decay of the topographic influence away from the surface.

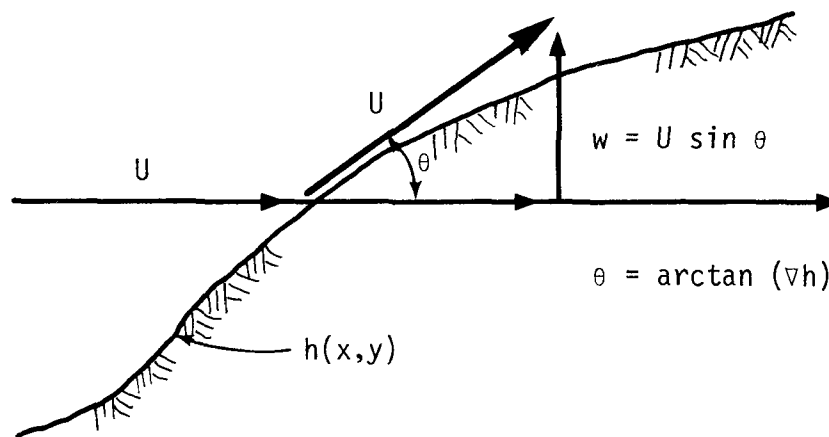


Figure 6. Schematic diagram of a flow contacting the slope of a hill

For low winds and stable conditions, the kinetic energy of the air-stream approaching a hill may be too small to overcome the potential energy required to lift it over the obstacle. As a result, the flow is diverted around the hill.\* The physical processes governing the occurrence of these phenomena are rather complex, and they have only recently received the attention of air pollution researchers. As a first attempt to characterize this effect, Eq. (13) was further modified by a multiplicative factor (see Figure 7),

---

\* The impingement of plumes upon cold mountain slopes, a phenomenon that is well known in recent air pollution studies, is related to this situation.

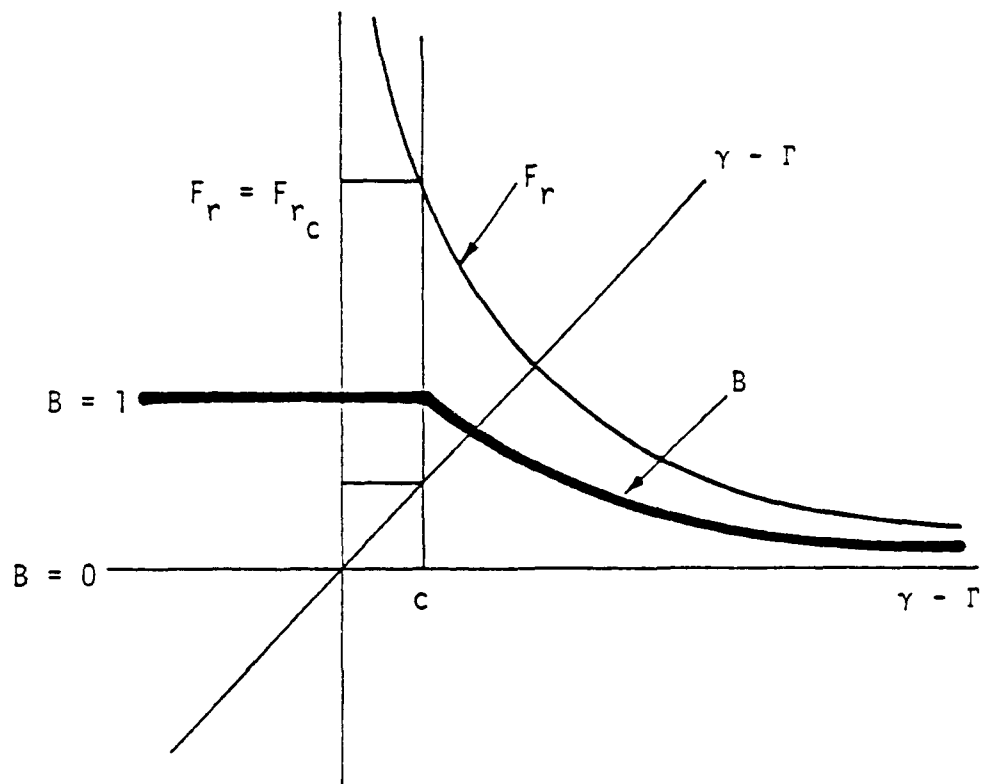
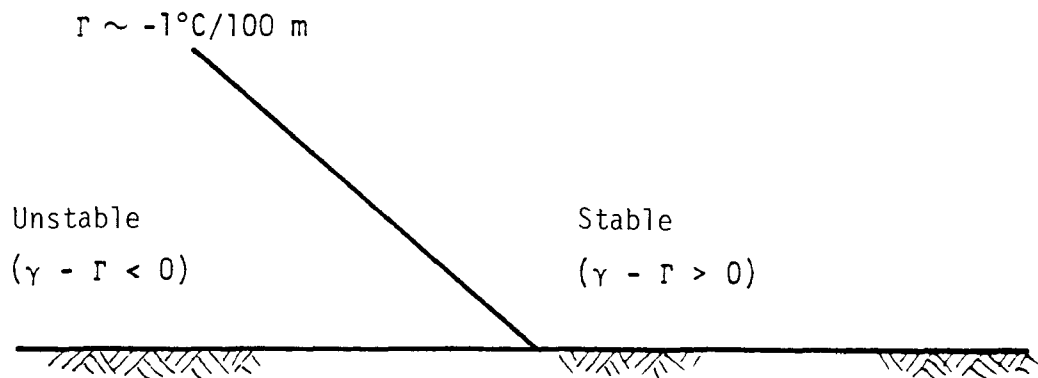


Figure 7. Parameters used in defining the diversion effect

$$B(F_r) = \begin{cases} 1 & \text{if } \gamma - \Gamma \leq c \\ F_r/F_{r_c} & \text{if } \gamma - \Gamma > c \end{cases}, \quad (14)$$

where

$\gamma$  = environmental temperature lapse rate,

$\Gamma$  = adiabatic lapse rate,

$$F_r = \frac{U}{\sqrt{\frac{g(\gamma - \Gamma)}{T_\infty} \Delta h}} \quad (\text{Froude number}),$$

$$\Delta h = h_{\max} - h(x, y),$$

$T_\infty$  = free-stream (unperturbed) temperature

$g$  = acceleration of gravity

$$c = \frac{U^2}{\frac{g}{T_\infty} (F_c \Delta h)^2} \quad (\text{a cut-off constant}),$$

$F_c$  = a critical Froude number where no flow diversion takes place.

Modification of the temperature lapse rate,  $\gamma$ , as air flows over a hill has been neglected as a first approximation herein. According to an analysis by Lilly (1973), the critical Froude number can be taken as 0.5 for an ellipsoidal mountain and 1.0 for a conical mountain.

## 2. Boundary Layer Effects

It is well known that surface friction plays an important role in determining the distribution of the horizontal wind, particularly the vertical wind profile in the atmospheric boundary layer. According to Blasius (1908), the vertical velocity in the boundary layer can be obtained from the similarity solution as follows:

$$\frac{w(z_i)}{U_\infty} = \eta_i \left[ \frac{\gamma'(z_i) - \gamma(z_i)}{\sqrt{Re_x}} \right] \quad (15)$$

where

$U_\infty$  = the free-stream (unperturbed) velocity,

$Re$  = the Reynolds number,

$w(z_i)$  = the vertical velocity at height  $z_i$ ,

$$\eta_i = \frac{\Delta z_i}{\Delta x} \sqrt{\frac{Re}{2}},$$

$$\gamma'_i = u(z_i)/U_\infty:$$

Equation (15) is used to parameterize the frictional effect in the atmosphere, from which the following equation is derived:

$$\begin{aligned} w(z_i) - w(z_{i-1}) &\cong \frac{\Delta z_i}{\Delta x} \left[ U(z_i) - U(z_{i-1}) \right] \\ &\cong \frac{u_*}{k} \frac{\Delta z_i}{\Delta x} \left[ \frac{kU(z_i)}{u_*} - \frac{kU(z_{i-1})}{u_*} \right] \\ &\cong \frac{u_*}{k} \frac{\Delta z_i}{\Delta x} \left[ f(z_i) - f(z_{i-1}) \right] \\ &\cong U(z_{i-1}) \frac{\Delta z_i}{\Delta x} \left[ \frac{f(z_i)}{f(z_{i-1})} - 1 \right], \end{aligned} \quad (16)$$

where  $u_*$  is the friction velocity,  $k$  is von Karman's constant, and the dimensionless  $f(z)$  can be computed from relationships obtained empirically by Businger et al. (1973).

for the stable case,

$$f(z) = \ln\left(\frac{z}{z_0}\right) + 4.7\left(\frac{z - z_0}{L}\right) ; \quad (17)$$

for the unstable case,

$$\begin{aligned} f(z) = & \ln\left[\frac{1 - g\left(\frac{z}{L}\right)}{1 + g\left(\frac{z}{L}\right)}\right] - \ln\left[\frac{1 - g\left(\frac{z_0}{L}\right)}{1 + g\left(\frac{z_0}{L}\right)}\right] \\ & + 2 \tan^{-1}\left[\frac{1}{g\left(\frac{z}{L}\right)}\right] - 2 \tan^{-1}\left[\frac{1}{g\left(\frac{z_0}{L}\right)}\right] , \end{aligned} \quad (18)$$

and

$$g\left(\frac{z}{L}\right) = \left[1 - 15\left(\frac{z}{L}\right)\right]^{-1/4} .$$

where  $z_0$  is the aerodynamic surface roughness length and  $L$  is the Monin-Obukhov length.

### 3. Thermal Effects

It is also known that flow can be induced by the conditions of uneven surface heating. On the scale of interest to this study, over complex terrain in urban settings, two types of atmospheric circulation were deemed important:

- > Flows induced by an urban heat island
- > Mountain and valley winds (upslope and downslope flows).



a. Urban Heat Island

Airflow over a heated island has been shown to have an appearance similar to that over a mountain (Stern and Malkus, 1953). According to Stern and Malkus, an "equivalent mountain" function is defined as follows:

$$M(x,y) = \begin{cases} \frac{T(x,y)}{\gamma - \Gamma} & \text{if } \gamma - \Gamma > 0 \\ 0 & \text{if } \gamma - \Gamma \leq 0 \end{cases} \quad (19)$$

where  $T(x,y)$  is the spatial distribution of surface temperature. In parallel to the discussions that led to Eq. (13), it can be assumed that the vertical motion generated by heat island effects is

$$w = U \cdot \sin (\arctan \nabla M) \cdot e^{-k_2 z} \quad (20)$$

The reader should note that in the absence of a driving wind,  $U$ , vertical fluxes due to the urban heat island are zero. Furthermore, the equivalent mountain formation was derived for flat terrain situations; therefore, this parameterization is used only for flat portions of the modeling grid. In sloping terrain, the treatment described in the following section is used.

b. Mountain-Valley Winds

Slope winds are micro/mesoscale breezes that blow normal to the topographic gradients due to temperature-dependent density differences. During the night, radiative cooling of the slope cools the air just above it. This process causes the air close to the ground to become denser than the air at the same altitude but farther above the sloping surface. As a result, the cold air slides down the slope. The reverse process occurs during the day when the sun's radiation warms the slope and the air just above the slope.

Defant (1933) proposed the following expression to describe the steady-state, average speed of a cold current gliding down a slope of average elevation angle  $\alpha$ :

$$U_{\text{slope}} = \left[ \frac{g\bar{h}(T_C - T_E)\sin \alpha}{C_D T_C} \right]^{1/2}, \quad (21)$$

where

$C_D$  = a drag coefficient

$\bar{h}$  = the mean height of the cold current,

$g$  = gravitational acceleration,

$T_C, T_E$  = the temperatures of the current and environment, respectively.

The reader will note that a driving wind is not necessary to induce down-slope flow with Eq. (21).

Adapting Eq. (21) to our grid system but retaining the important functional dependences, one can obtain the following expression for both upslope and downslope flow:

$$U_{\text{slope}} = \text{constant} \left[ \left( \frac{T_C - T_E}{T_C} \right) \left( \frac{H_{\text{max}} - H}{H_{\text{max}}} \right) \right]^{1/2}, \quad (22)$$

where  $H$  is the average surface elevation in the grid cell and  $H_{\text{max}}$  is the highest terrain elevation affecting local flow. The terrain involving the heights is substituted for the " $\sin \alpha$ " term in Eq. (21) because the " $\sin \alpha$ " term is qualitatively correct only for estimating average slope velocity and only if the elevation angle is uniform along the entire slope. In the modeling grid, however, the velocity is computed at any point along

a slope, not just the average slope velocity, and elevation angles are rarely uniform along a slope. The substitution allows qualitatively realistic spatially resolved estimates of upslope and downslope flow behavior. With a proper selection of the constant in Eq. (22), quantitatively correct estimates should also be possible.

As in Defant's algorithm, Eq. (22) contains no dependence on driving wind. In our model, therefore, the vertical fluxes for the mountain-valley winds are self-generating. Since down- and up-slope flows have both horizontal and vertical components, the model must account for the self-generating horizontal component as well as the vertical component to maintain consistency. Therefore, the parameterization of mountain-valley winds is entered through the vertical flux term and through the horizontal boundary conditions. All previous parameterizations of vertical fluxes described are dependent upon the horizontal wind and are intrinsically consistent with the horizontal flow component; thus, no adjustments to boundary conditions are necessary for them.

### C. NUMERICAL SOLUTION PROCEDURE

To obtain a solution to Eq. (11) with complex boundary conditions, a numerical technique is required. Several direct Poisson solvers are available that are based on block-cyclic reduction of a set of finite difference equations (Buzbee, Golub, and Nielson, 1970; Swarztrauber and Sweet, 1975). Although these solvers are convenient and inexpensive to use, their application is restricted to simple rectangular modeling regions. This presents a rather serious drawback for the present formulation because, as described earlier, the terrain may intersect the modeling region.

Thus, an alternative solution technique was chosen that can accommodate the exclusion of portions of the modeling region with irregular shapes and yet incur only a modest increase in computation time over the direct solution techniques. The general form of the Poisson equation is

$$\nabla^2 \phi = \frac{\partial^2 \phi}{\partial x^2} + \frac{\partial^2 \phi}{\partial y^2} = f(x,y) \quad , \quad (23)$$

and the five-point difference approximation to Eq. (23) is

$$\frac{\phi_{i-1,j} - 2\phi_{i,j} + \phi_{i+1,j}}{(\Delta x)^2} + \frac{\phi_{i,j-1} - 2\phi_{i,j} + \phi_{i,j+1}}{(\Delta y)^2} = f_{i,j} \quad , \quad (24)$$

$$i = 1, \dots, M \text{ and } j = 1, \dots, N \quad ,$$

where

- $\phi$  = the potential function,
- $f(x,y)$  = the forcing function,
- $x, y$  = orthogonal Cartesian coordinates,
- $i, j$  = the grid cell indices of a grid system that  
is superimposed on the modeling region and that  
has  $M$  grid cells in the  $x$ -( $i$ -) direction and  $N$   
grid cells in the  $y$ -( $j$ -) direction.

Equation (24) is valid for all points within the modeling region, but for those along the modeling boundary some additional computations are required. Along the boundaries, the normal derivatives of  $\phi$  (i.e.,  $d\phi/dx$  or  $d\phi/dy$ --often referred to as Neumann-type boundary conditions) are specified, and these are used to compute values of  $\phi$  at fictitious grid points outside the modeling region. For example, consider a grid cell ( $i,j$ ) that forms part of the left boundary of the modeling region as shown in Figure 8. To solve Eq. (24) for this point, one must specify some value for  $\phi_{i-1,j}$ , which exists at a point outside the modeling region. The study team simply computed  $\phi_{i-1,j}$  using

$$\phi_{i-1,j} = \phi_{i,j} - \left( \frac{d\phi}{dx} \right)_{ij} \Delta x \quad (25)$$

and substituted this expression in Eq. (24).

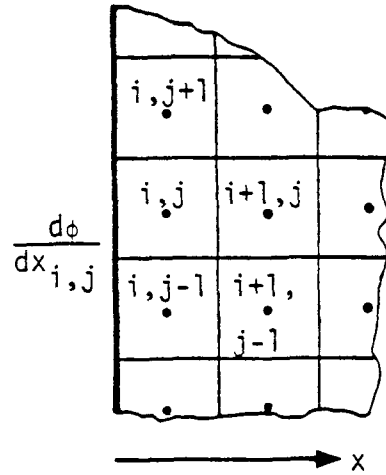


Figure 8. Sketch showing a grid cell  $(i,j)$  along the left boundary of the modeling region

The commonly used modified Gauss-Seidel iterative solution method was selected because it is very well suited to the solution of the five-point operator [Eq. (24)] for the Poisson equation (Dahlquist and Björck, 1974). Like all iterative techniques, it starts from a first approximation, which is successively improved until a sufficiently accurate solution is obtained. To simplify the description of this method, consider the linear system of equations

$$Ax = b \quad (26)$$

instead of the system described in Eq. (24). Equation (26) can be written as

$$x_i = \frac{-\sum_{j \neq i}^N (a_{ij}x_j + b_j)}{a_{ii}}, \quad i = 1, 2, \dots, n \text{ and } a_{ii} \neq 0. \quad (27)$$

In Gauss-Seidel's method, a sequence of approximations  $x^{(1)}$ ,  $x^{(2)}$ ,  $x^{(3)}$ , ... is computed by

$$x_i^{(k+1)} = \frac{-\sum_{j=1}^{i-1} a_{ij}x_j^{(k+1)} - \sum_{j=i+1}^n a_{ij}x_j^{(k)} + b_i}{a_{ii}}, \quad (28)$$

$$i = 1, 2, \dots, n.$$

Note that Eq. (28) can also be written as

$$x_i^{(k+1)} = x_i^{(k)} + r_i^{(k)}, \quad (29)$$

where  $r_i^{(k)}$  is the current residual of the  $i$ -th equation and

$$r_i^{(k)} = \frac{-\sum_{j=1}^{i-1} a_{ij}x_j^{(k+1)} - \sum_{j=i+1}^n a_{ij}x_j^{(k)} + b_i}{a_{ii}}. \quad (30)$$

Now, to improve the rate of convergence, one can slightly modify Eq. (29) to give

$$x_i^{(k+1)} = x_i^{(k)} + \omega r_i^{(k)}, \quad (31)$$

where  $\omega$  is called the relaxation parameter, which is chosen so that the rate of convergence is maximized. This improved iteration procedure is called the "successive overrelaxation method" (Dahlquist and Björck, 1974).

In the present study,  $\omega = 1.4$  was found to give the best rate of convergence in tests of the modified Gauss-Seidel solution to Eq. (24). In these tests, the criterion for complete convergence was defined so that

$$\max_i r_i^{(k)} \leq 0.01 x_i^{(k)}. \quad (32)$$

## V APPLICATION OF THE MODEL TO THE PHOENIX AREA

The Phoenix metropolitan area is located in central Arizona along the channel and flood plain of the Salt River. It is surrounded by flat desert wastelands and by barren mountain ridges ranging widely in elevation. The river level is about 350 m above mean sea level near downtown Phoenix, and mountain peaks rise as high as 1400 m above mean sea level within 20 km of the downtown area. Since Phoenix is located in the great southwest desert of the United States, it typically experiences clear skies and intense surface heating and radiational cooling during the days and nights, respectively. In light of the above comments, the Phoenix urban area is an ideal location in which to test the performance of the three-dimensional wind model described earlier, because all the following phenomena appear to occur there: topographic obstructions to wind flow, urban heat island effects, surface roughness effects, and mountain-valley winds (up- and down-slope flows). Therefore, the Phoenix area was chosen as the initial test location for the model.

In the next section, the data base used to carry out wind simulations for four days in Phoenix is described. Section B discusses the results of those simulations. Finally, Section C presents statistical analyses of the results.

### A. DATA BASE

Four days were selected for testing the wind model described in the previous chapter. On three of these days low wind speeds prevailed, and on one the wind speeds were high. The dates chosen were 15 and 16 February 1977 and 7 and 10 March 1977; these were chosen for completeness of data and phenomenological interest. On these days, a maximum of 15 surface wind stations collected data; however, for some hours a significant number of these stations reported missing or invalid data. Names and coordinates

of each of the 15 stations are shown in Table 1. No upper level wind or temperature measurements are made near the Phoenix area, and National Weather Service synoptic scale maps provided the only information about upper level flows on these days. The model was exercised for all 24 hours on each of the days.

The Phoenix metropolitan area and surrounding environs were divided into a 40- by 50-grid of 2- by 2-km squares as shown in Figure 9. Five vertical levels of 200 m each were chosen for the present application. For each grid element, the average surface elevation, elevation of most prominent terrain feature in the vicinity of the cell, and the aerodynamic roughness length were determined. Terrain height information was obtained from topographic maps of the area. Values of the roughness length were estimated using the bulk aerodynamic method devised by Lettau (1969). For this purpose, representative land use categories were established and percentages of them within each horizontal grid element determined using aerial photographs, results of visual ground surveys, street maps, and real estate maps and charts. A composite value for each of the elements was then derived by linear weighting of the percent coverage of each land use category existing within the element.

For all days simulated, the values of the coefficients used in the parameterization of heat island, frictional, and topographic vertical fluxes were identical: 1.0, 0.01, and 0.3, respectively. These were derived from previous model applications and sensitivity tests for other areas. Only the boundary condition flows and the mountain-valley wind coefficients were varied for each hour. Table 2 shows the mean flow imposed at the modeling boundaries and the mountain-valley wind coefficient used for each hour simulated on all four days. The computing costs on the LBL CDC 7600 for these runs were typically about \$50.00 per 24-hour simulation excluding plotting. Microfiche plots cost about \$20.00 per 24-hour simulation.



TABLE 1. PHOENIX AREA WIND MEASUREMENT STATION NAMES AND COORDINATES

Station Name	UTM* Coordinates		Grid Cell Model Coordinates	
	East	North	East	North
Central Phoenix	404.21	3702.44	32	21
South Phoenix	401.21	3696.36	31	18
Glendale	390.57	3714.82	25	27
West Phoenix	395.04	3708.31	27	24
North Phoenix	402.10	3713.71	31	27
North Scottsdale/Paradise Valley	414.27	3719.34	37	30
Scottsdale	415.83	3704.66	37	22
Mesa	423.85	3698.12	41	19
Mesa Wind	431.69	3697.50	46	19
Fire Station 13	409.13	3704.68	35	23
Fire Station 17	402.71	3708.81	31	24
Orange Grove	385.61	3725.60	22	33
Williams AFB	438.00	3685.00	49	13
Luke AFB	372.00	3711.00	16	26
Taylor	391.09	3687.72	25	14

\* Universal Transverse Mercator

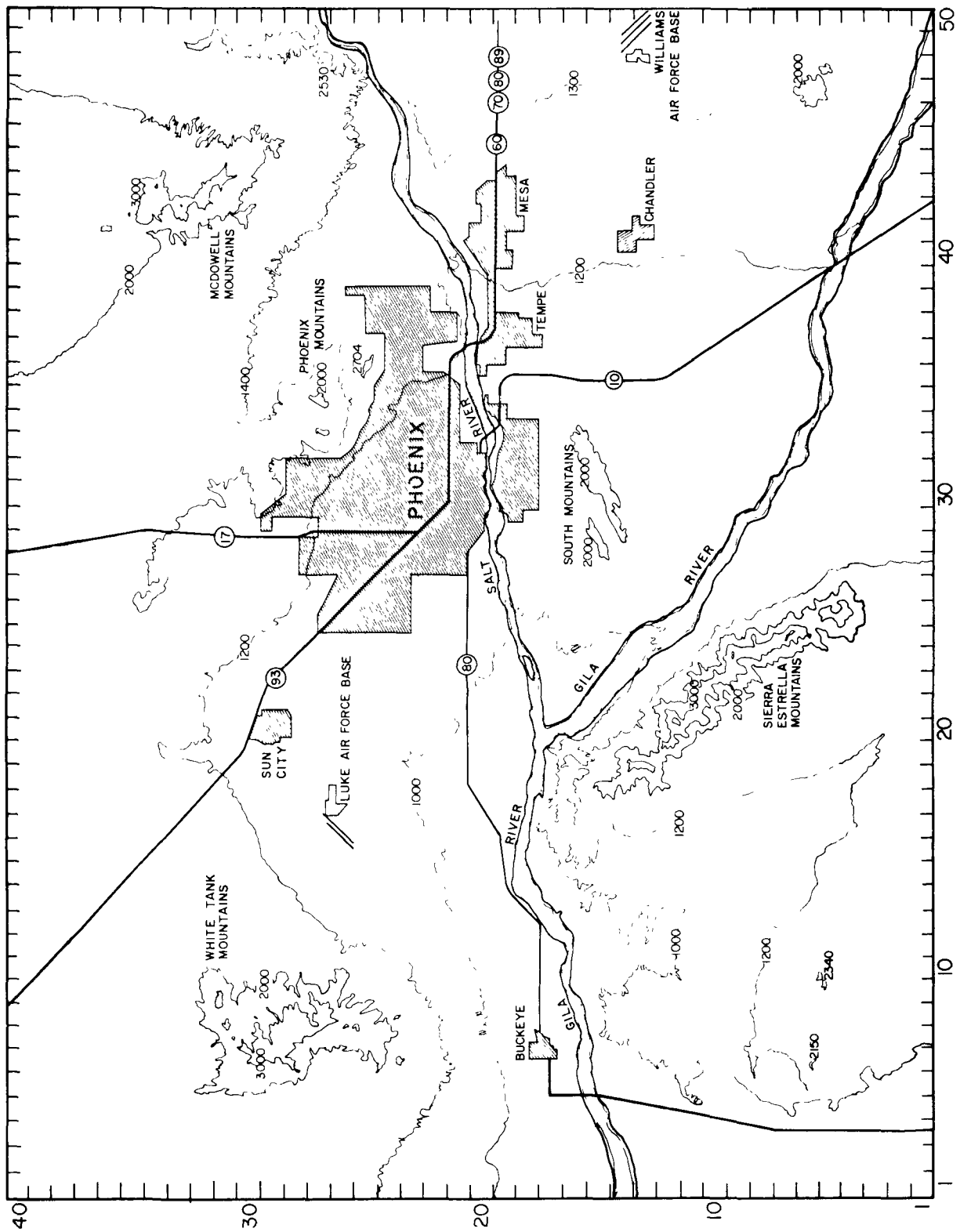


Figure 9. Modeling grid indicated on a topographic map of the Phoenix area

TABLE 2. MEAN FLOW IMPOSED AT MODEL BOUNDARIES AND MOUNTAIN-VALLEY WIND COEFFICIENT USED FOR PHOENIX WIND SIMULATIONS

Hour	15 February 1977				16 February 1977				7 March 1977				10 March 1977			
	Wind Speed (mph)	Wind Direction (°from)	Mountain-Valley Wind Coefficient	Wind Speed (mph)	Wind Direction (°from)	Mountain-Valley Wind Coefficient	Wind Speed (mph)	Wind Direction (°from)	Wind Speed (mph)	Wind Direction (°from)	Mountain-Valley Wind Coefficient	Wind Speed (mph)	Wind Direction (°from)	Mountain-Valley Wind Coefficient	Wind Speed (mph)	Wind Direction (°from)
0000	3	200	-0.07	5	230	-0.02	2	210	2	210	-0.1	20	220	0	0	0
0100	3	210	-0.06	3	230	-0.03	2	210	2	210	-0.1	20	250	0.0	0.0	0.0
0200	3	180	-0.06	2	180	-0.05	2	210	2	210	-0.1	18	270	0.0	0.0	0.0
0300	3	200	-0.06	5	230	-0.03	3	210	3	210	-0.08	17	260	0.0	0.0	0.0
0400	3	180	-0.05	3	230	-0.02	3	210	3	210	-0.06	18	280	0.0	0.0	0.0
0500	6	200	-0.04	2	250	-0.05	3	260	3	260	-0.04	20	280	0.0	0.0	0.0
0600	8	240	-0.02	3	250	-0.05	4	260	4	260	-0.04	18	280	0.0	0.0	0.0
0700	5	230	0.0	2	270	-0.04	6	240	6	240	0.0	17	290	0.0	0.0	0.0
0800	4	240	0.0	4	270	-0.02	6	180	6	180	0.0	22	290	0.0	0.0	0.0
0900	5	220	0.0	8	270	0.02	7	220	7	220	0.0	22	290	0.0	0.0	0.0
1000	12	220	0.01	6	270	0.04	5	270	5	270	0.0	19	290	0.0	0.0	0.0
1100	10	270	0.01	5	270	0.04	5	220	5	220	0.0	20	320	0.0	0.0	0.0
1200	6	270	0.0	4	300	0.04	6	300	6	300	0.0	20	320	0.0	0.0	0.0
1300	4	310	0.05	2	360	0.08	6	300	6	300	0.0	20	320	0.0	0.0	0.0
1400	5	310	0.02	2	45	0.08	6	300	6	300	0.0	23	340	0.0	0.0	0.0
1500	5	310	0.01	3	80	0.05	6	320	6	320	0.0	23	320	0.0	0.0	0.0
1600	4	40	0.04	5	90	0.04	4	310	4	310	0.08	20	330	0.0	0.0	0.0
1700	3	30	0.02	6	130	0.03	4	120	4	120	0.05	20	340	0.0	0.0	0.0
1800	5	40	0.01	3	110	0.02	4	120	4	120	0.0	18	340	0.0	0.0	0.0
1900	4	40	-0.005	3	240	-0.02	5	160	5	160	-0.06	15	340	0.0	0.0	0.0
2000	3	190	-0.07	3	260	-0.03	5	170	5	170	-0.08	13	340	0.0	0.0	0.0
2100	3	220	-0.06	2	270	-0.05	4	190	4	190	-0.08	13	340	0.0	0.0	0.0
2200	3	220	-0.05	2	260	-0.05	2	180	2	180	-0.08	11	330	0.0	0.0	0.0
2300	3	240	-0.05	3	260	-0.05	2	190	2	190	-0.1	10	320	0.0	0.0	0.0

## B. DISCUSSION OF THE RESULTS

The measured surface winds are plotted along with the corresponding predictions for the lowest layer of the modeling grid in Appendix B for every second hour on the four days. The predictions for all five layers not presented herein are contained on microfiche.\* The contours shown on the predicted wind field plots represent terrain that is above the top elevation of that particular grid layer; they are included so that the reader may more easily elucidate the impact of elevated terrain and terrain slope. Computations are not made by the model for grid cells within these contours.

A glance at the measured winds on the days selected for application of the wind model to Phoenix should convince most readers that complex flow situations existed on three of the four days (15 and 16 February and 7 March 1977). Generally, chaotic wind patterns were observed on these three days owing to weak synoptic flow and the dominance of local effects. Stronger synoptic flow existed on the fourth day (10 March 1977), resulting in more regular flow patterns. Certainly, the main goal of this study is to determine whether the wind model developed here can at least qualitatively match such diverse wind patterns as were observed on these four days in the Phoenix area. Success in this task would indicate that most of the important phenomena have been treated and have been parameterized reasonably well.

Beyond this study, continued efforts to achieve a better quantitative match of predicted and measured winds are suggested that would focus on systematic adjustment of empirical parameters for a given application site. For the present application, such adjustments have not been carried out. Analyses of quantitative results presented later in this section are intended to provide a benchmark against which to compare future improvements in model performance, rather than an estimate of the model's ultimate prediction accuracy; optimization of empirical coefficients in the model are certain to improve its performance.

---

\* The microfiche format was selected for compact presentation of all of the 576 plots generated in this study. The microfiche are available on request from the Project Officer.

On the basis of a qualitative comparison of the wind model predictions with wind measurements, the results of this application of the model to the Phoenix area are encouraging. The model reproduced the wind field on the high wind speed day (10 March 1977) very well and required no mountain-valley wind contribution. This finding is consistent with the intuitive notion that these effects would be relatively insignificant under strong synoptic flow conditions. Furthermore, this result indicates that the model's treatment of topographic blocking, frictional, and urban heat island effects is adequate.

In the early hours of 10 March the large scale flows appear to have been generally out of the southwest at about 15 to 23 mph. Flows gradually began to shift to a more westerly direction by 0200. By 0500 they were northwesterly, and they became almost northerly in the early afternoon. Flow velocities began to diminish somewhat at about 1800, slowing to about 10 mph by 2300. Throughout the day, significant amounts of diversion can be seen in the model predictions around the Sierra Estrella, South, and Maricopa mountain features. Some minor flow disturbances can also be seen in the vicinity of the mountain just north of Phoenix (e.g., Camelback, Phoenix Mountain). The presence of these topographic features frequently tends to produce localized areas of convergence and divergence in the Avondale and Tempe-Mesa vicinities and along the Gila River. There is some indication that these are consistent with the location of pollutant "hot-spots" in the Phoenix area (Berman, 1978).

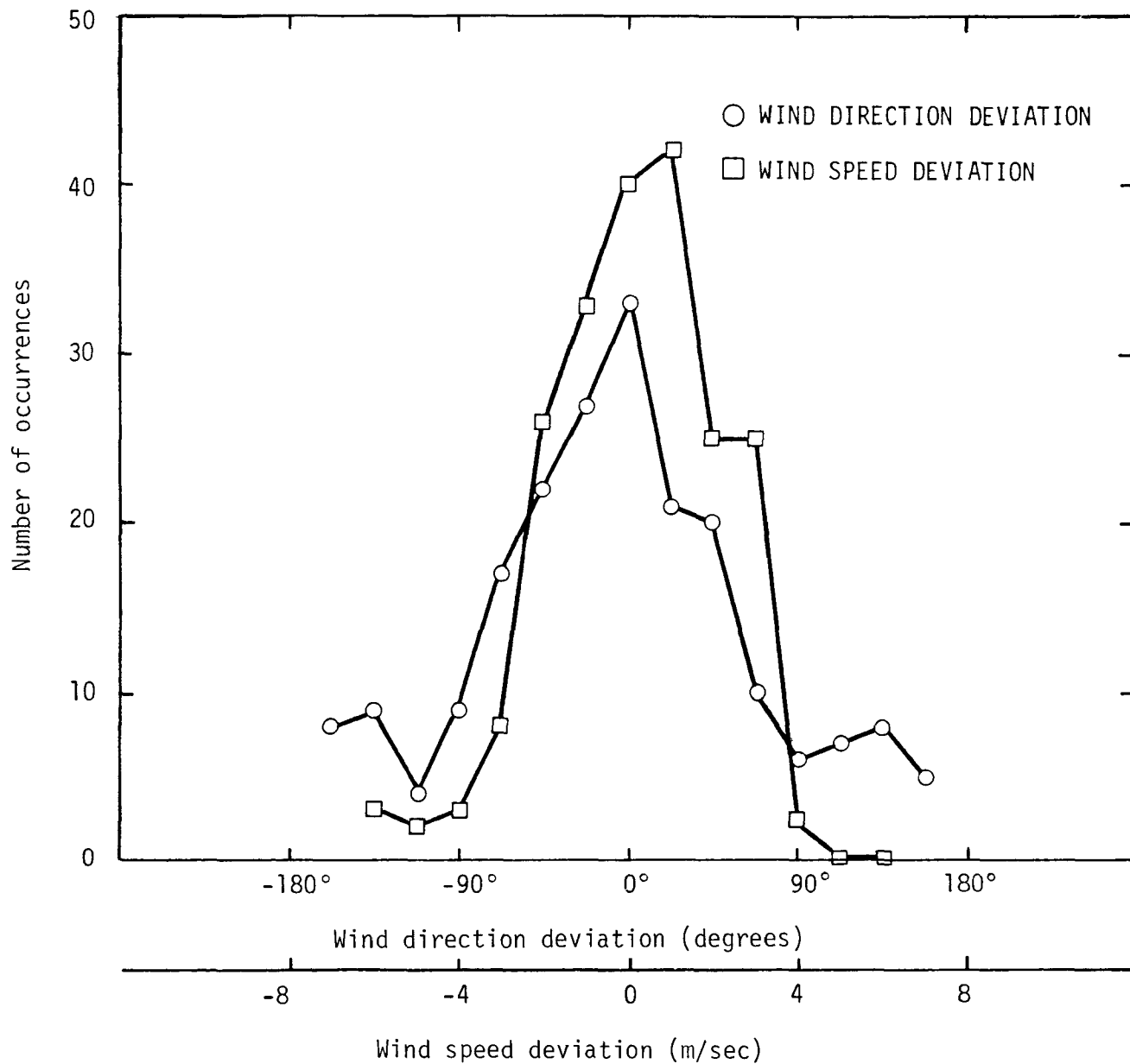
On the low wind speed days, it appears that microscale (less than 2 km) and mesoscale (larger than 2 km) drainage and upslope flows dominate the chaotic flow situation. Although the model did not reproduce the flow characteristics exactly for these days, it appears to have predicted the most important mesoscale drainage and upslope influences. On these days, 15 and 16 February and 7 March 1977, large scale flows were light, ranging from 2 to 10 mph, and generally out of the west (varying between southwest and northeast). As can be seen in the model predictions, local effects essentially mask the large scale flow characteristics, particularly in the lowest levels. A significant amount of downslope flow can be seen to persist around all

significant terrain features. For example, up- and down-slope flows associated with the gradually steepening terrain toward the McDowell Mountains to the northwest dominate over a large part of the modeling region. Up- and down-slope flows from the South Mountains have a significant impact on the wind in Phoenix proper. Down-slope flows persist during the hours of darkness on all three days. The down-slope flows desist just after dawn and a few hours later the effects of up-slope flow on major terrain features can be seen. These diminish in the early evening, followed by the onset of down-slope flow a few hours later. Areas of convergence and divergence caused by opposing flows up and down adjacent terrain features can be observed in the vicinity of Phoenix, especially in the Tempe, Mesa and Gila River areas. These patterns are fairly consistent with the distribution of pollutants observed in those areas. A specific example is the large area of convergence at night in West Phoenix. This area typically has high concentrations of inert pollutants like carbon monoxide during nighttime hours in light wind and clear sky situations (Berman, 1978).

Some of the measured wind values on these days appear to reflect strong local (microscale) effects (Pitchford, 1976). Although we cannot state categorically that an aberrant wind speed or direction is the result of these influences, this possibility should be kept in mind in evaluating the model's performance. Some of the measurement stations appear to have poor exposure, e.g., the south Phoenix station is immediately adjacent to a large tree. Our analysis of prediction statistics was performed using all available data, although some may be representative of local or short-time scale phenomena.

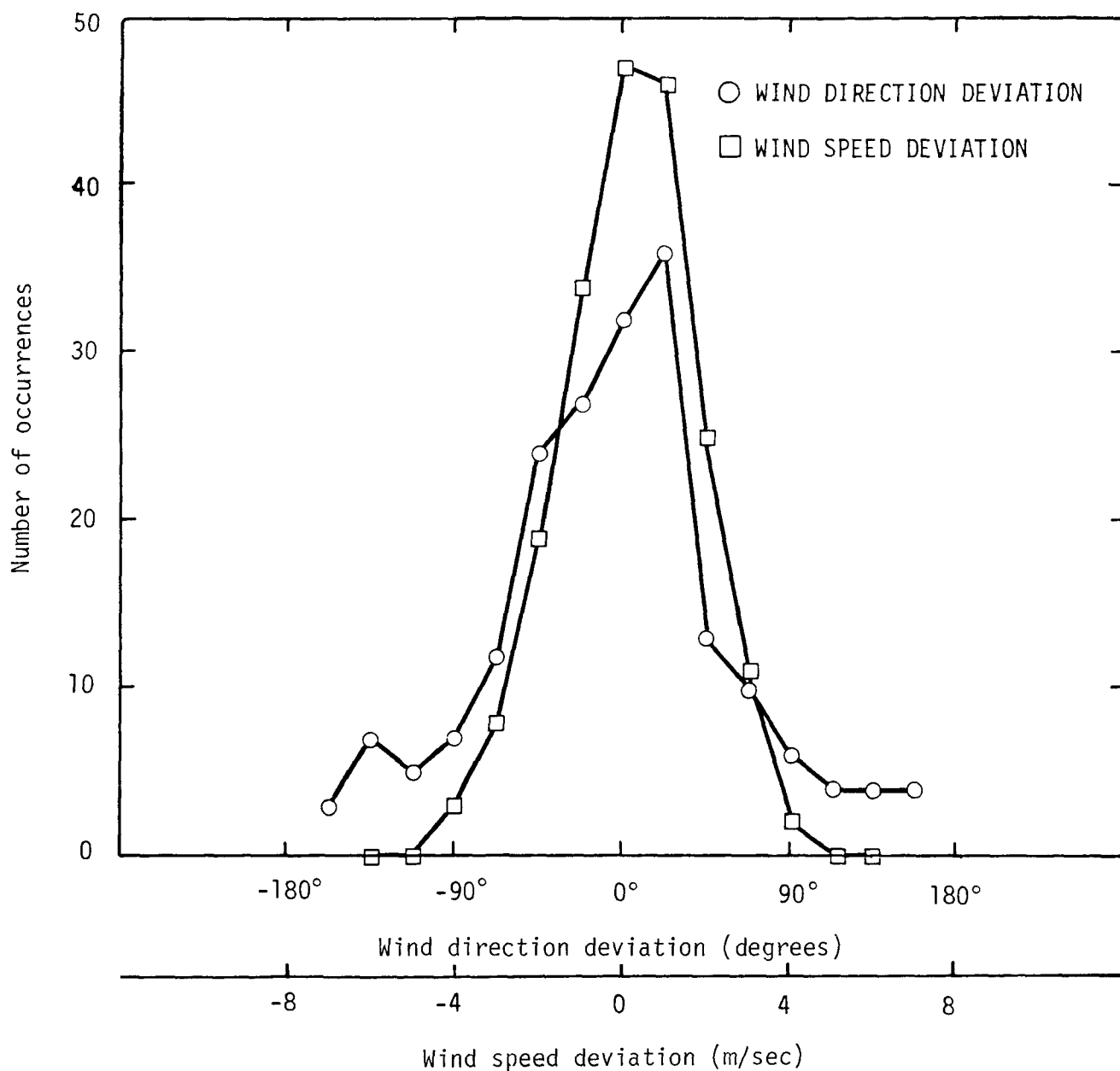
### C. STATISTICAL ANALYSIS OF THE RESULTS

The wind model predictions at the surface were compared with the corresponding surface-level measurements taken each hour throughout the four test days. Based on these data, frequency distributions of the deviation in predicted wind speed and wind direction as a function of the measured values were constructed. Also, estimates of the mean (or expected value of) deviations in these predicted parameters were computed. These frequency distributions and means of deviations in wind speed and wind direction are shown in Figures 10 through 13 for the four test days: 15 February,



Note: The mean absolute wind speed deviation is 1.58 m/sec, and the mean absolute wind direction deviation is 58.98°.

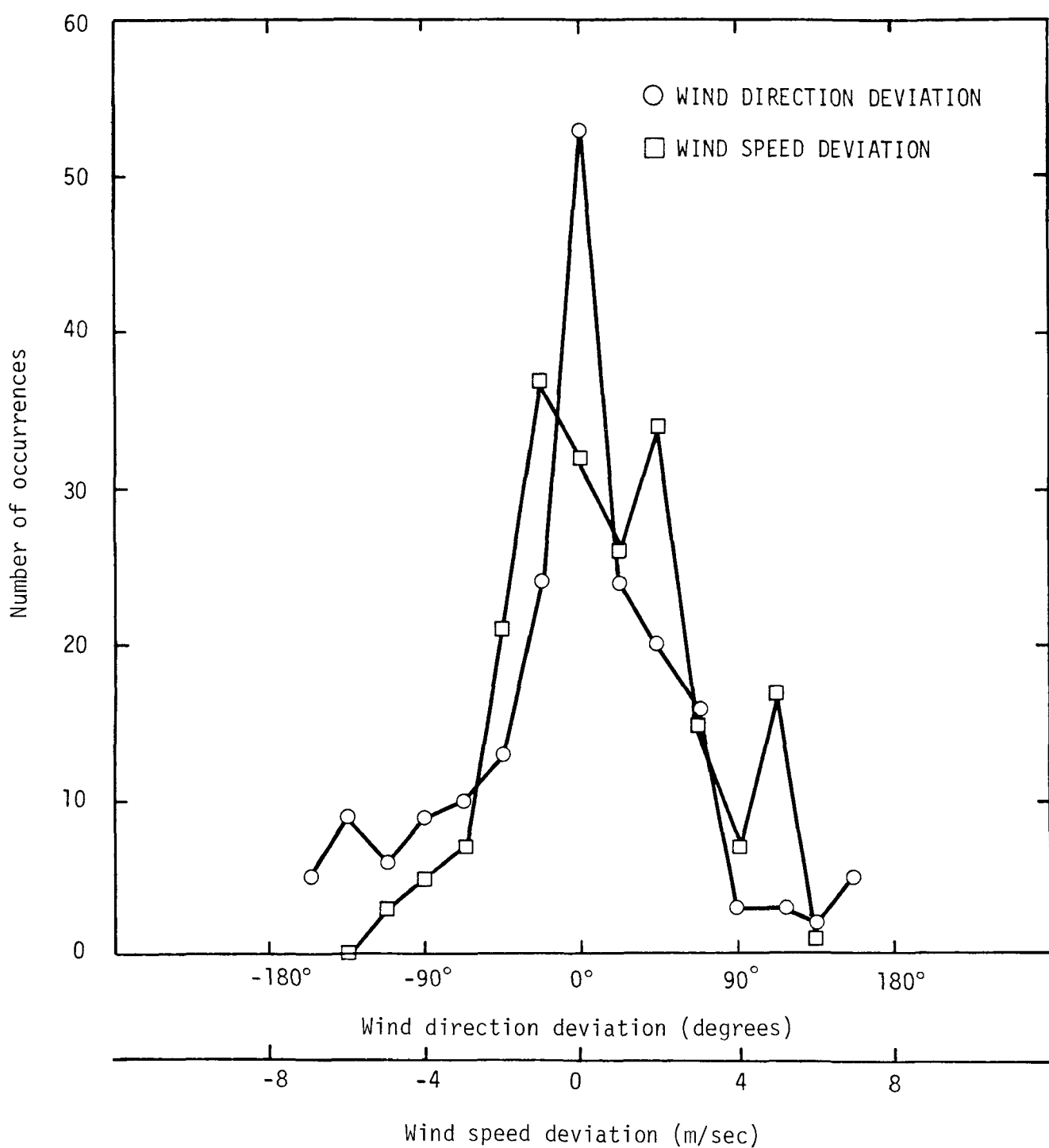
Figure 10. Frequency distributions of wind speed and wind direction deviations for 15 February 1977



Note: The mean absolute wind speed deviation is 1.28 m/sec, and the mean absolute wind direction deviation is 49.52°.

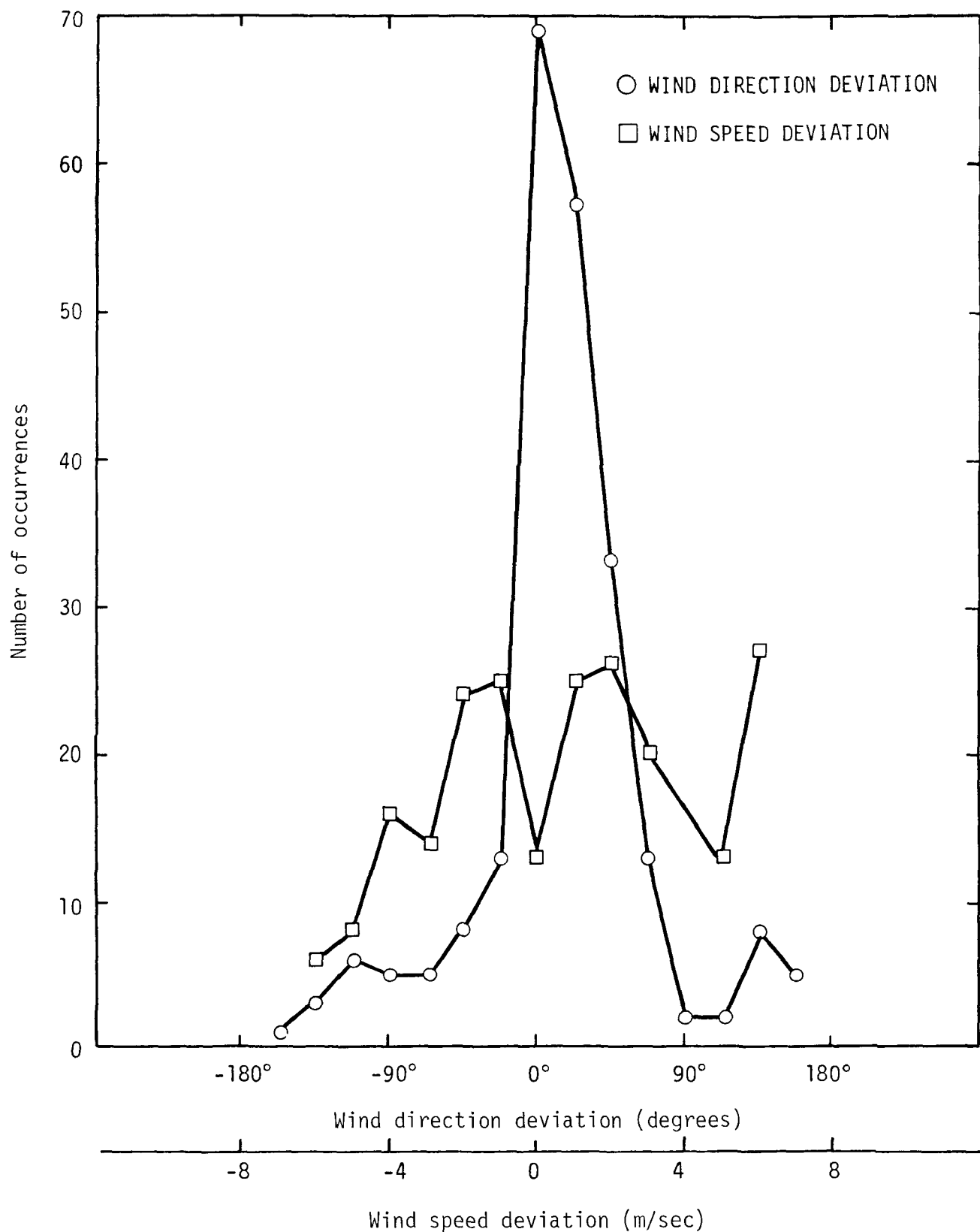
Figure 11. Frequency distributions of wind speed and wind direction deviations for 16 February 1977





Note: The mean absolute wind speed deviation is 1.9 m/sec, and the mean absolute wind direction deviation is 40.58°.

Figure 12. Frequency distributions of wind speed and wind direction deviations for 7 March 1977



Note: The mean absolute wind speed deviation is 3.08 m/sec, and the mean absolute wind direction deviation is 40.05°.

Figure 13. Frequency distributions of wind speed and wind direction deviations for 10 March 1977

16 February, 7 March, and 10 March 1977. In these figures, wind direction data points are indicated with circles, and wind speed data points with squares. All measured wind data reported on these days were used to construct these distributions and means. As noted earlier, many stations in the Phoenix area may be influenced by microscale effects; consequently, this statistical evaluation of the wind model's performance is quite stringent, yet the performance of the model for these days in Phoenix is quite encouraging.

These extensive statistical analyses of the predicted and measured wind speeds and wind directions were also carried out to detect possible systematic biases and random errors in the model. The figures illustrate that the model generally predicts winds that are higher in magnitude (by about 1.5 m/sec) and more clockwise in direction (by about 1 compass point on a 16-point scale) than are the corresponding surface measurements. This finding is not surprising because the predictions are averages for a layer between the ground and 200 m above the ground, whereas the measurements were obtained by sensors situated between about 10 and 20 m above ground.

The mean absolute deviation in wind speed predictions for all four days combined is 1.96 m/sec, based on 831 hourly averaged wind measurements. The four-day mean of absolute wind direction deviations is 49.8°. Both of these values indicate that the performance of the model is reasonable when applied to a complex and chaotic flow situation. Notice that the lower wind speed days (15 and 16 February and 7 March) have lower mean wind speed deviations than the higher wind speed day (10 March). In contrast, the mean direction deviation is smaller for the high wind speed day, on which an organized synoptic flow existed over the area. These results basically agree with the observations in the preceding paragraph. Over 64 percent of all wind direction deviations are within  $\pm 45^\circ$  or  $\pm 1$  compass point for all four days.

## VI CONCLUSIONS AND RECOMMENDATIONS

A three-dimensional diagnostic wind model has been developed for rugged terrain based on mass continuity. The model is composed of several horizontal layers of variable thicknesses. For each layer, Poisson equation is written with the wind convergence as the forcing function. Many types of wind perturbations over rugged terrain are considered in this model, including diversion of the flow due to topographical effects, modification of wind profiles due to boundary layer frictional effects, convergence of the flow due to urban heat island effects, and mountain and valley winds due to thermal effects. Wind data collected during a comprehensive field measurement program at Phoenix, Arizona, were used to test the model. The average deviation between the predicted and observed wind speeds, based on 831 hourly measurements, is 1.96 m/sec. The corresponding average wind direction deviation is 49.8°. These gross statistics seem to indicate that the performance of the model is reasonable when applied to a complex and chaotic flow situation.

Further improvement of the model is certainly possible. Among the areas for which continued developmental effort would be most fruitful are:

- > A better, more objective procedure to prescribe the boundary conditions for initiating the model calculations.
- > A systematic analysis of the model responses to optimize the *empirical coefficients in the parameterization schemes*.
- > Further refinement of the model by including other physical processes, such as the wind direction shear, if proven important.

APPENDIX A  
DECOMPOSITION OF A VELOCITY VECTOR

## APPENDIX A

### DECOMPOSITION OF A VELOCITY VECTOR

In its most general form, any velocity vector can be decomposed into two parts, one of which represents a potential flow:

$$\begin{aligned}\bar{v} &= \bar{A} + \bar{B} \\ &= \nabla\phi + \bar{B} \quad .\end{aligned}\tag{A-1}$$

This decomposition is obviously not unique, because any potential flow can be used for  $\bar{A}$ . By imposing the additional condition,

$$\nabla \cdot \bar{B} = 0 \quad ,\tag{A-2}$$

one can show that a unique decomposition can be constructed, and the second vector,  $\bar{B}$ , can be given by a vector potential,  $\tilde{B}$ , (Aris, 1962):

$$\bar{B} = \nabla \times \tilde{B} \quad .\tag{A-3}$$

This vector potential will satisfy Poisson's equation,

$$\nabla^2 \tilde{B} = -\omega \quad ,\tag{A-4}$$

where  $\omega$  is the vorticity of the flow. This is the well-known Helmholtz's decomposition for incompressible flow.

Alternatively, one can write

$$\bar{v} = \bar{A} + \bar{B} \quad ,\tag{A-5}$$

$$\bar{A} = \nabla\phi \quad ,\tag{A-6}$$

$$\bar{B} = \nabla \times \tilde{B} \quad .\tag{A-7}$$

If the vortical component  $\tilde{\mathbf{B}}$  is restricted to be in the plane perpendicular to the vorticity vector itself, namely,

$$\tilde{\mathbf{B}} \cdot \nabla \times \tilde{\mathbf{B}} = 0 \quad , \quad (\text{A-8})$$

then it can be represented by two scalar functions,

$$\tilde{\mathbf{B}} = \psi \nabla \chi \quad .$$

Such a vector was termed complex lamellar by Lord Kelvin (Truesdell, 1954).

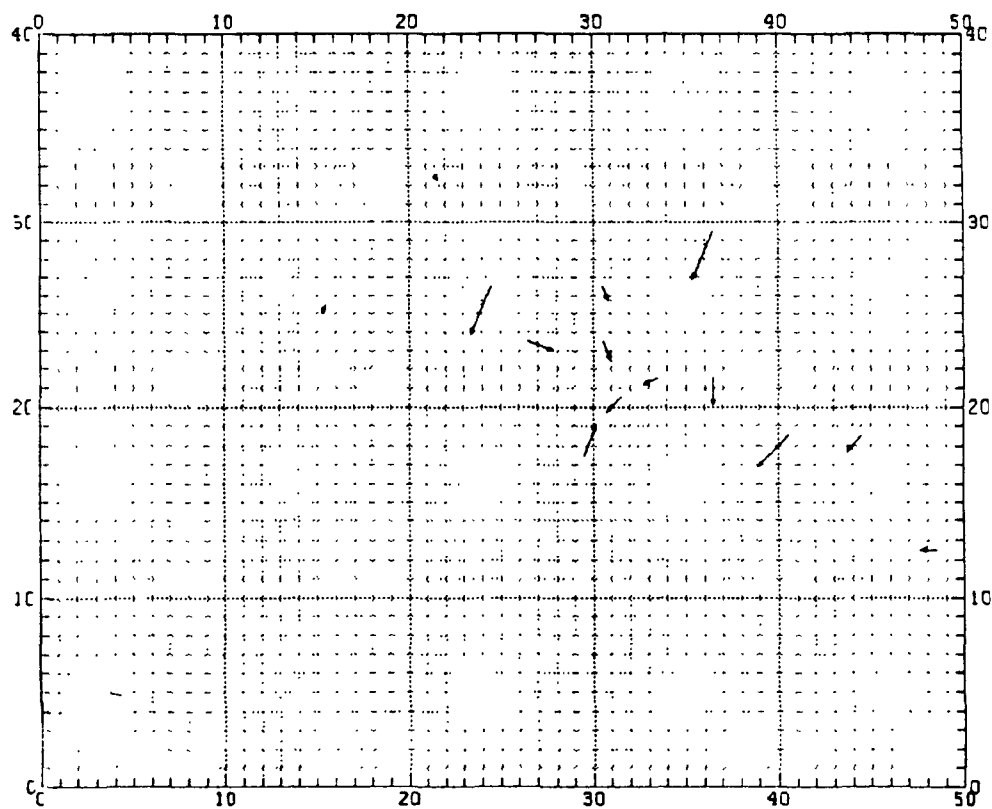
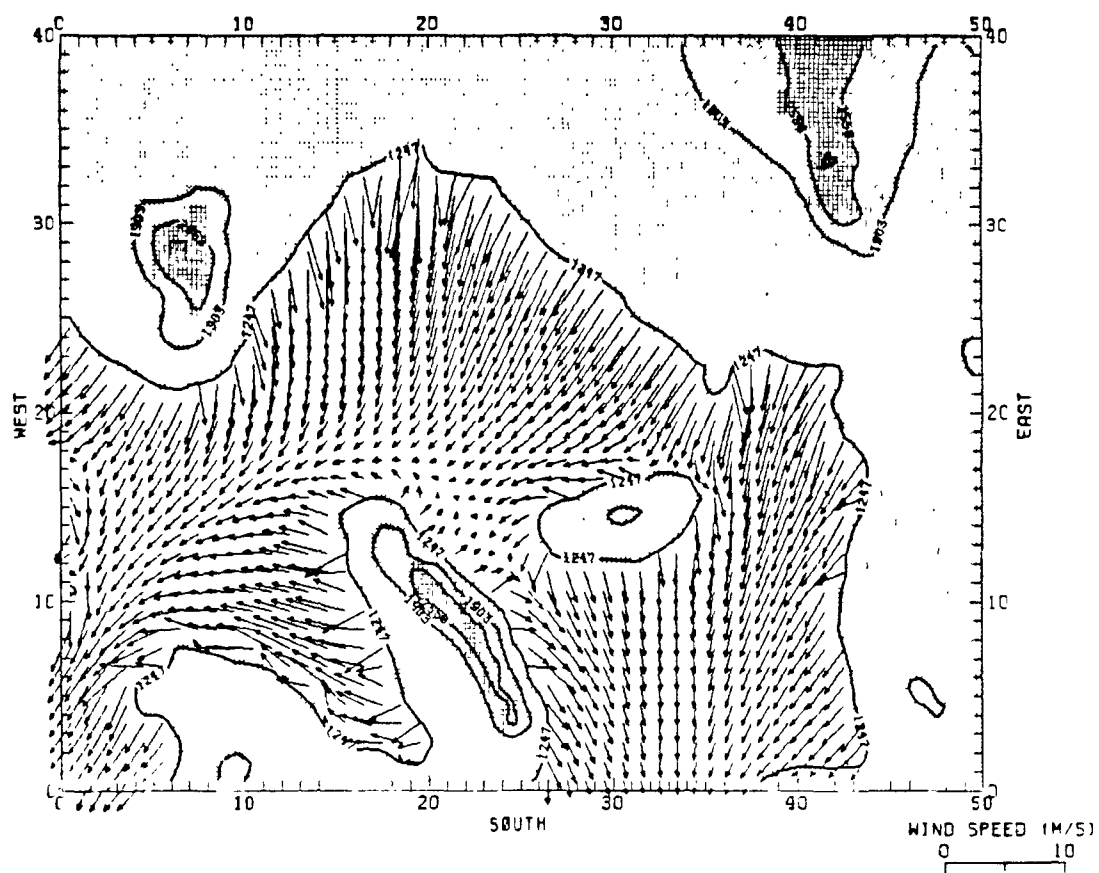
APPENDIX B  
COMPARISON OF PREDICTED AND MEASURED  
SURFACE WINDS IN PHOENIX



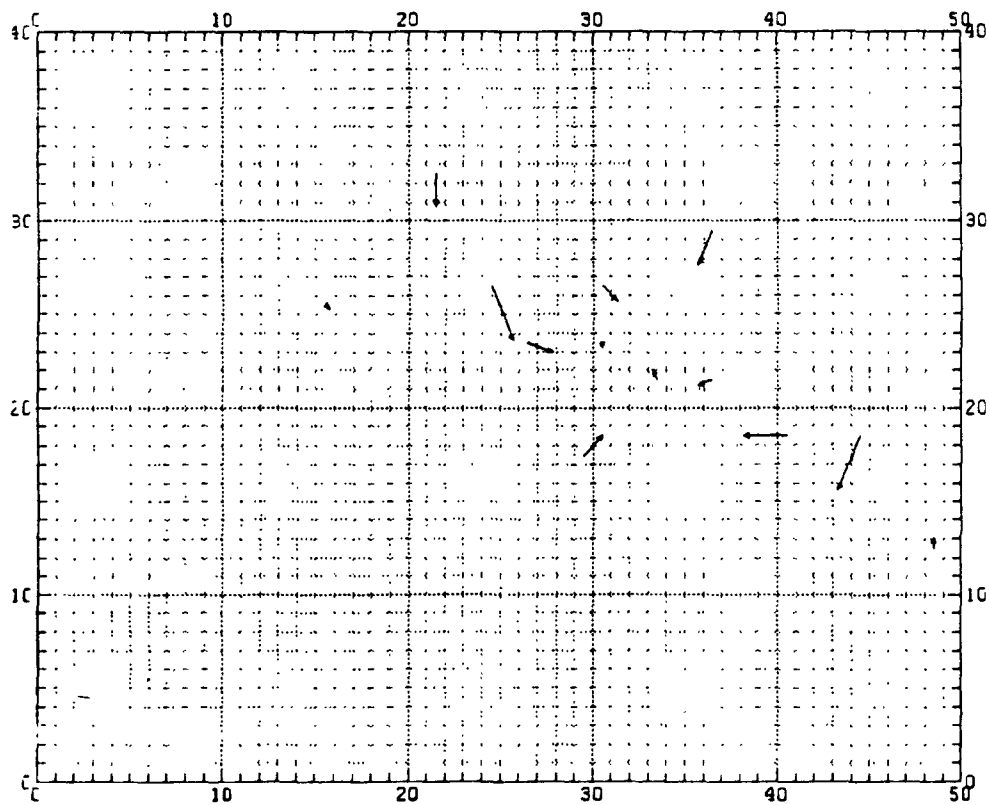
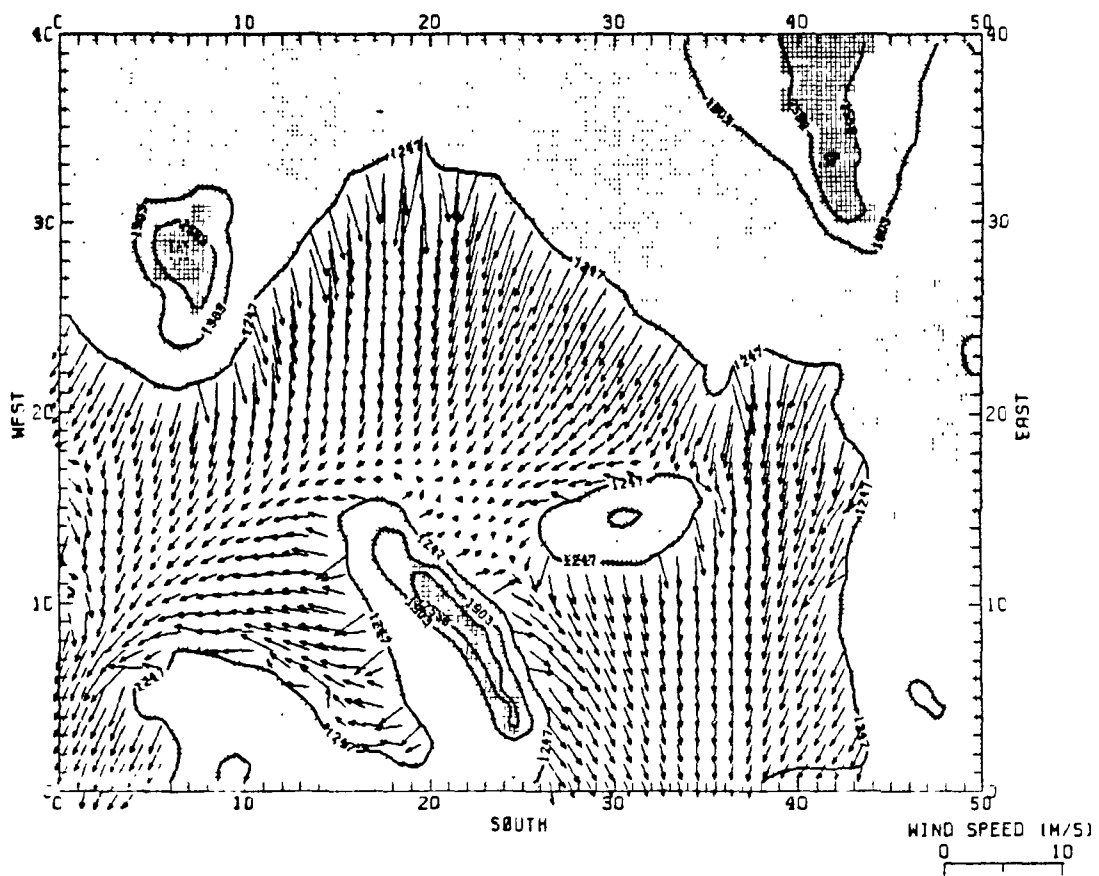
APPENDIX B  
COMPARISON OF PREDICTED AND MEASURED  
SURFACE WINDS IN PHOENIX

This appendix presents a comparison of the predicted and measured surface winds in Phoenix every second hour for the four test days in 1977: 15 and 16 February and 7 and 10 March 1977. Each pair of comparisons shows the predictions on the top of the page and the corresponding measurements on the bottom labeled in mountain standard time (MST).

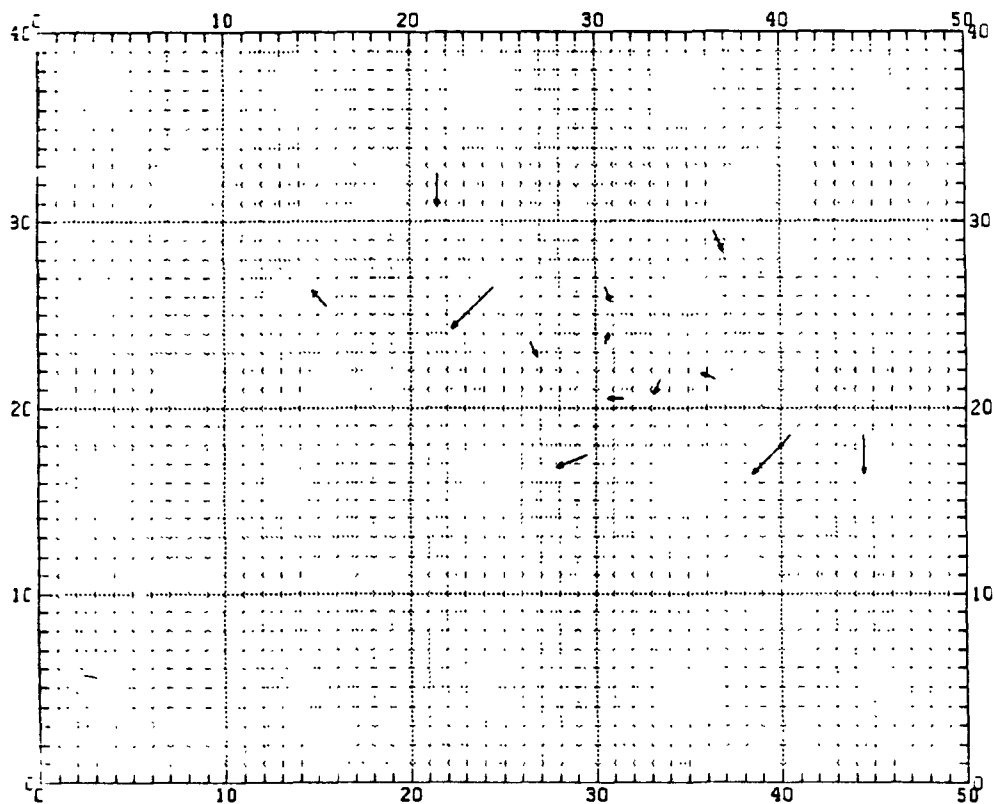
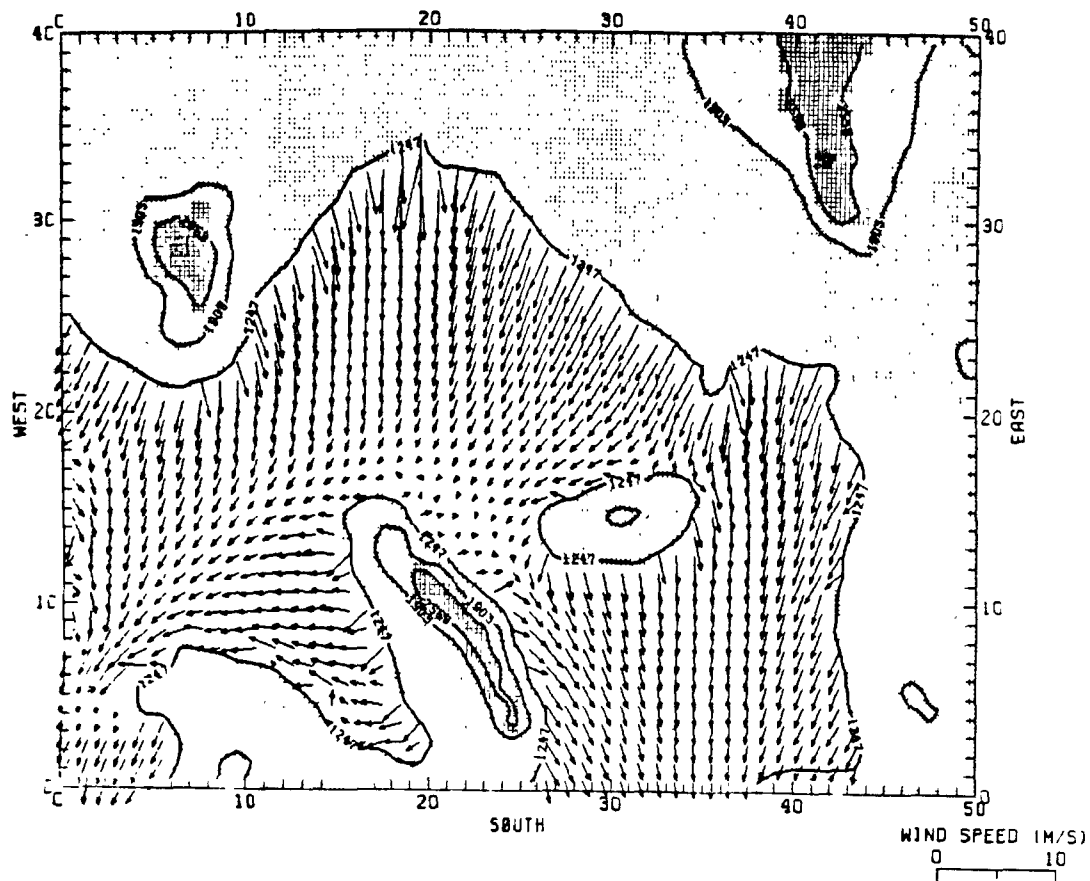
PART 1--15 FEBRUARY 1977



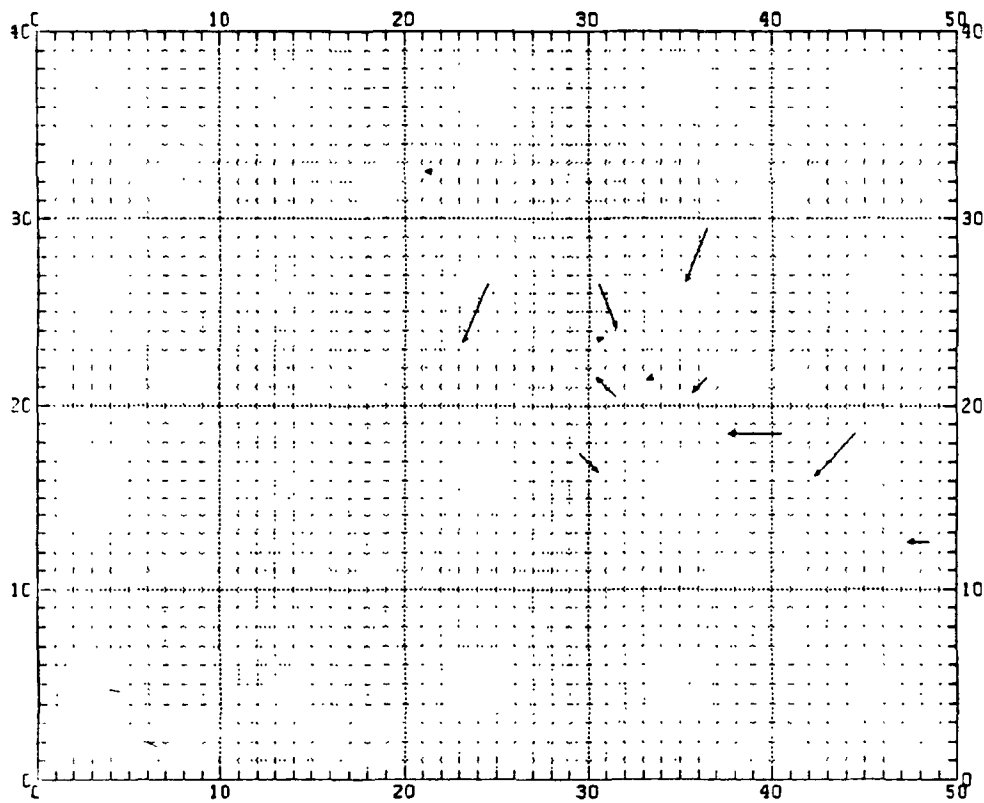
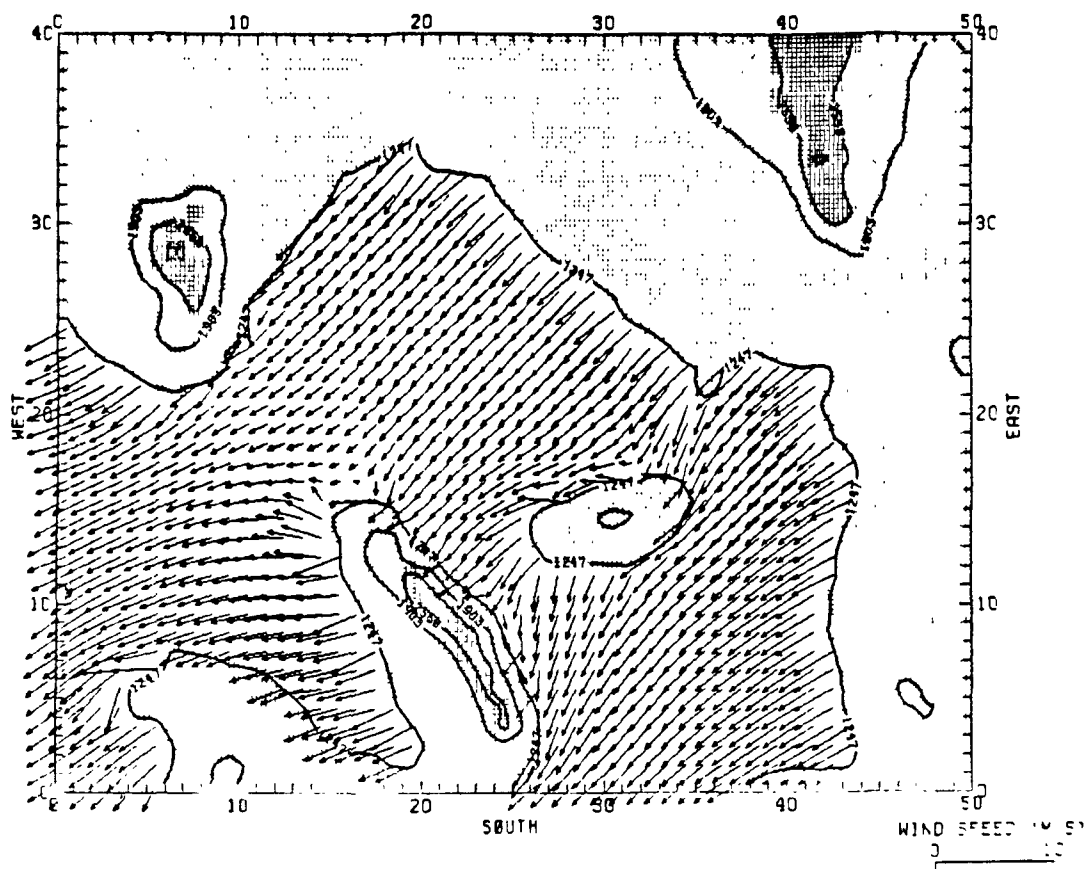
0000 MST

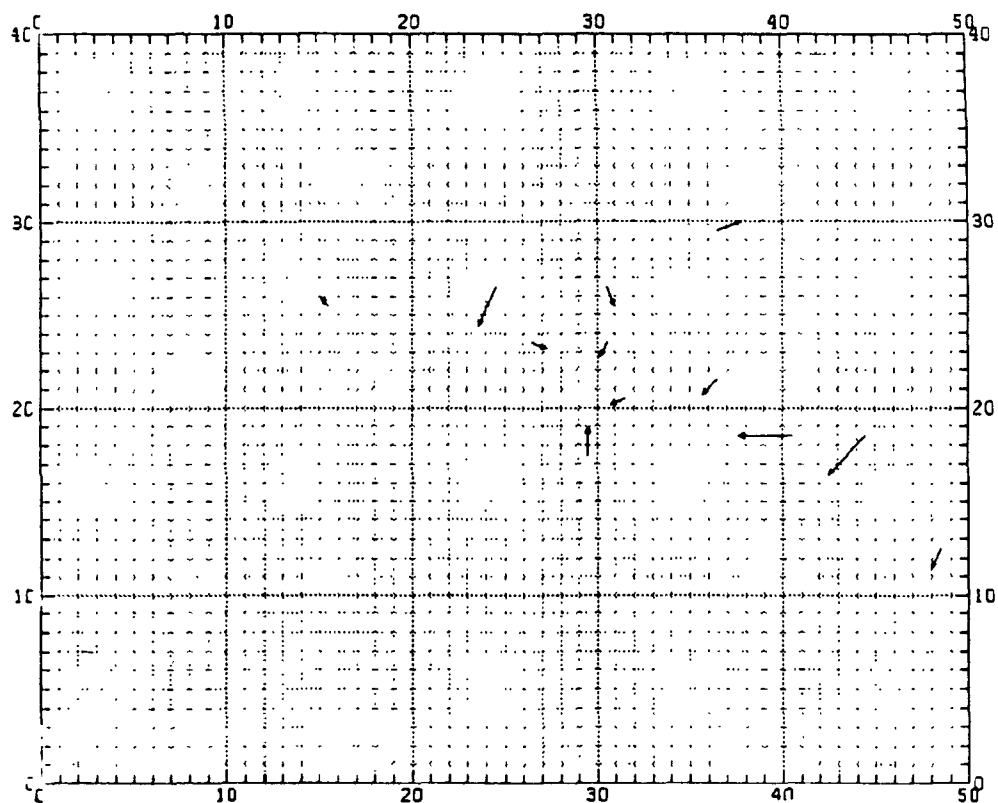
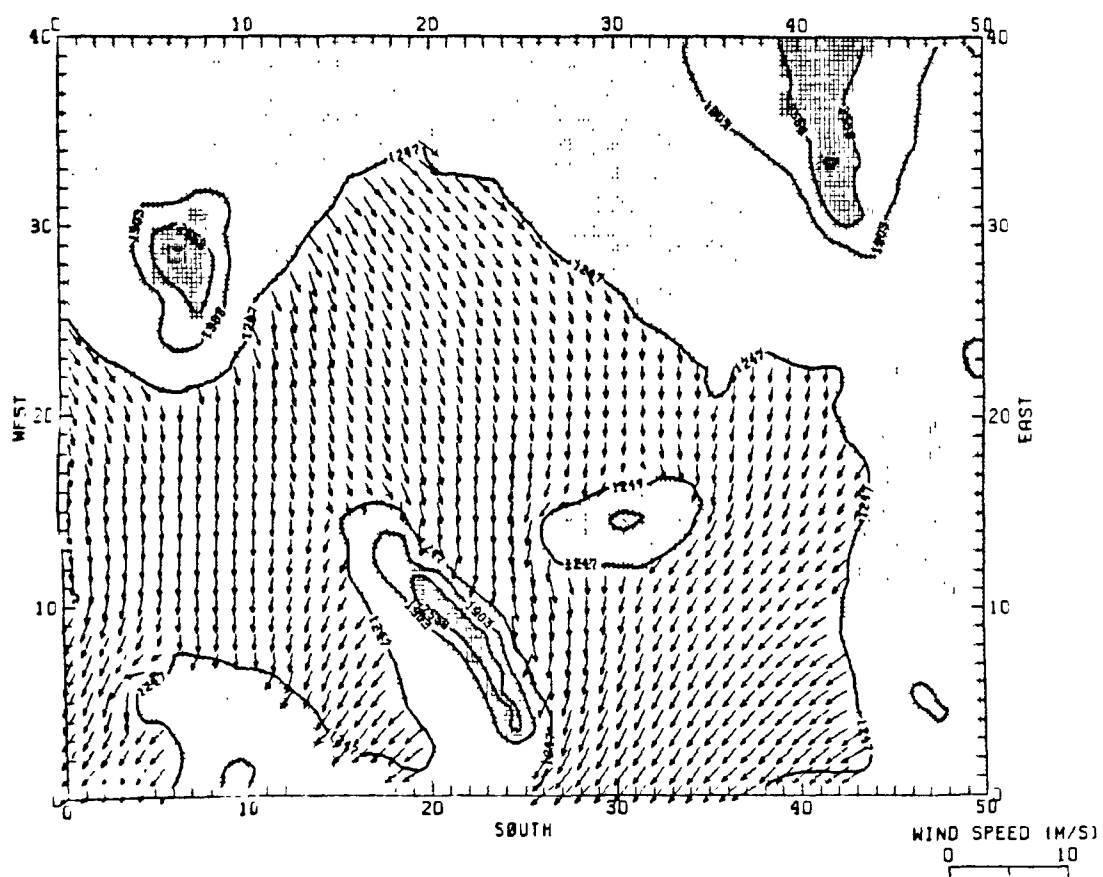


0200 MST

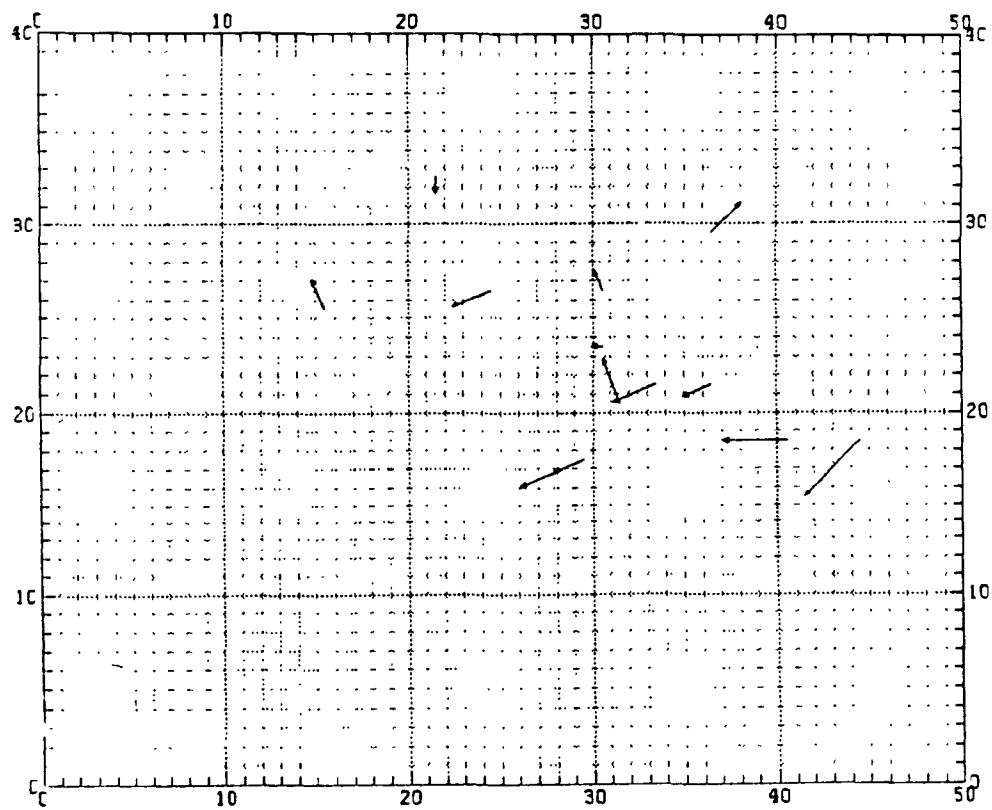
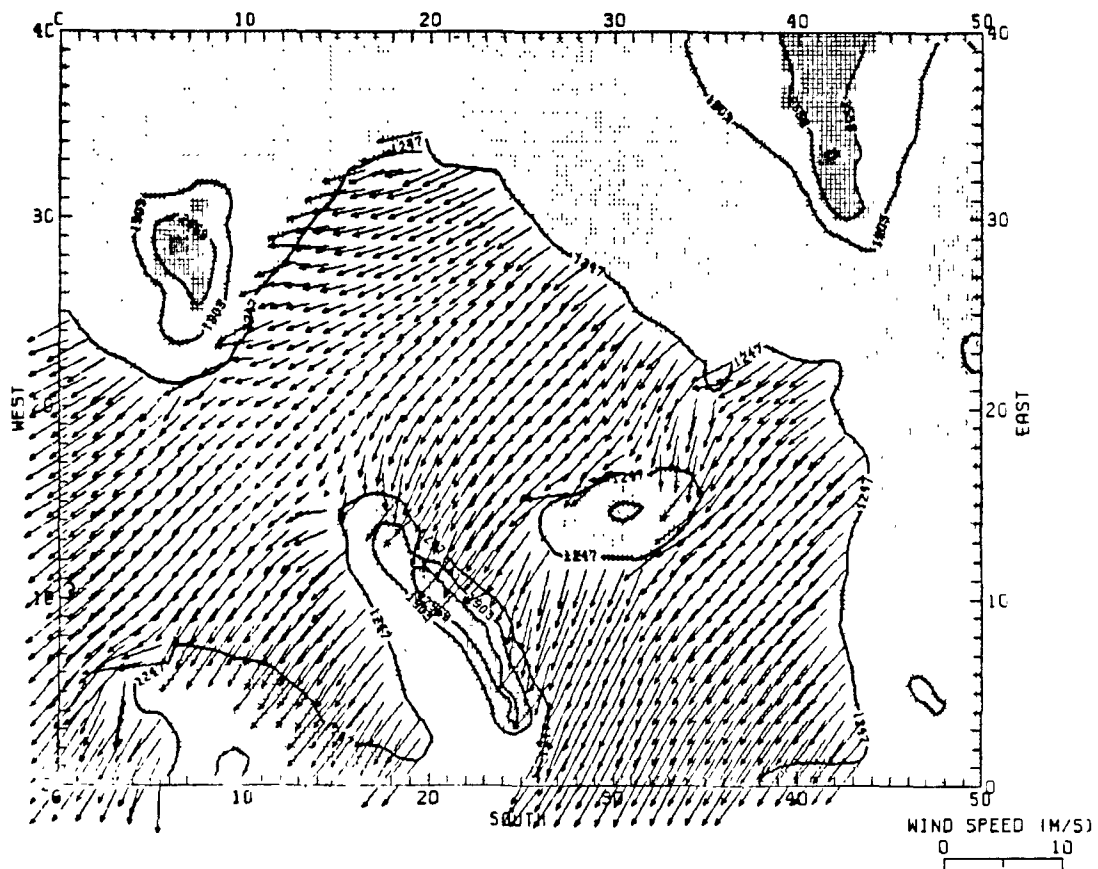


0400 MST

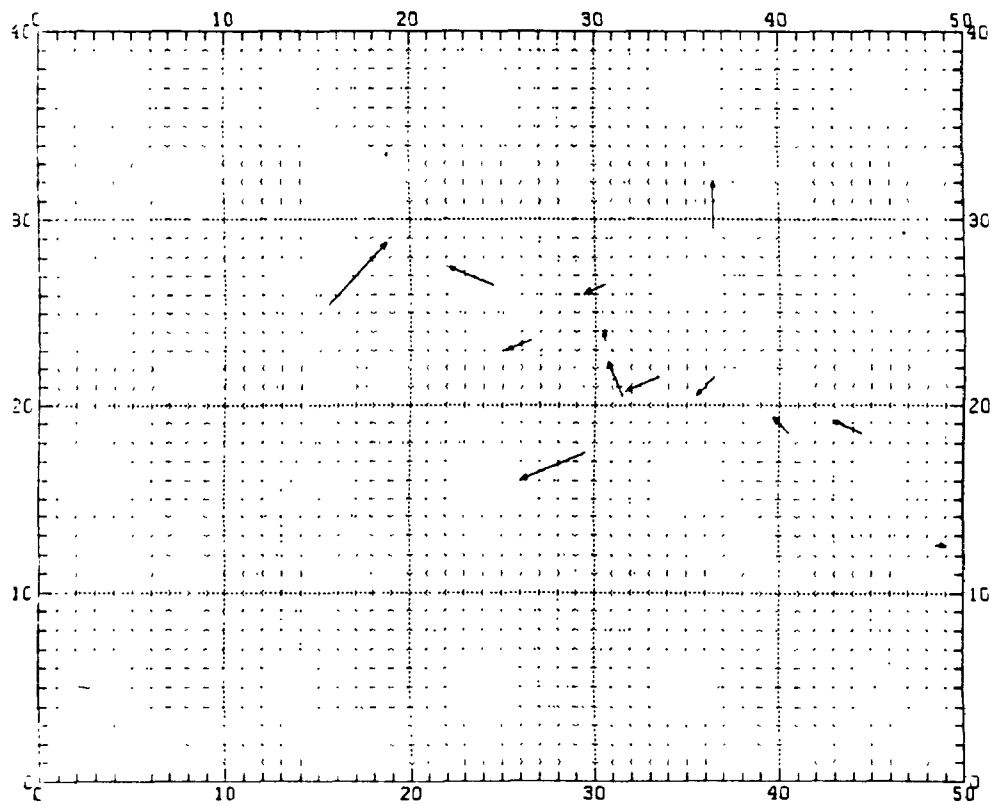
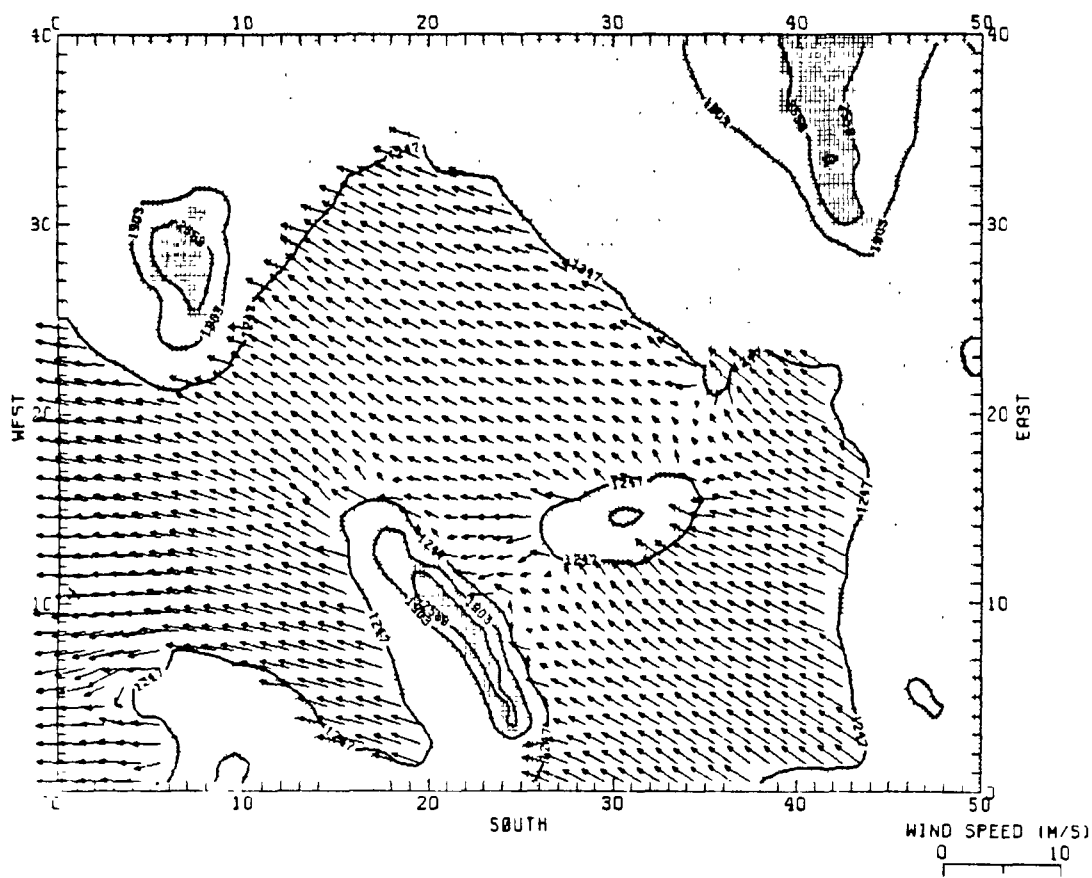




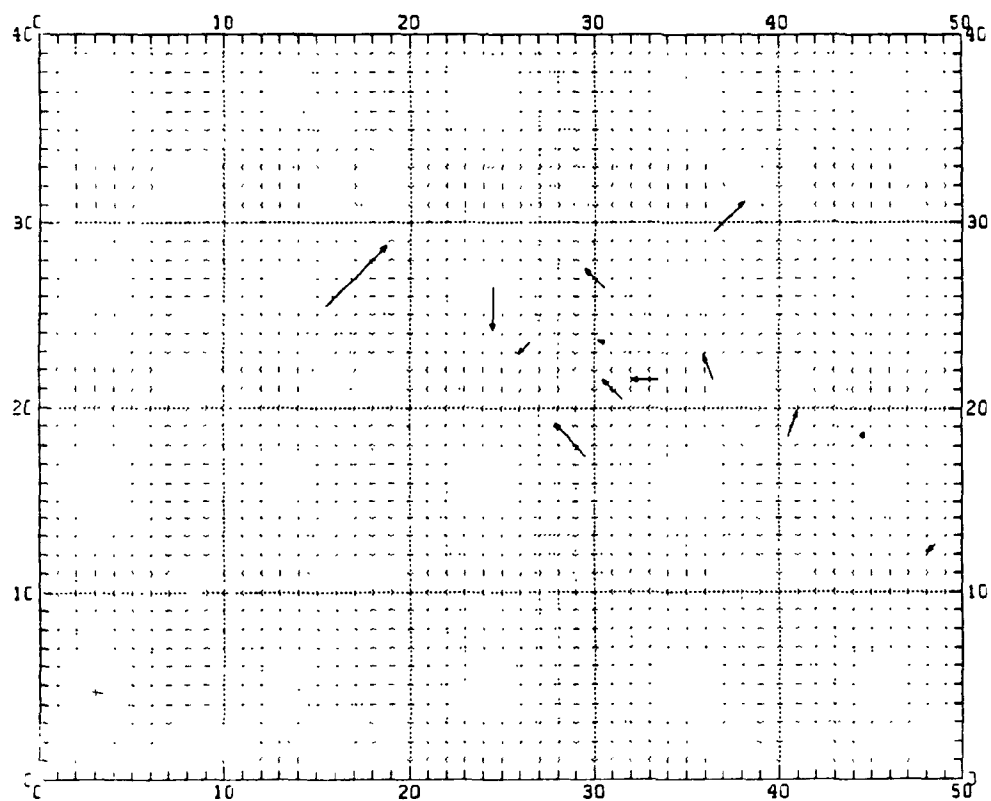
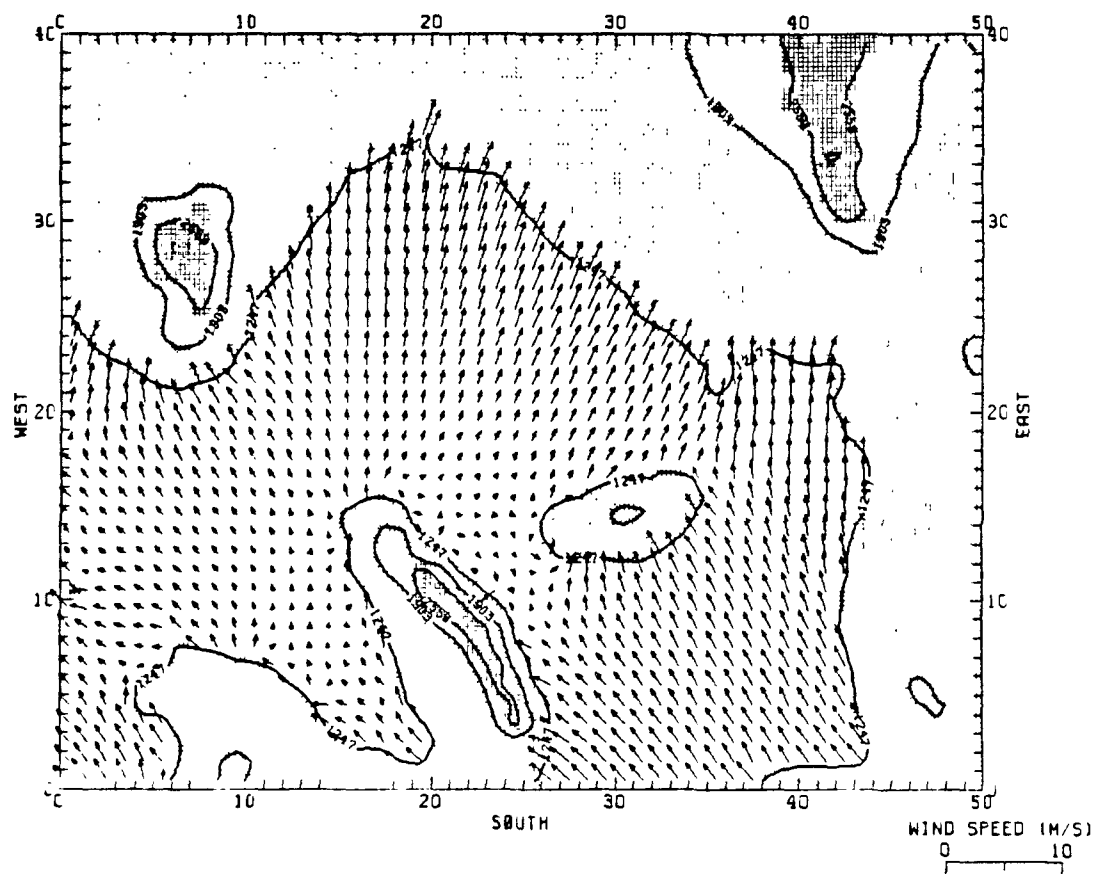
0800 MST



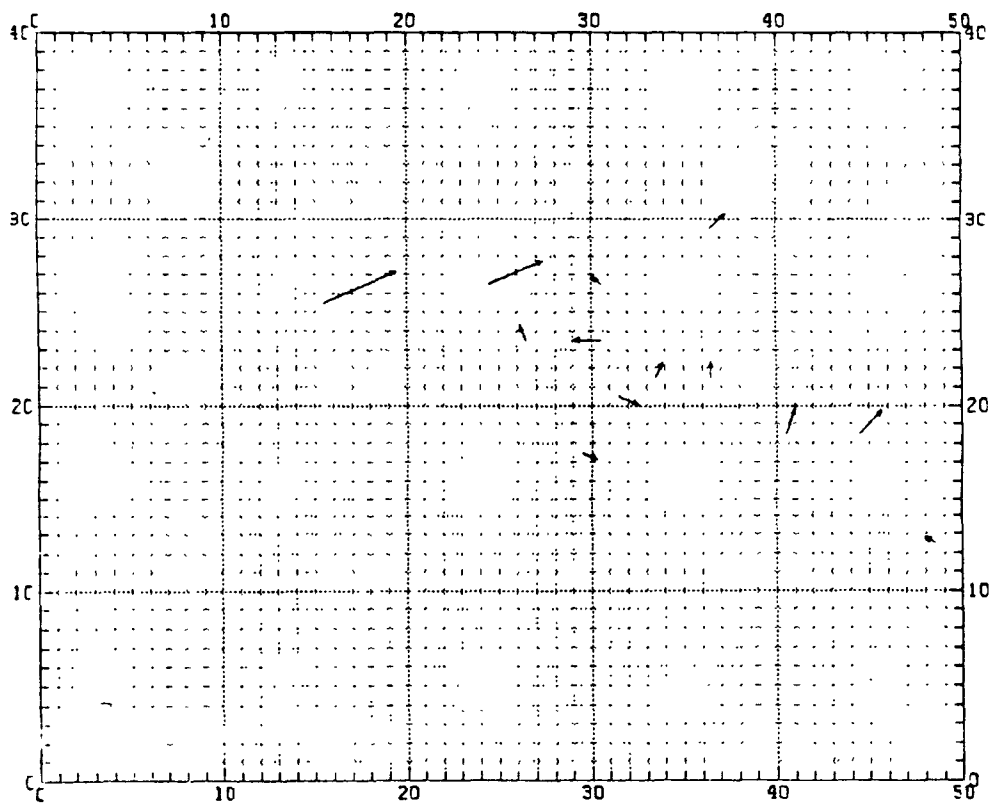
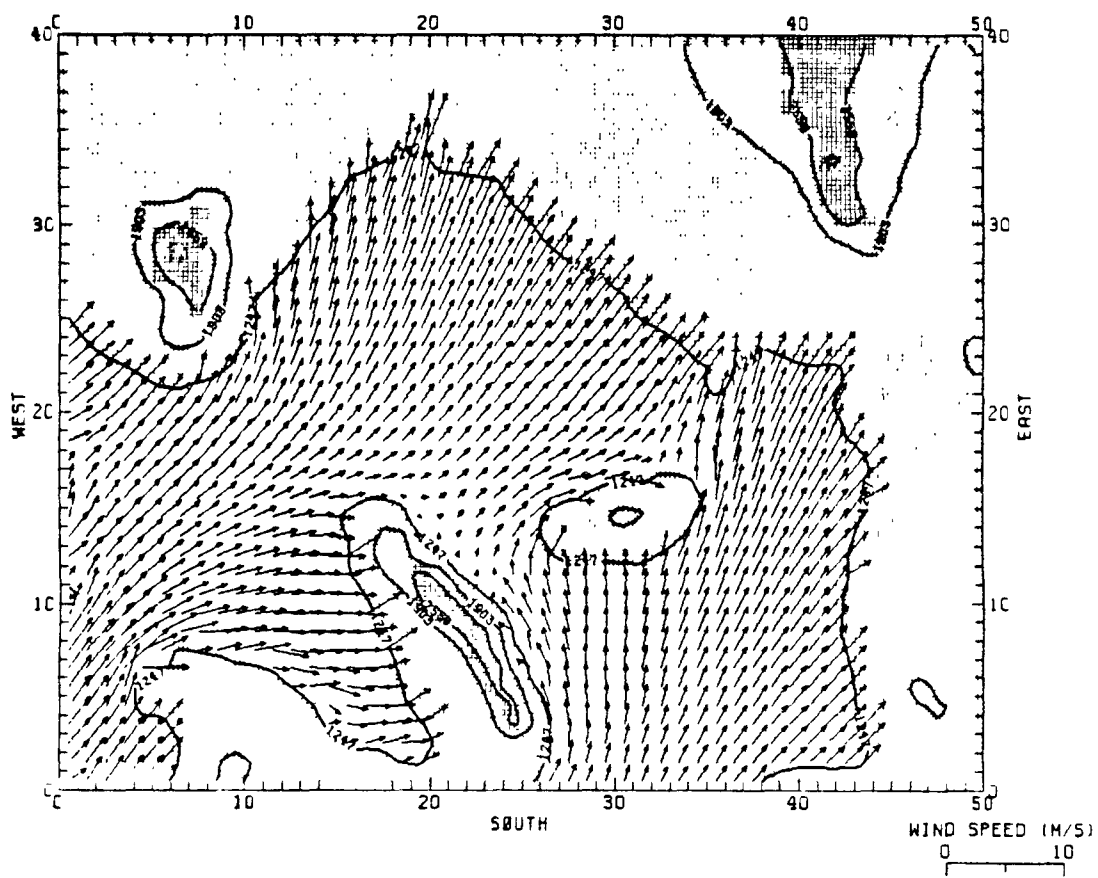


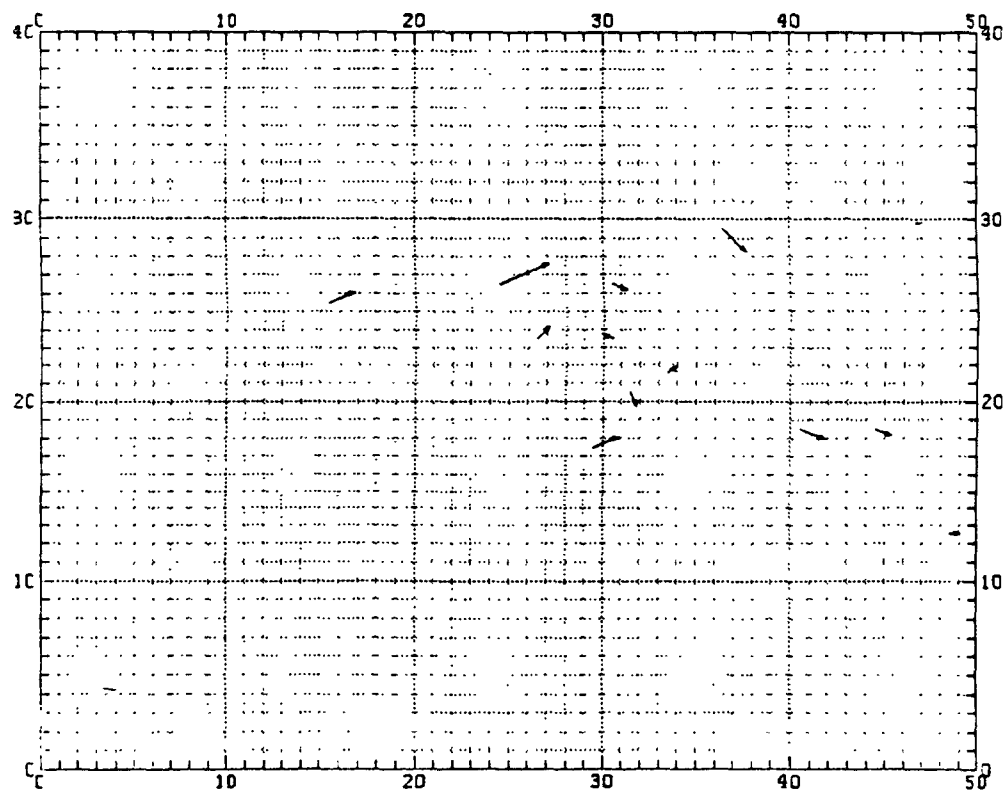
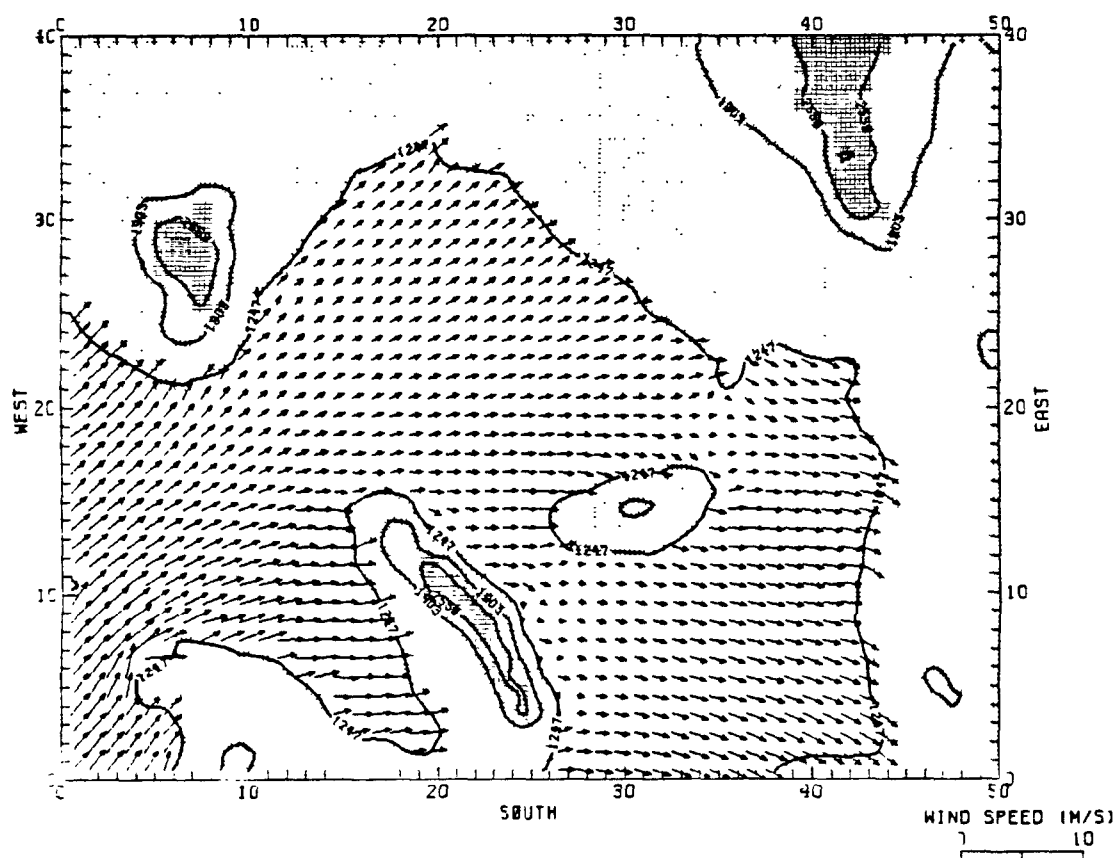


1200 MST

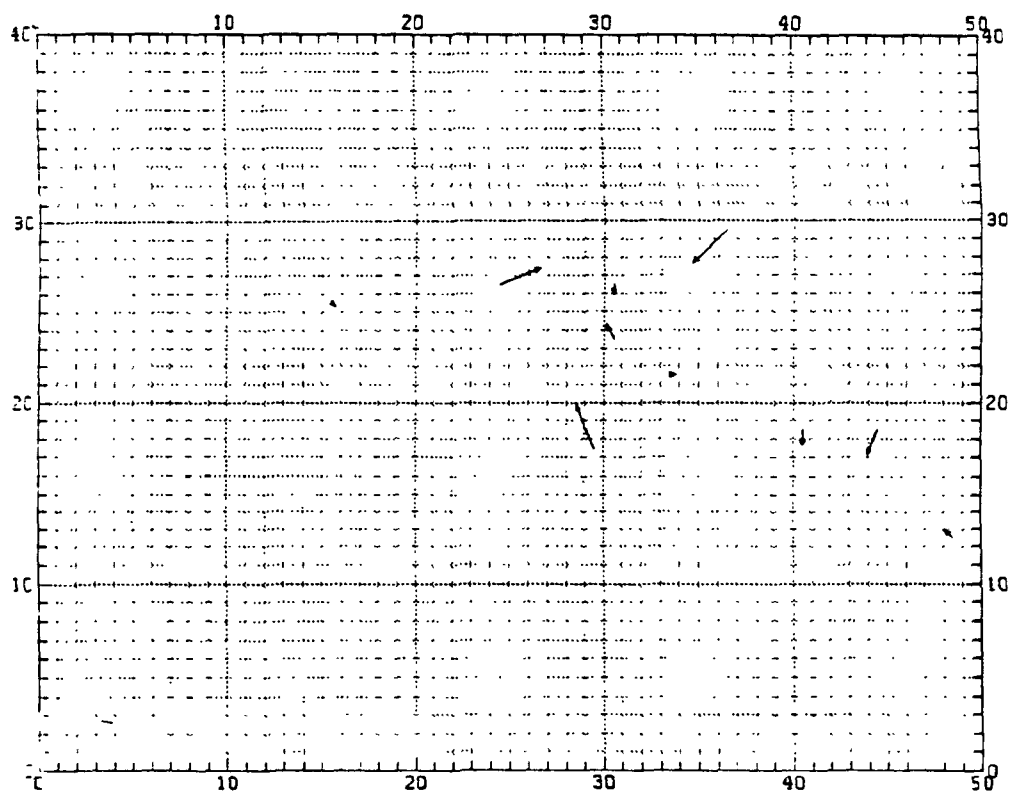
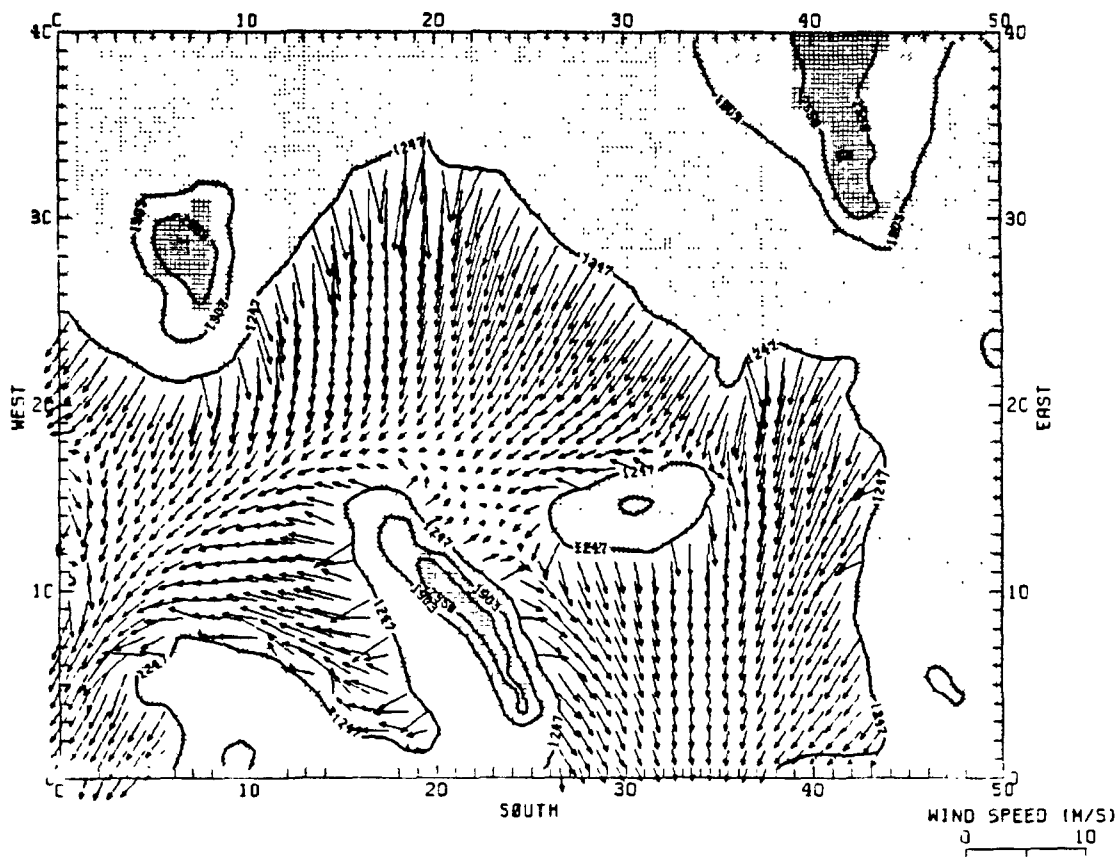


1400 MST

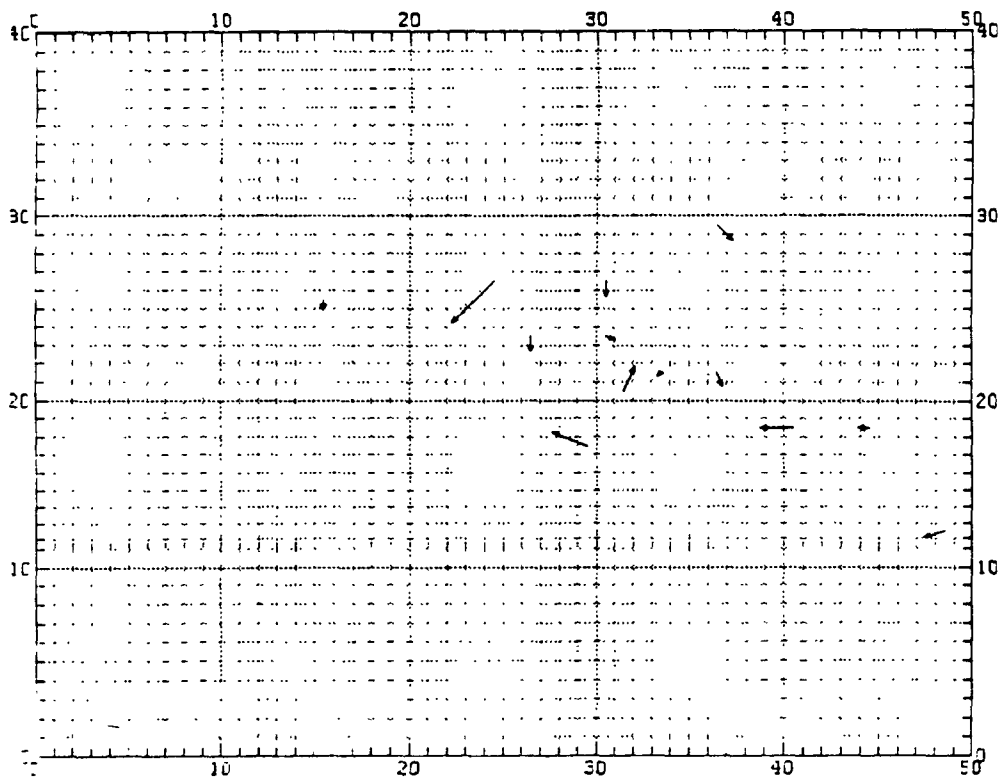
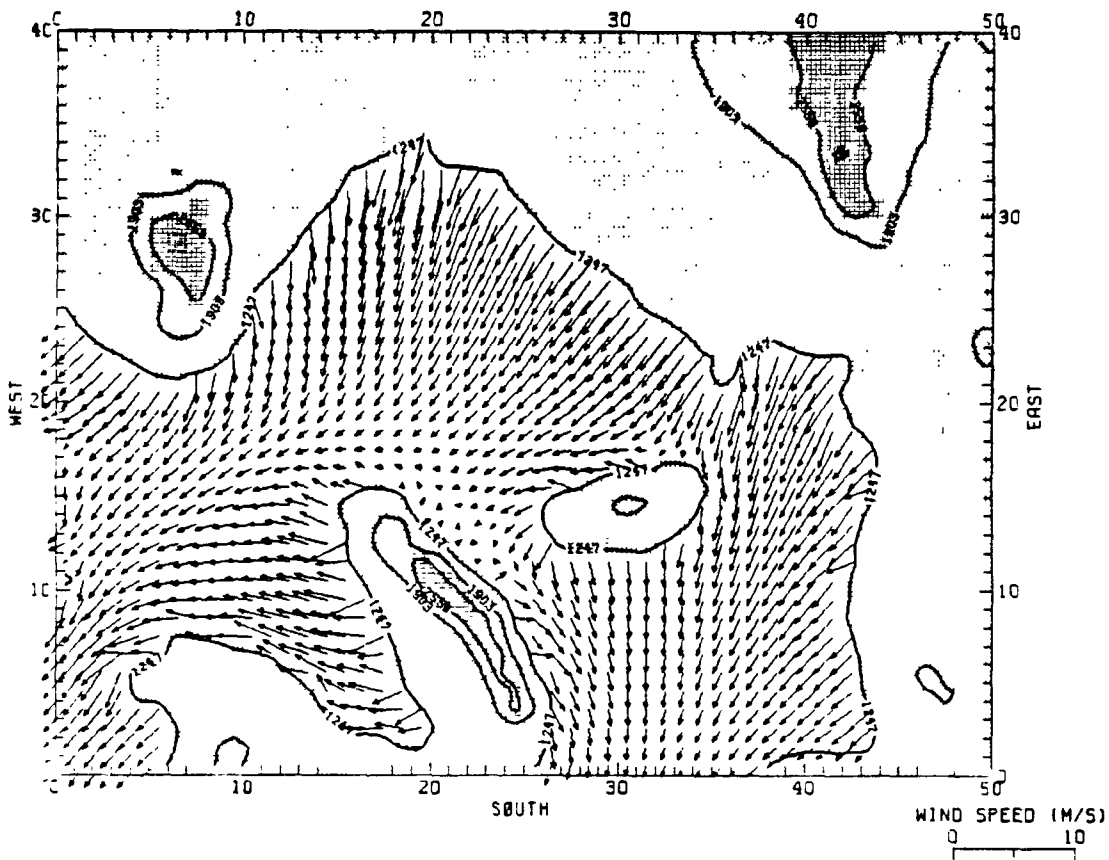




1800 MST

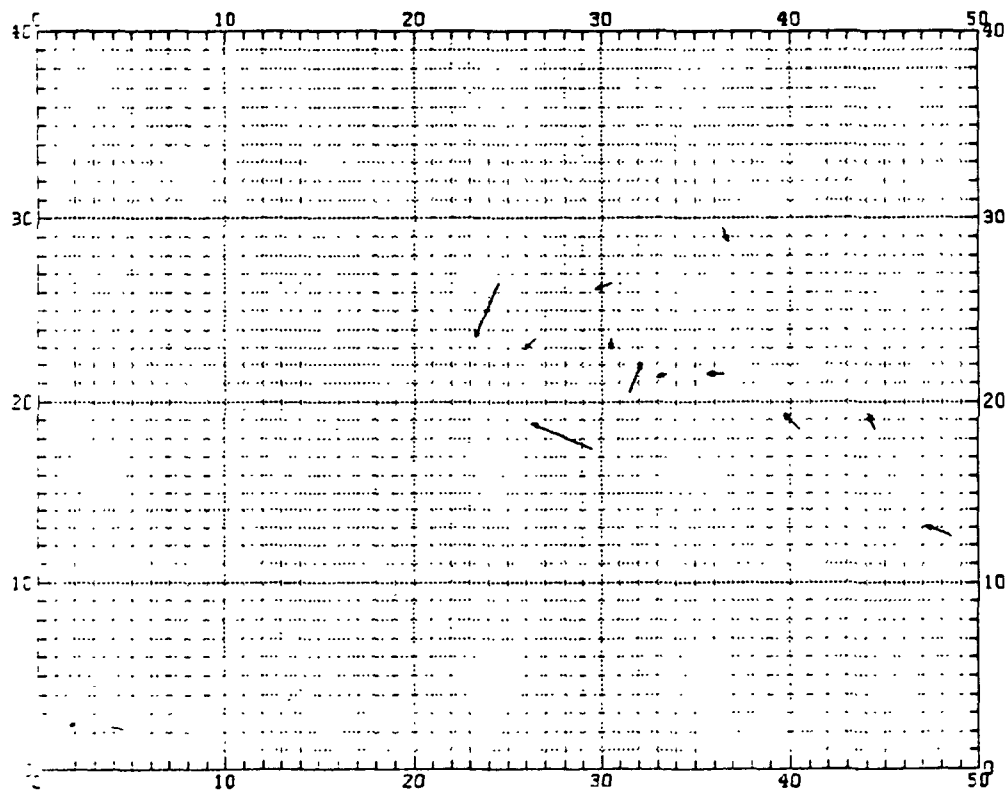
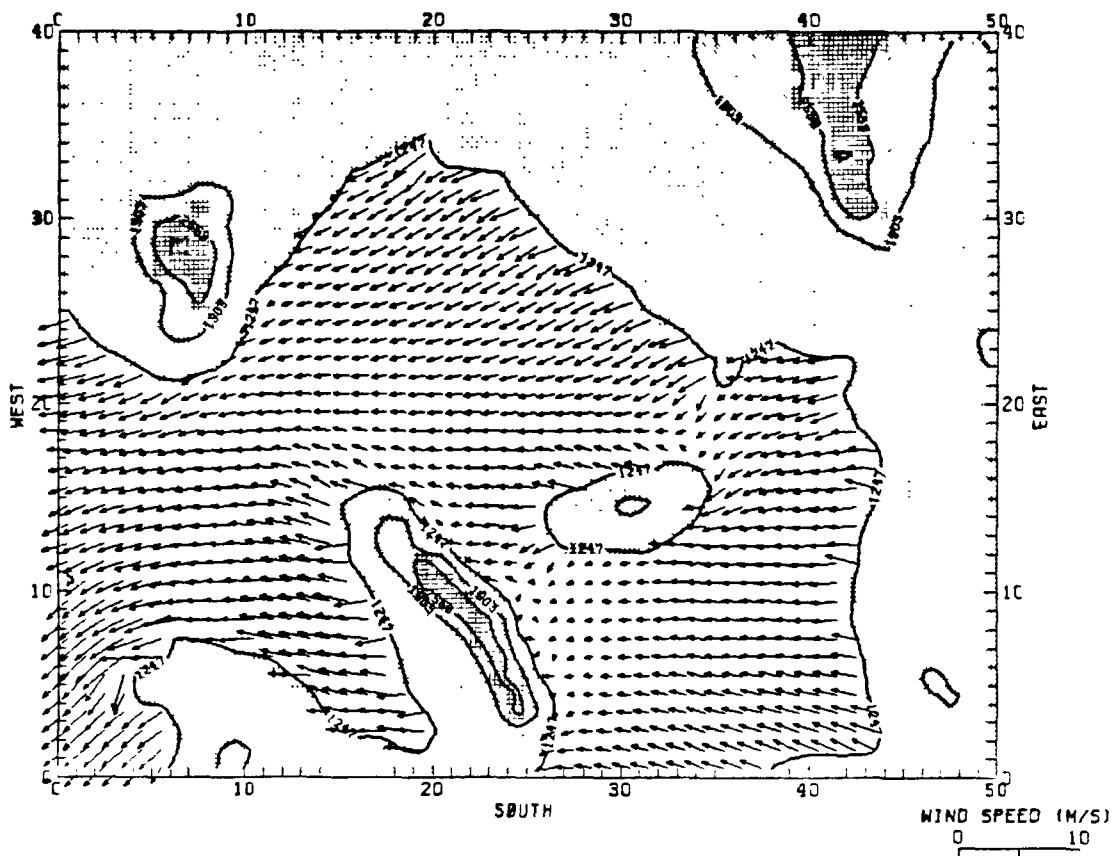


2000 MST



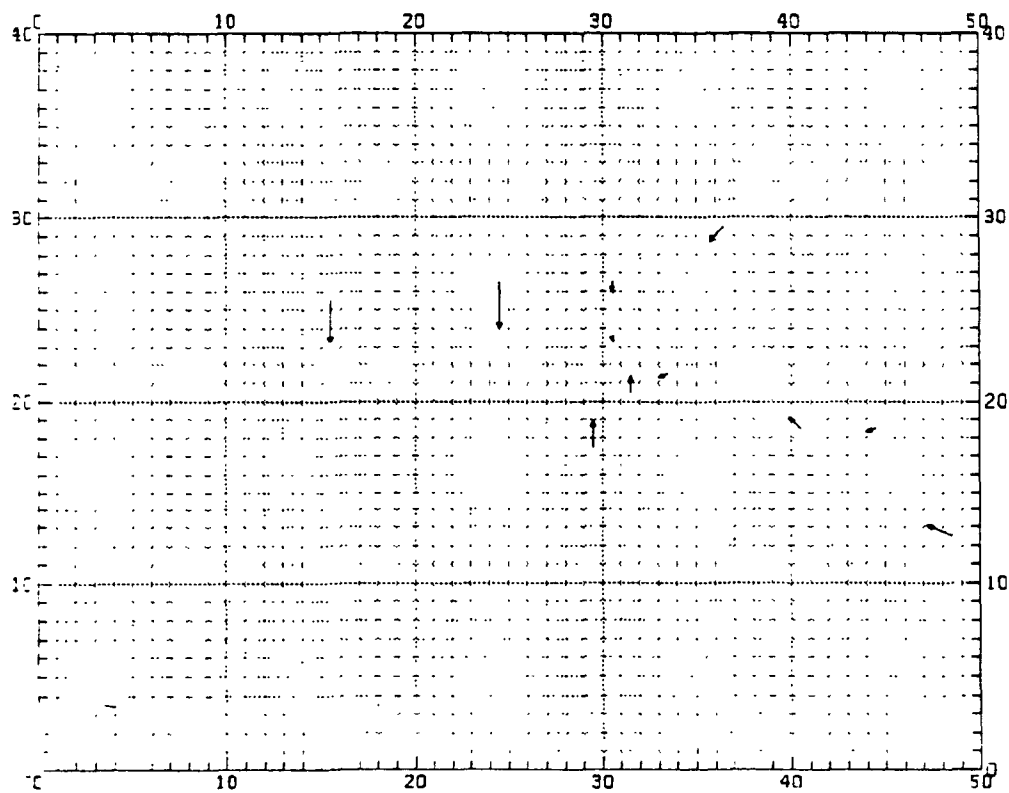
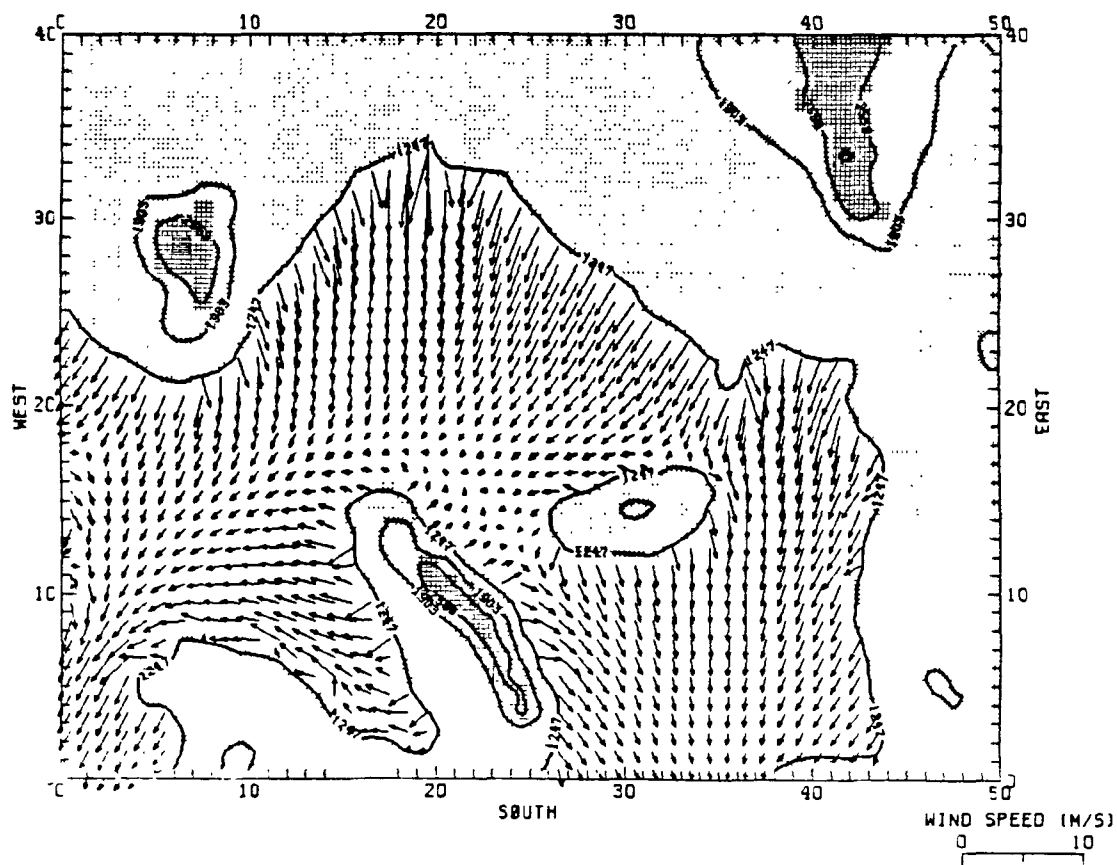
2200 MST

PART 2--16 FEBRUARY 1977

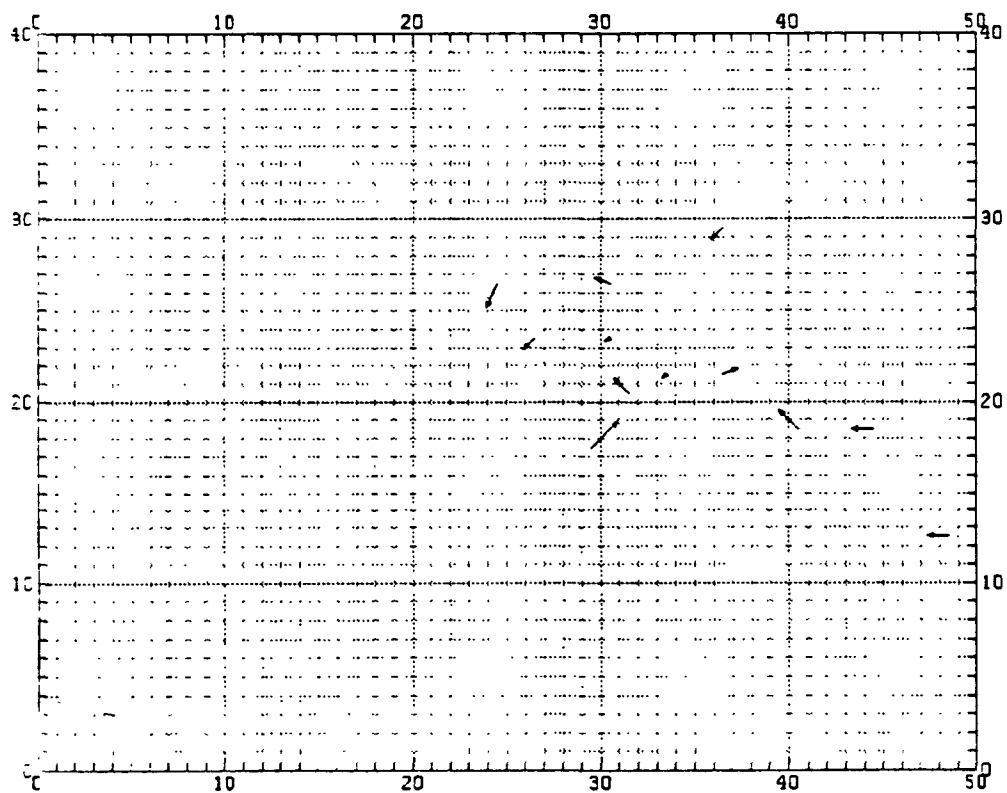
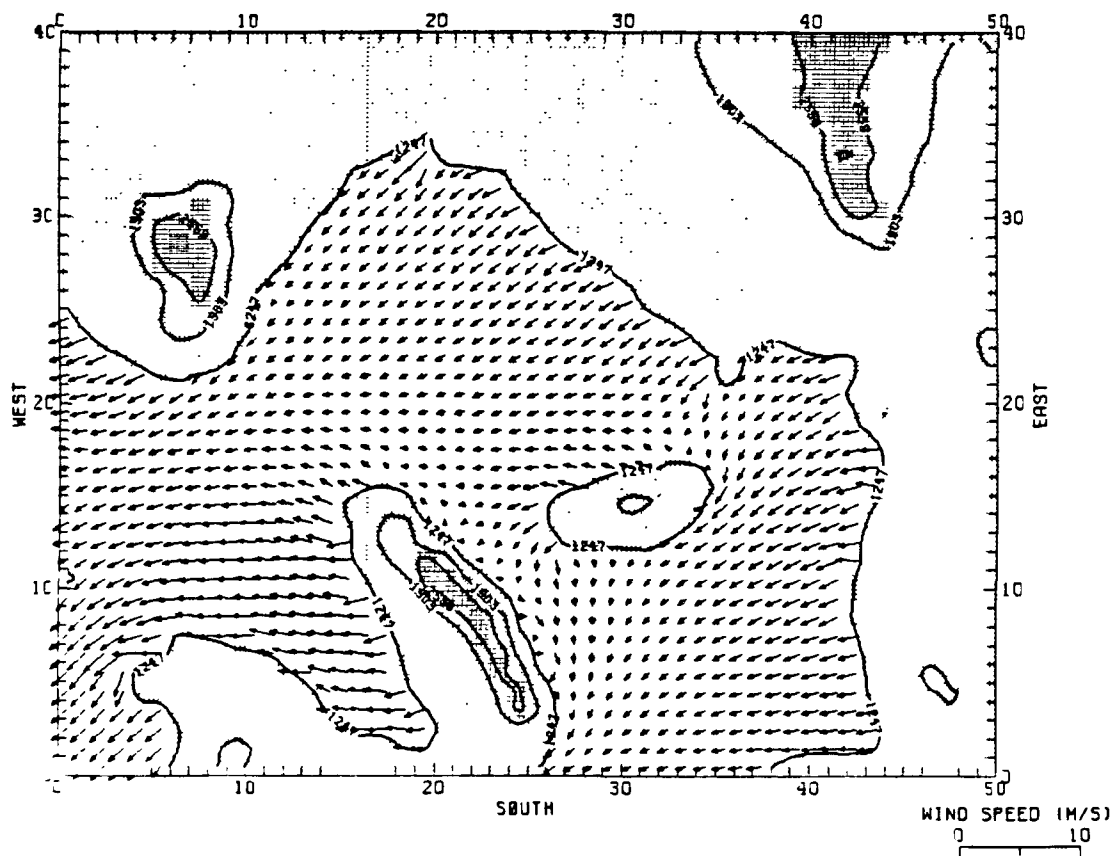


0000 MST

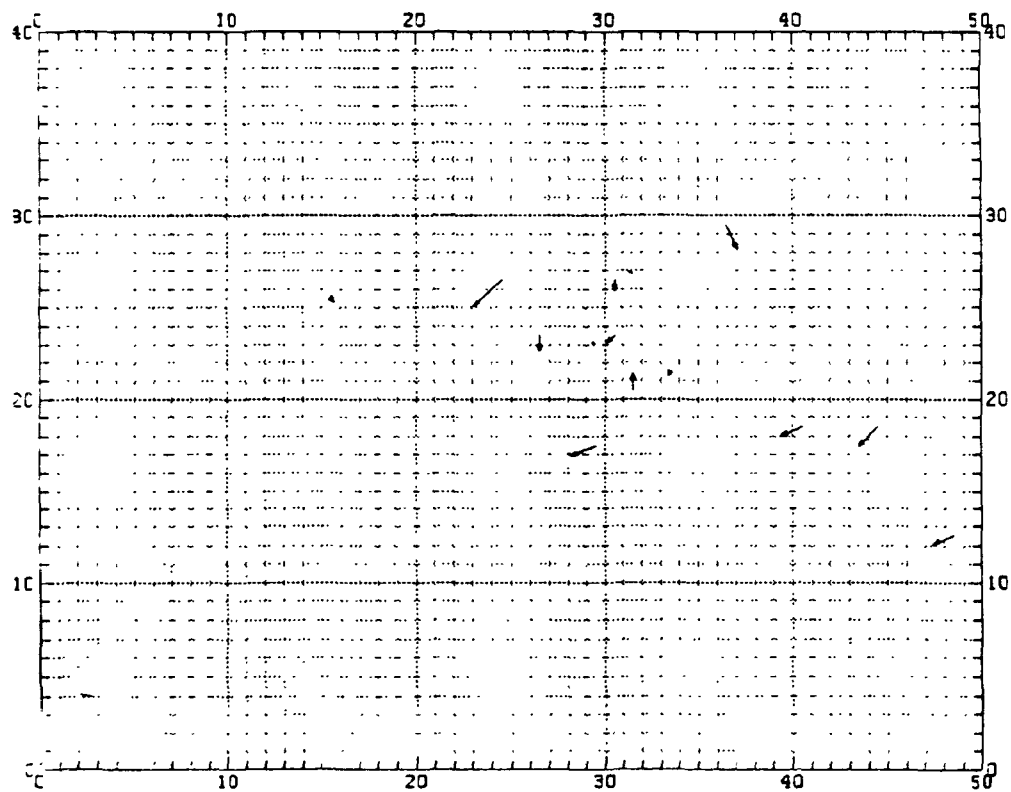
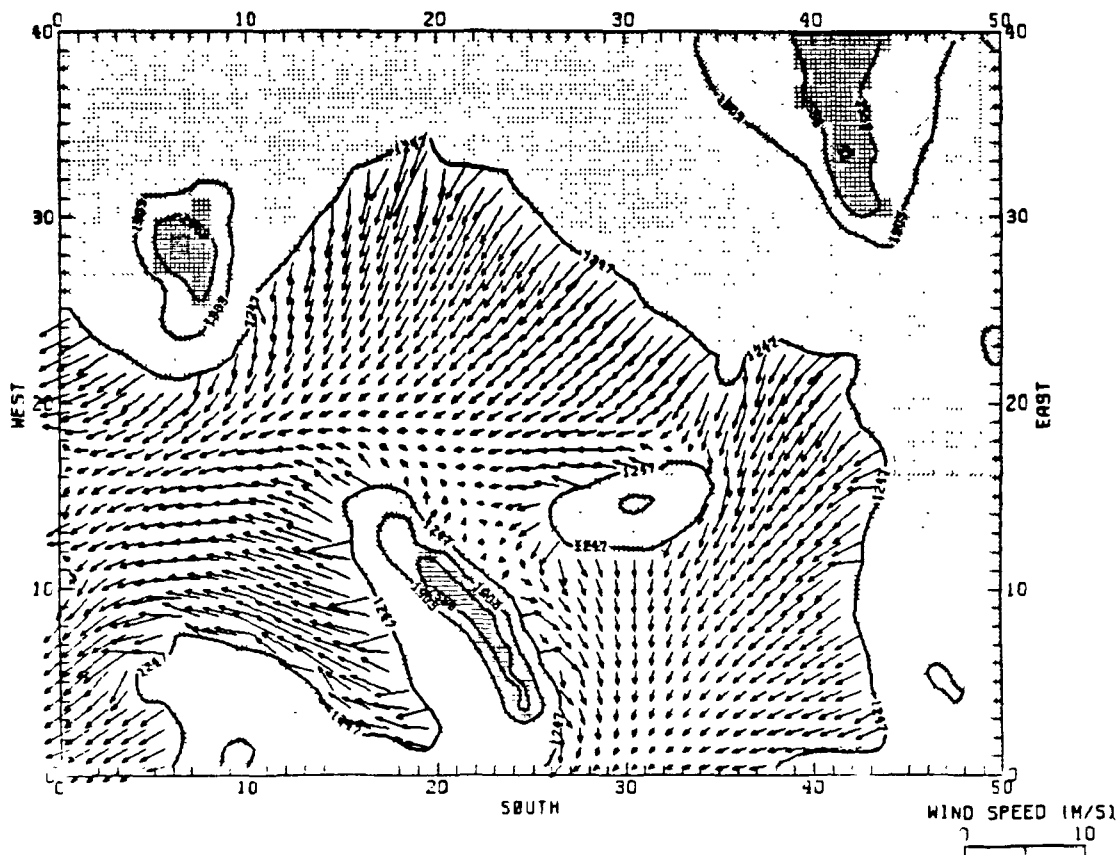




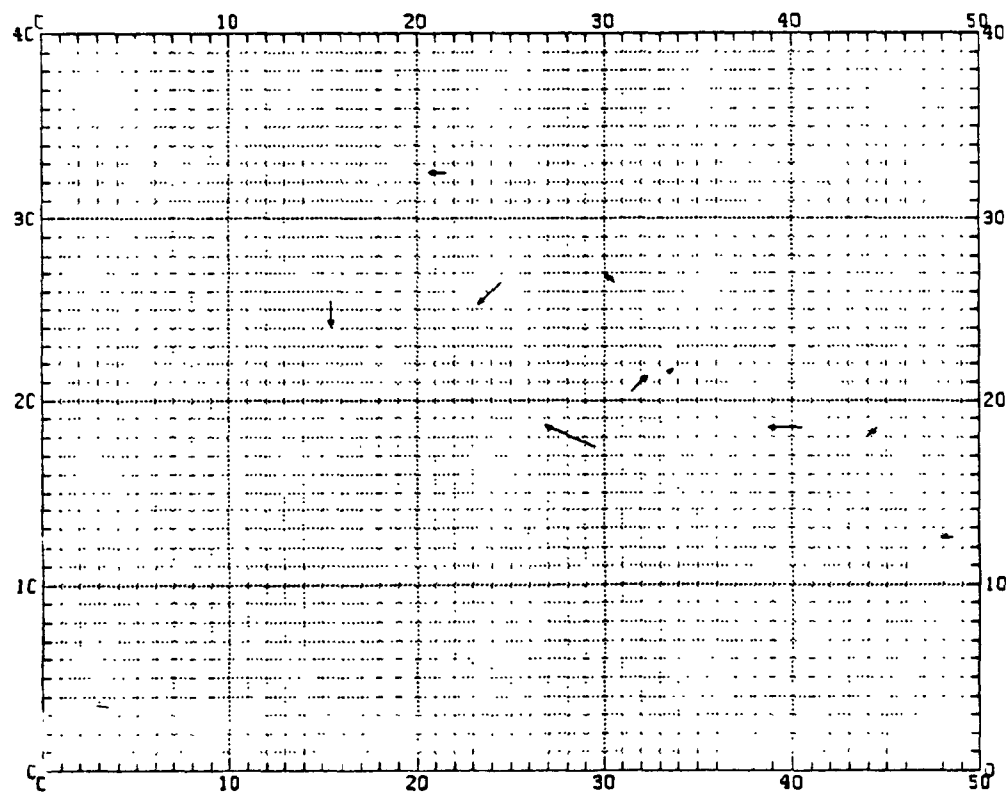
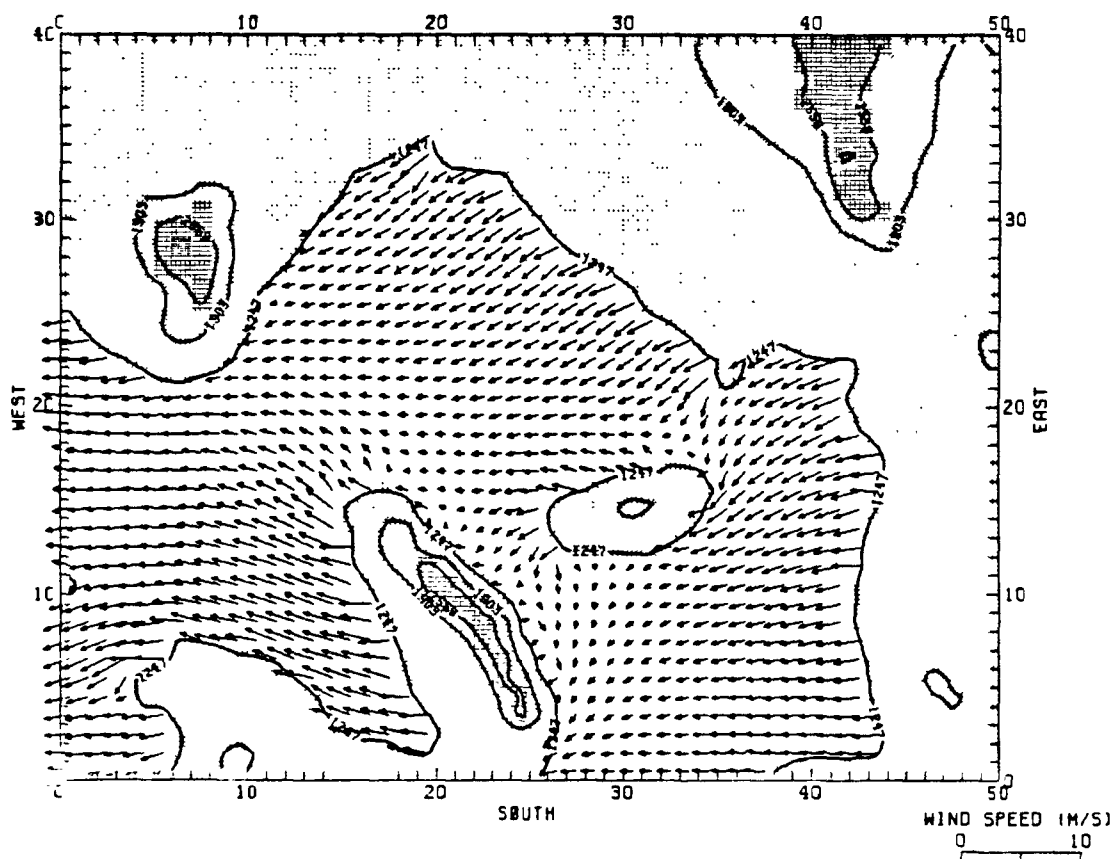
0200 MST



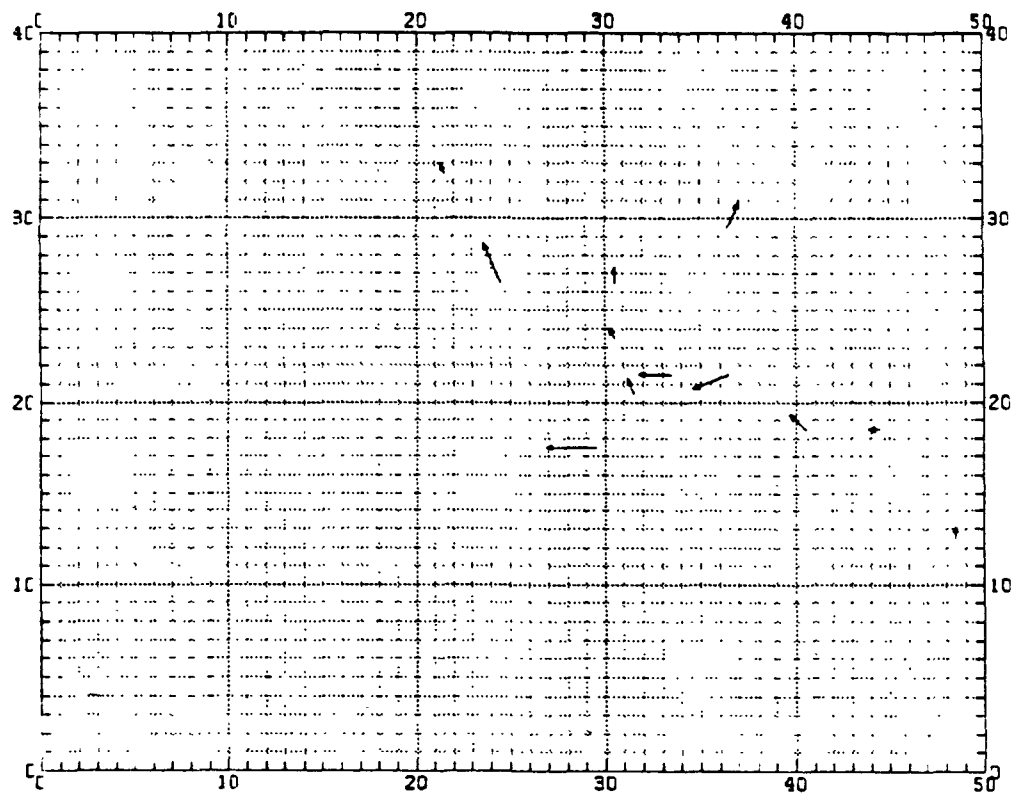
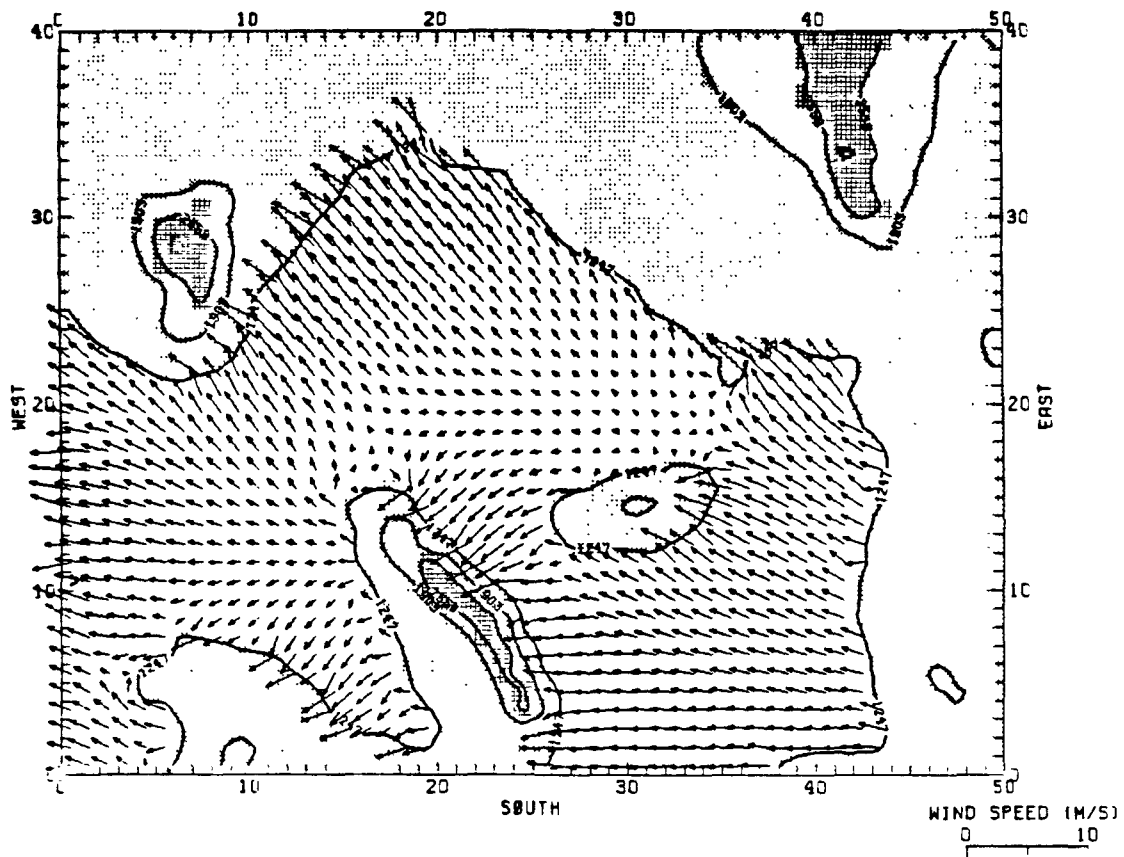
0400 MST



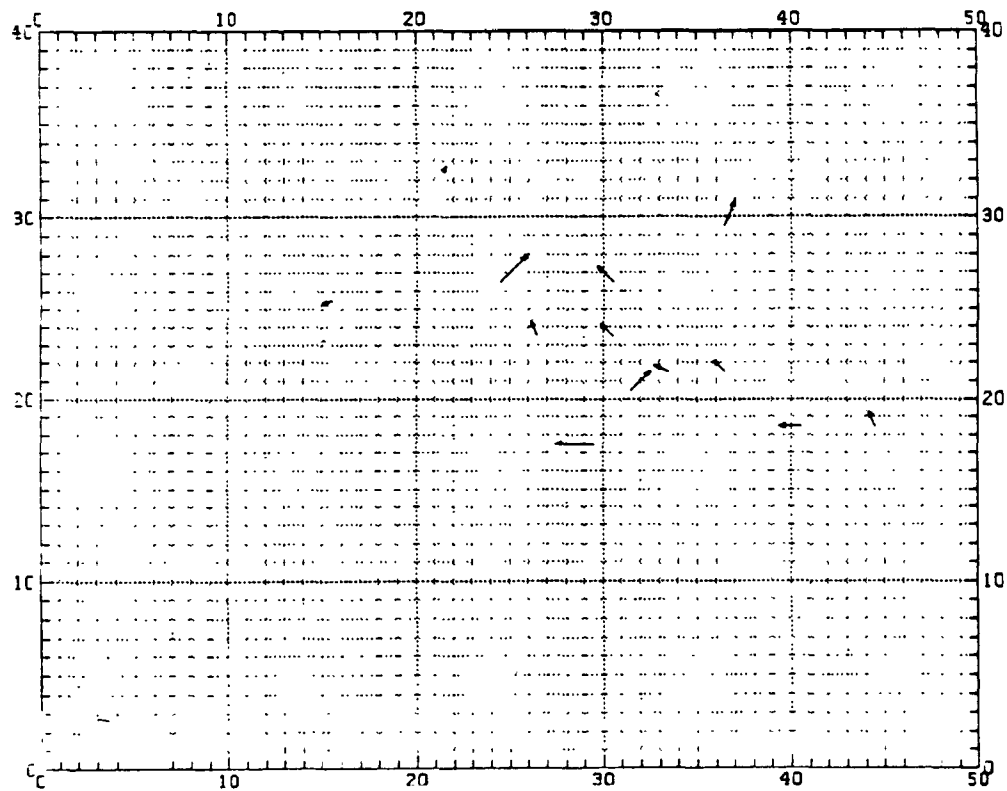
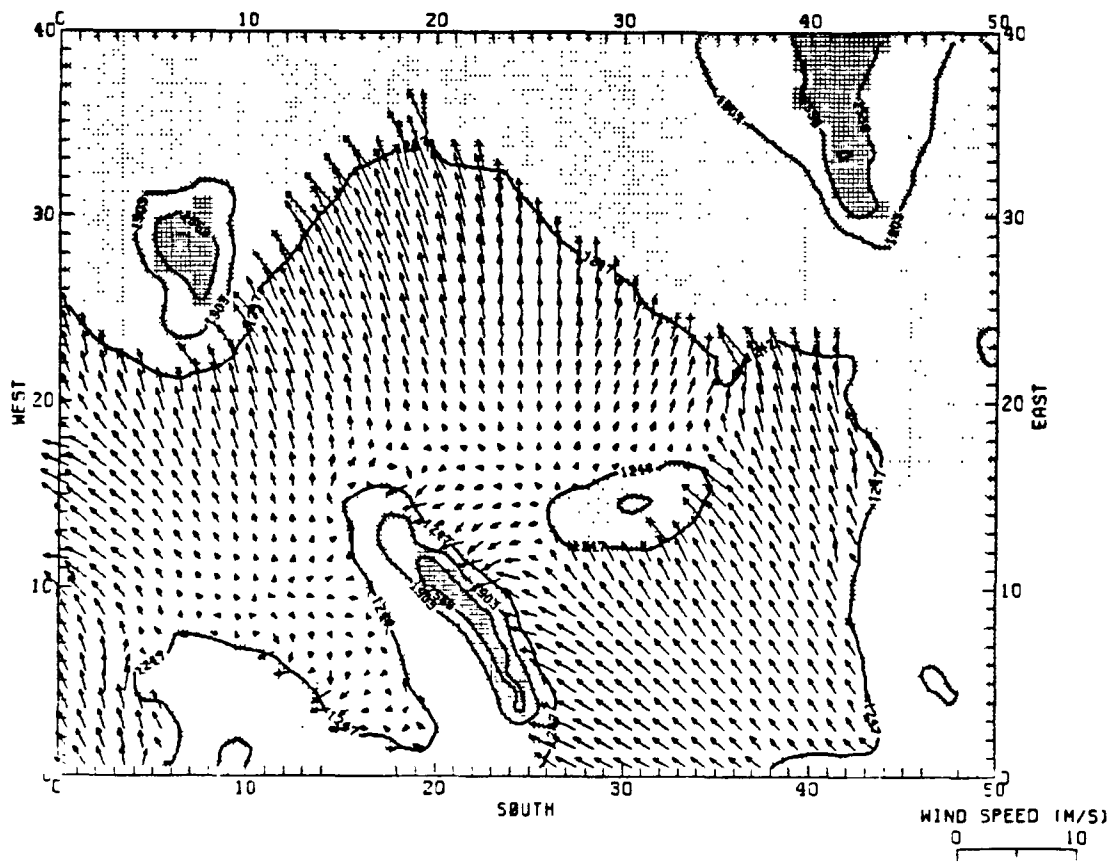
0600 MST



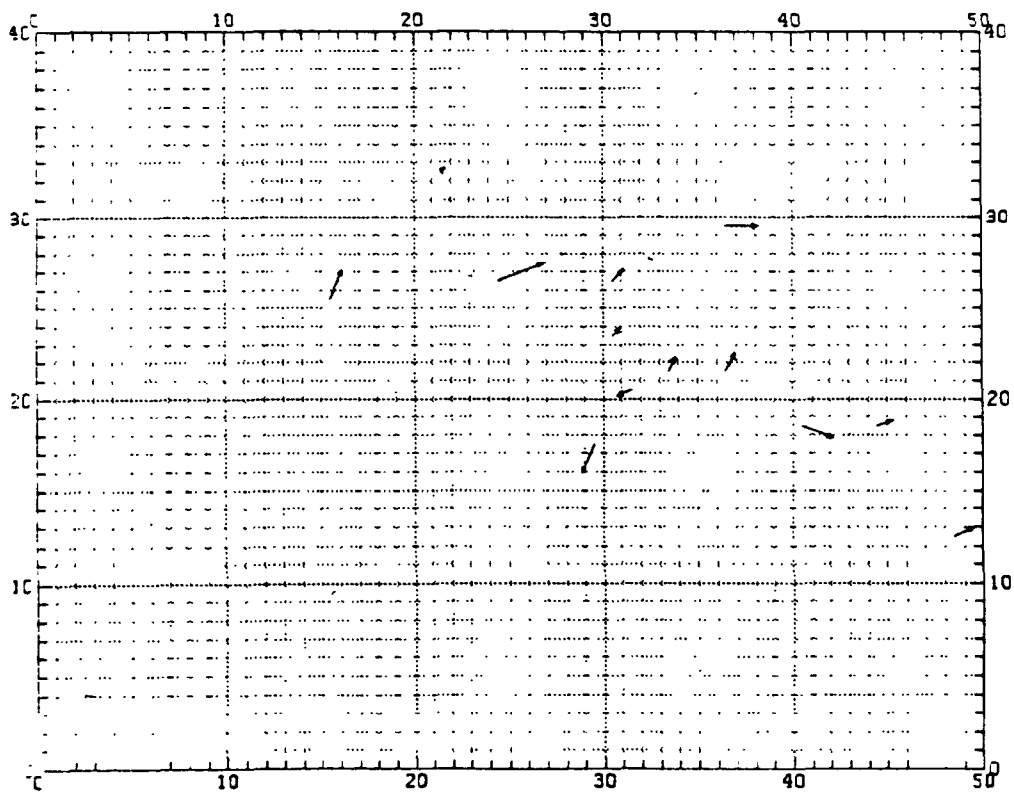
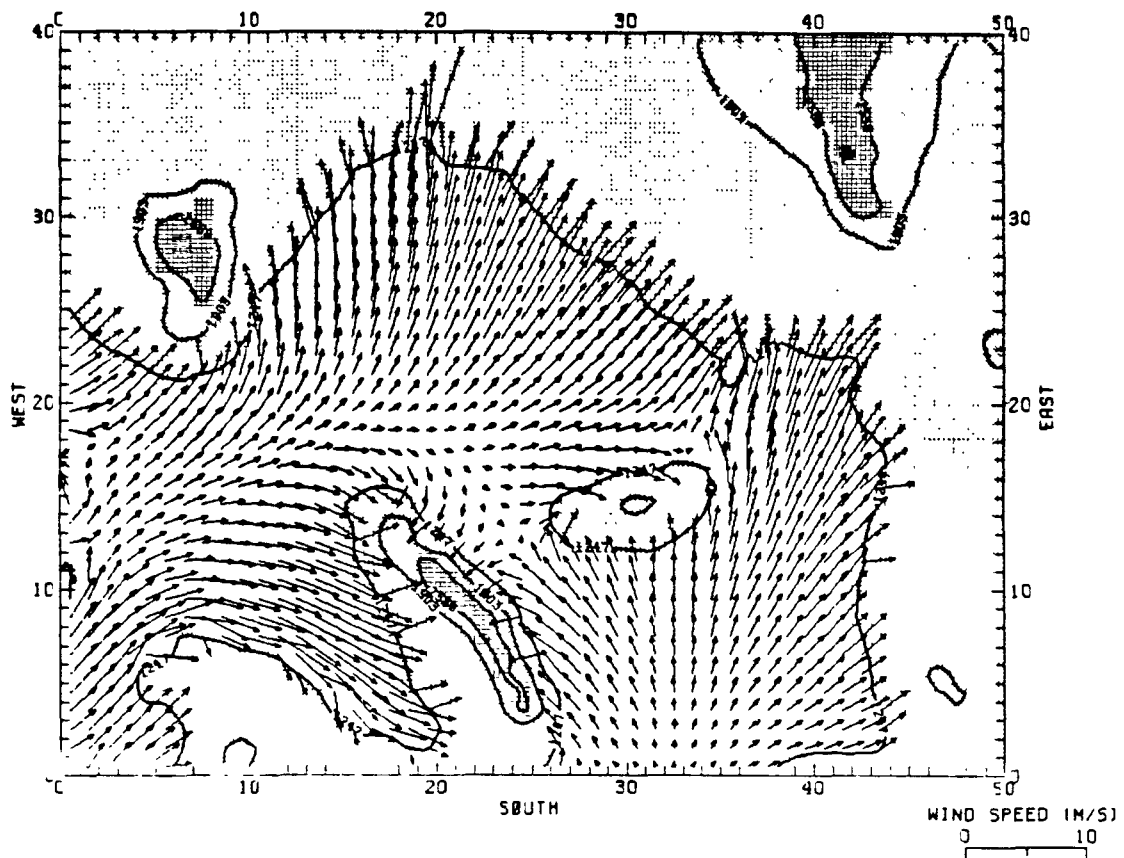
0800 MST



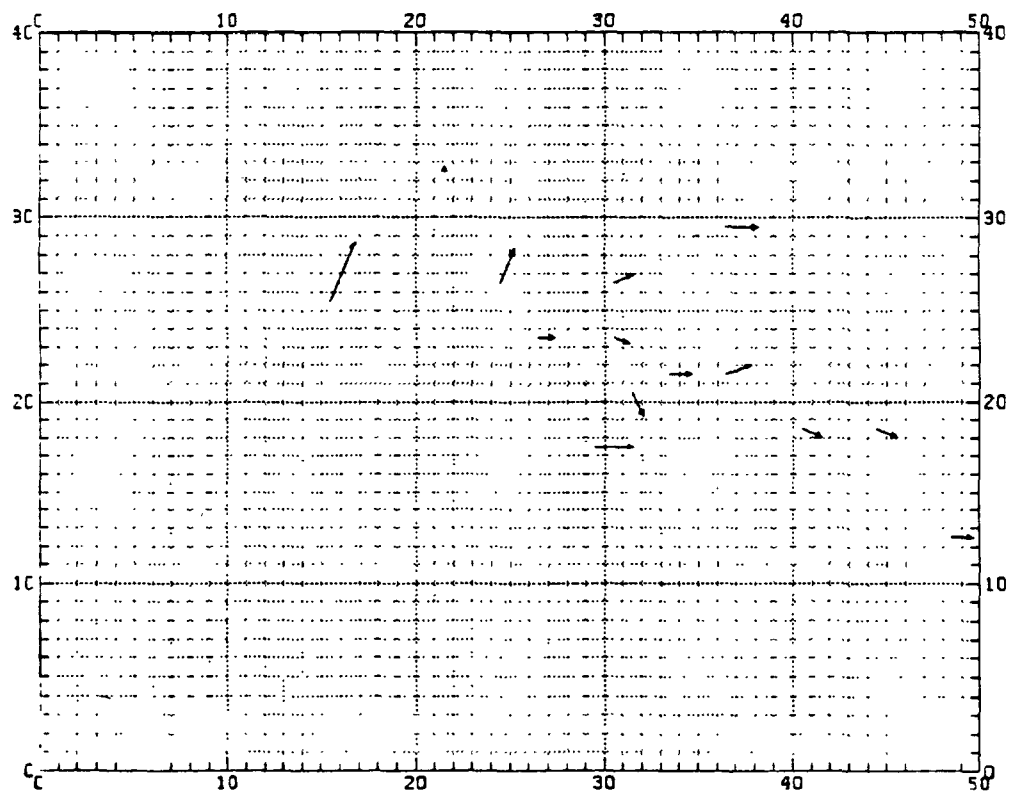
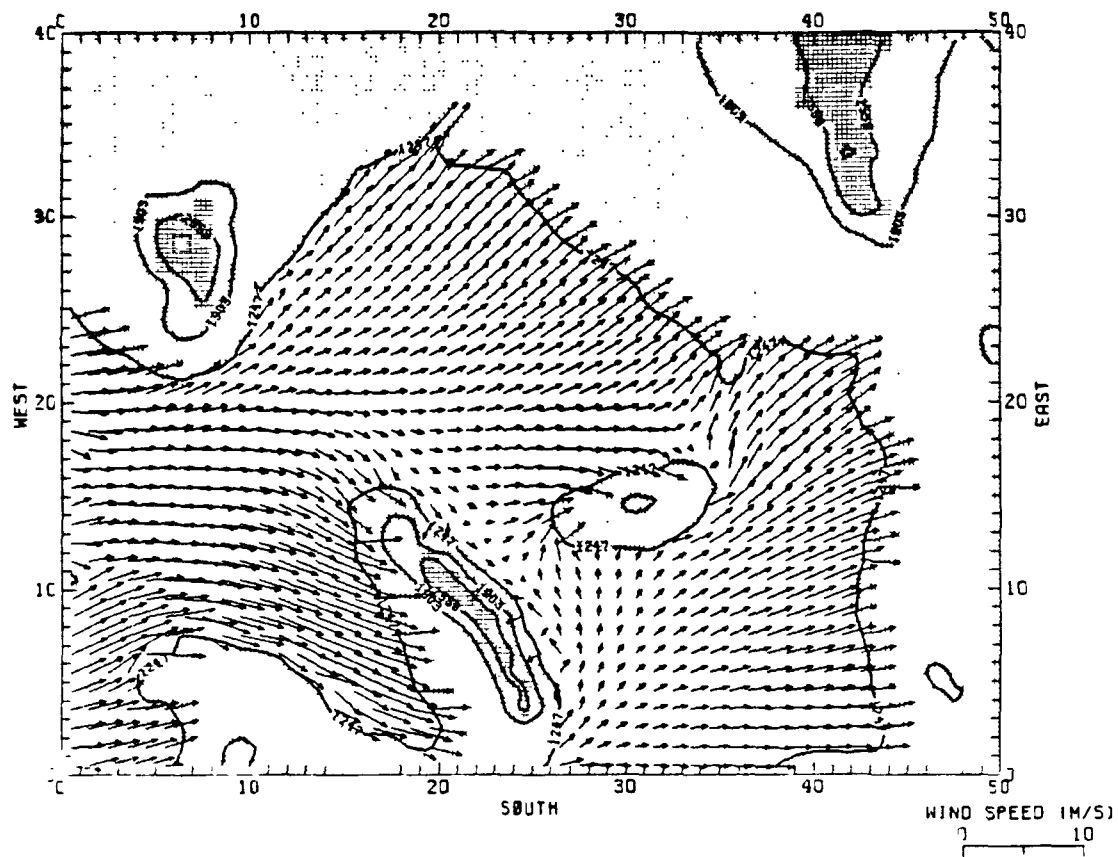
1000 MST



1200 MST

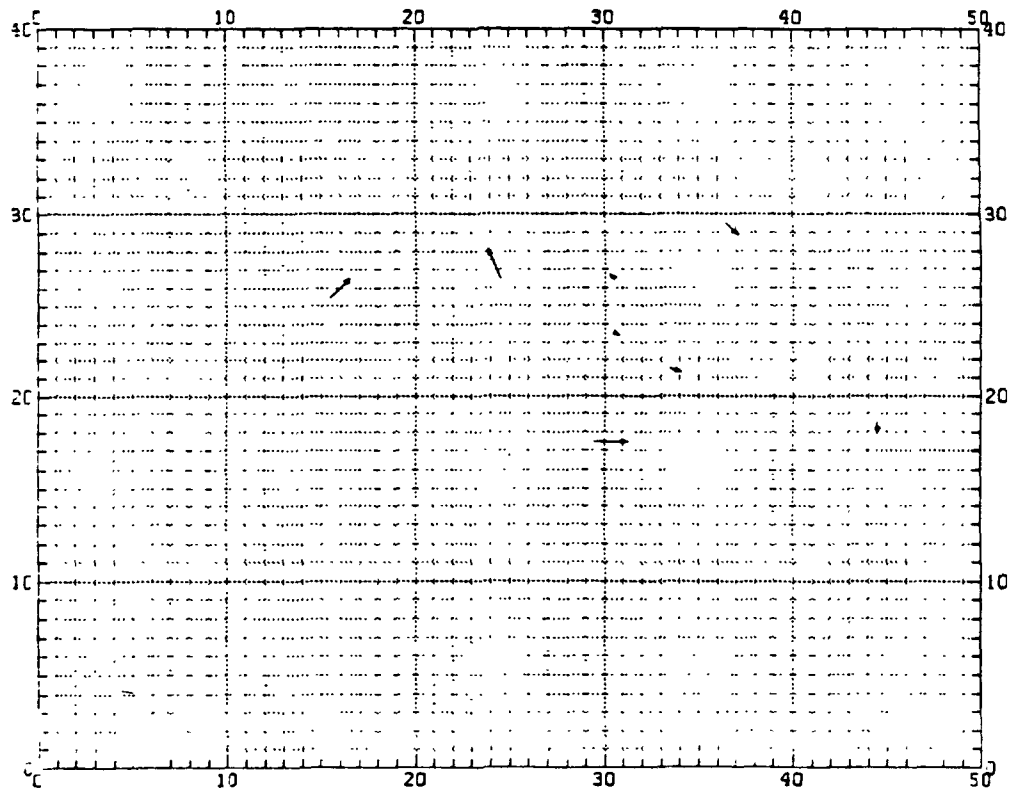
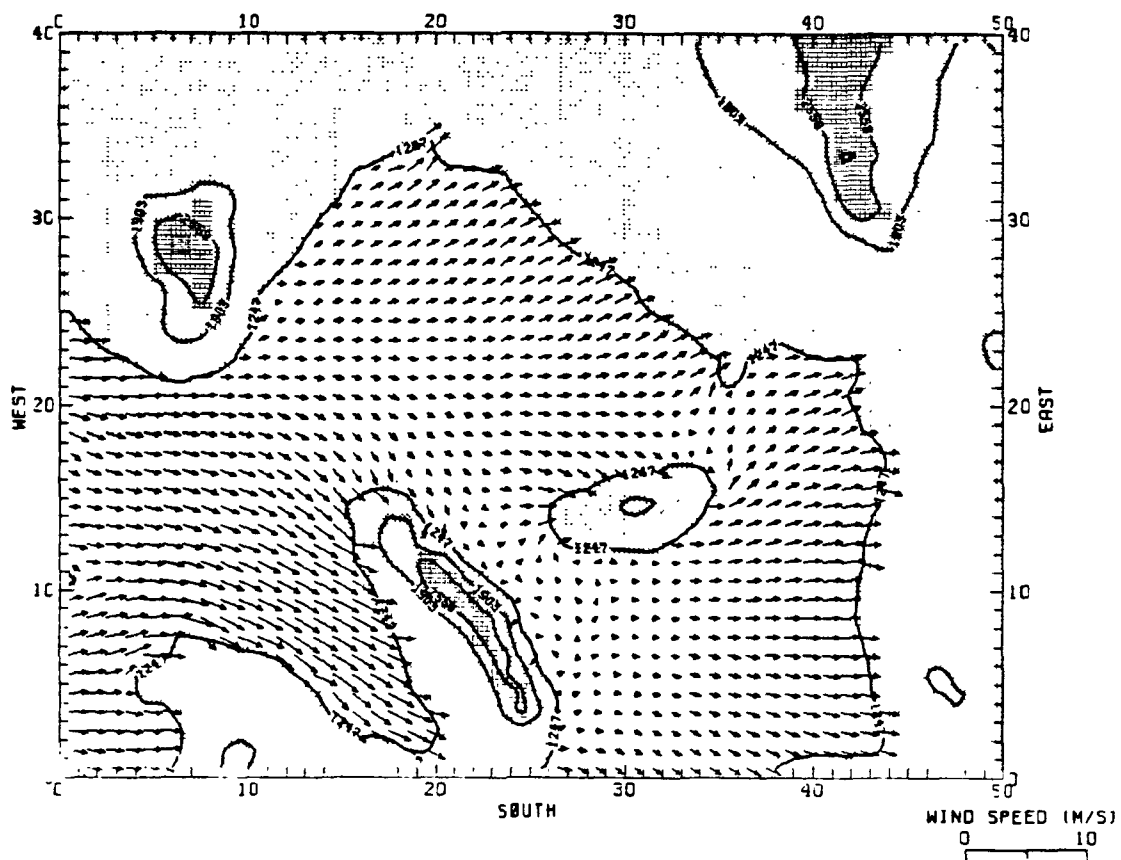


1400 MST

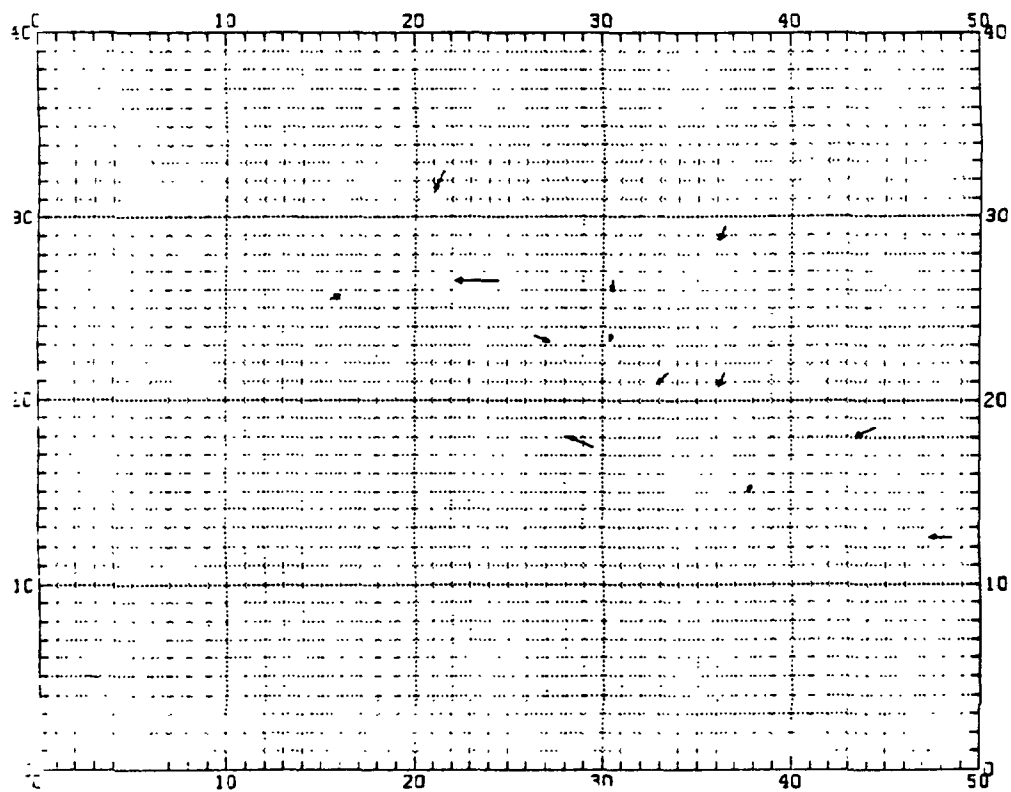
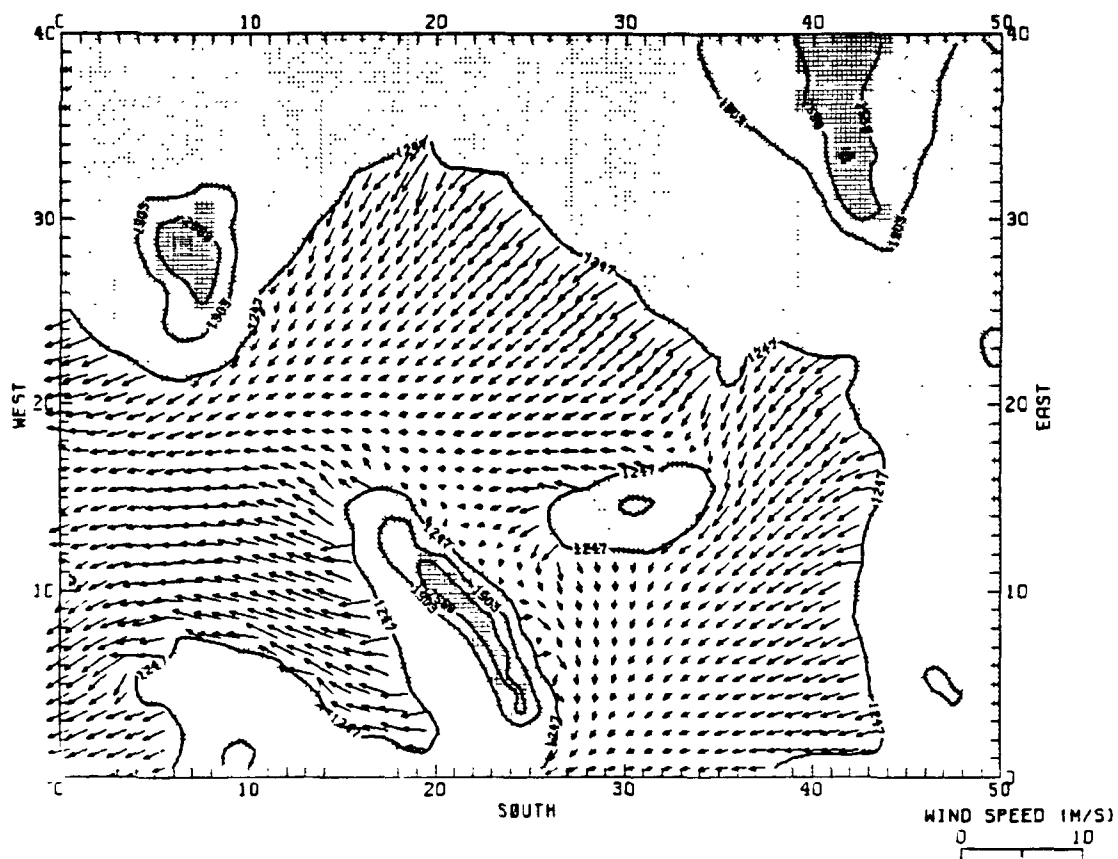


1600 MST

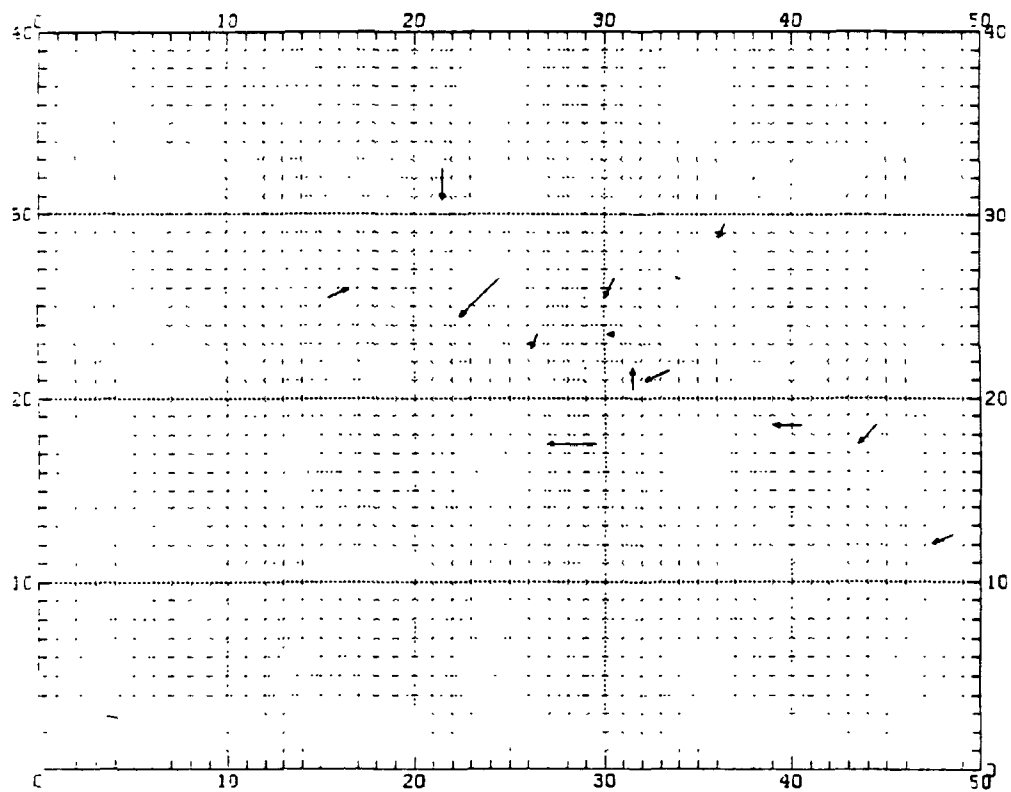
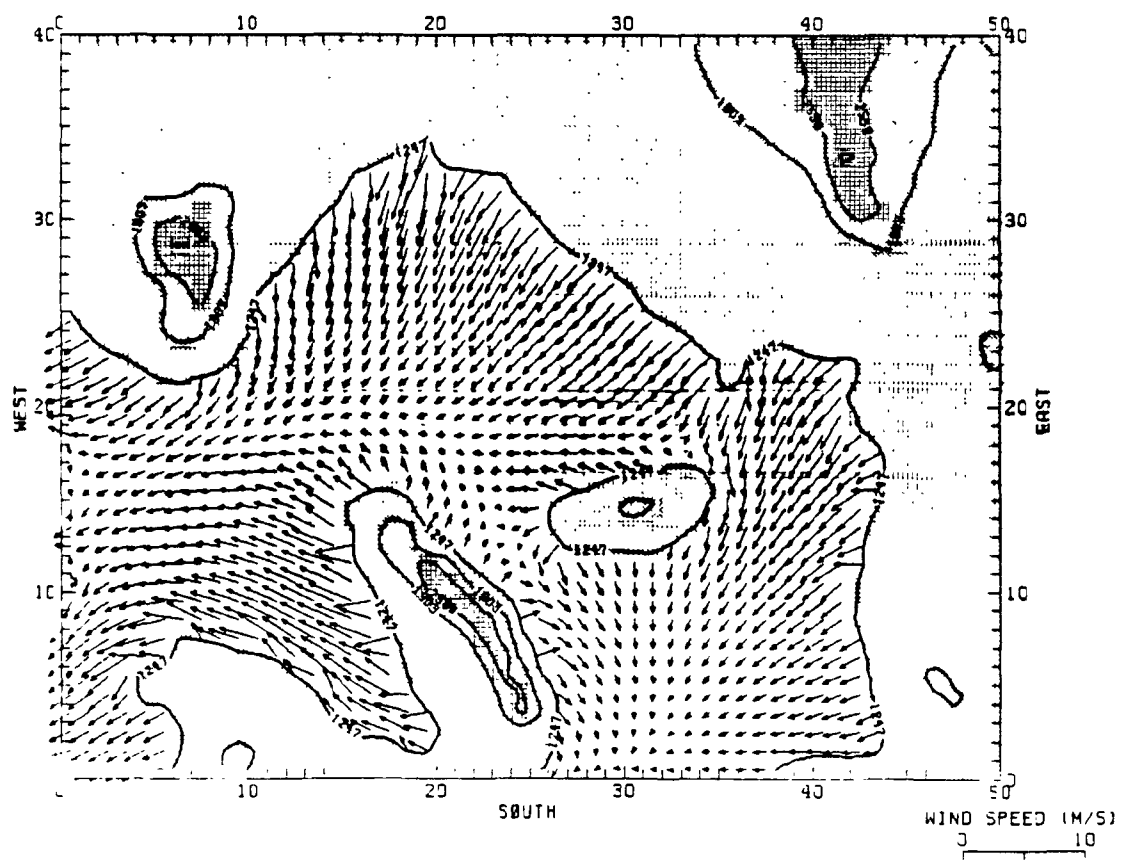




1800 MST

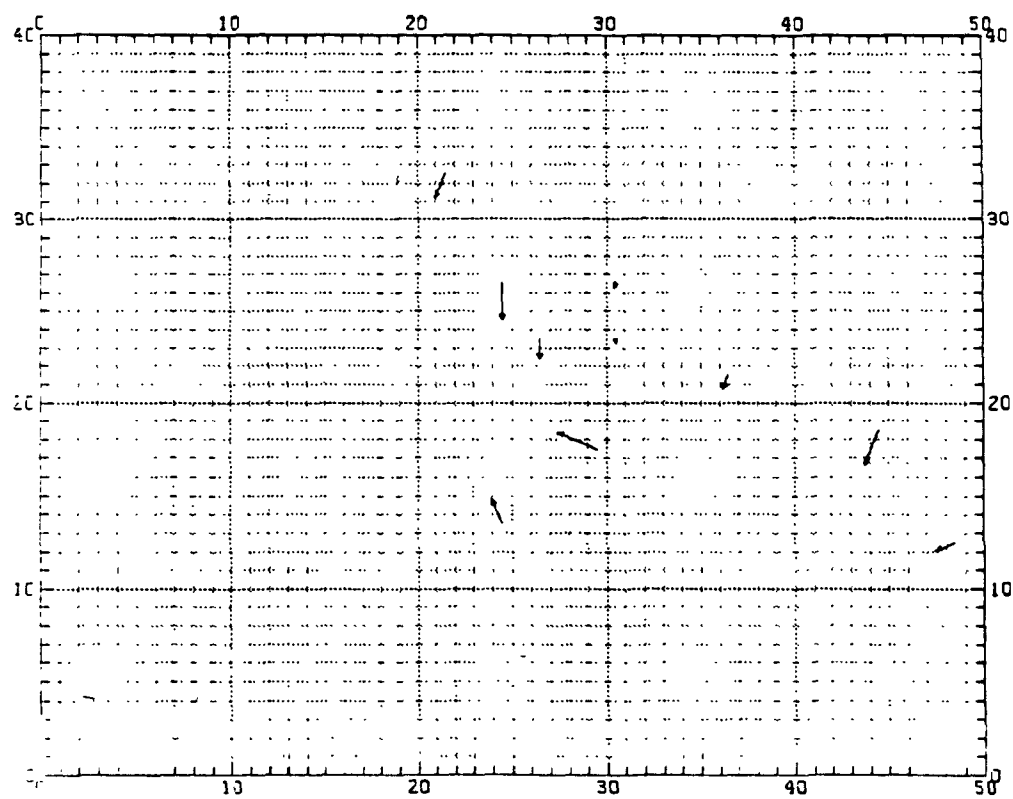
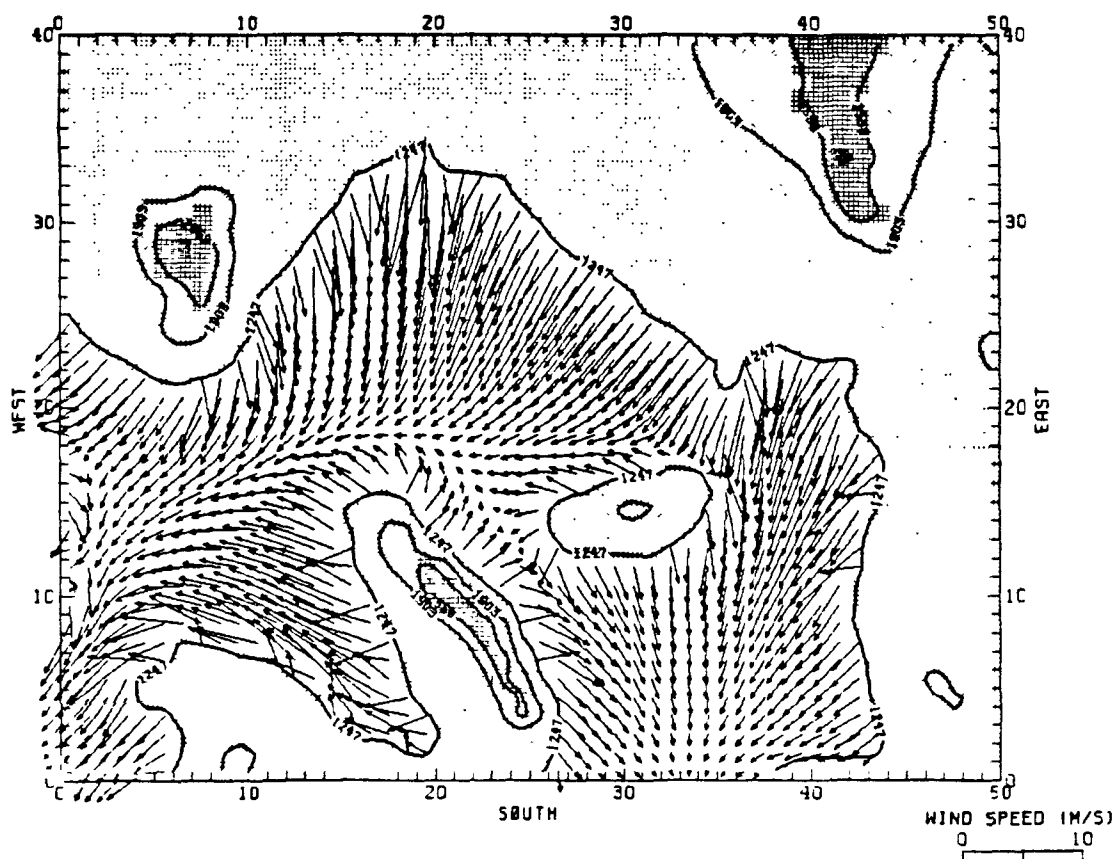


2000 MST

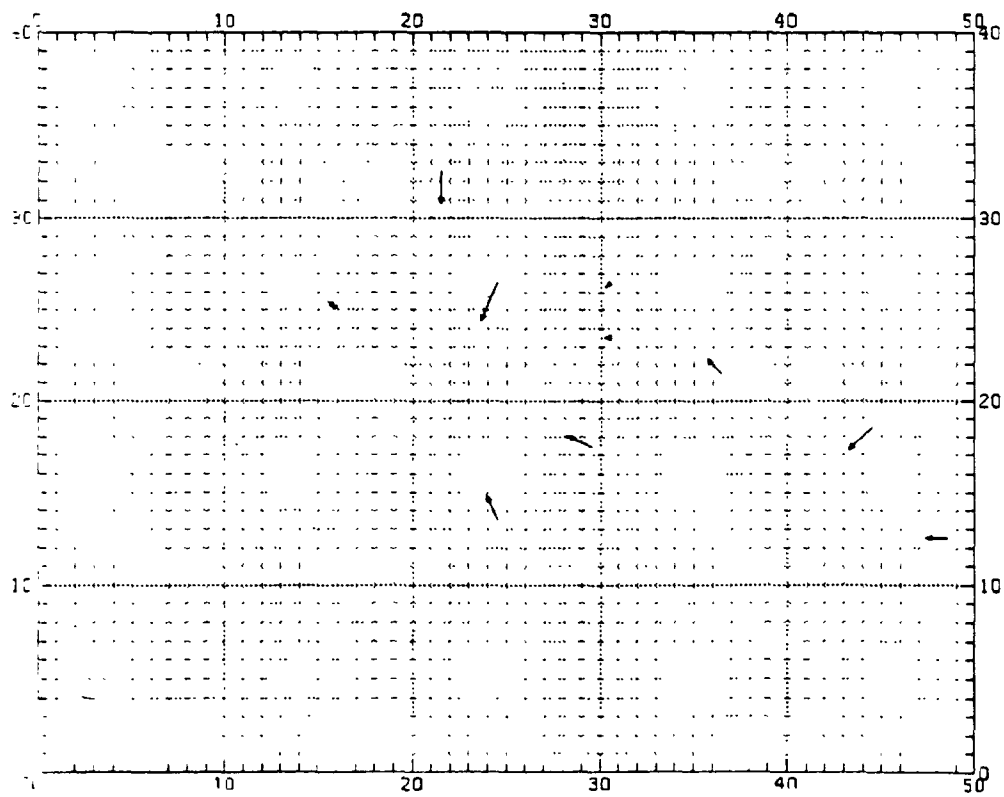
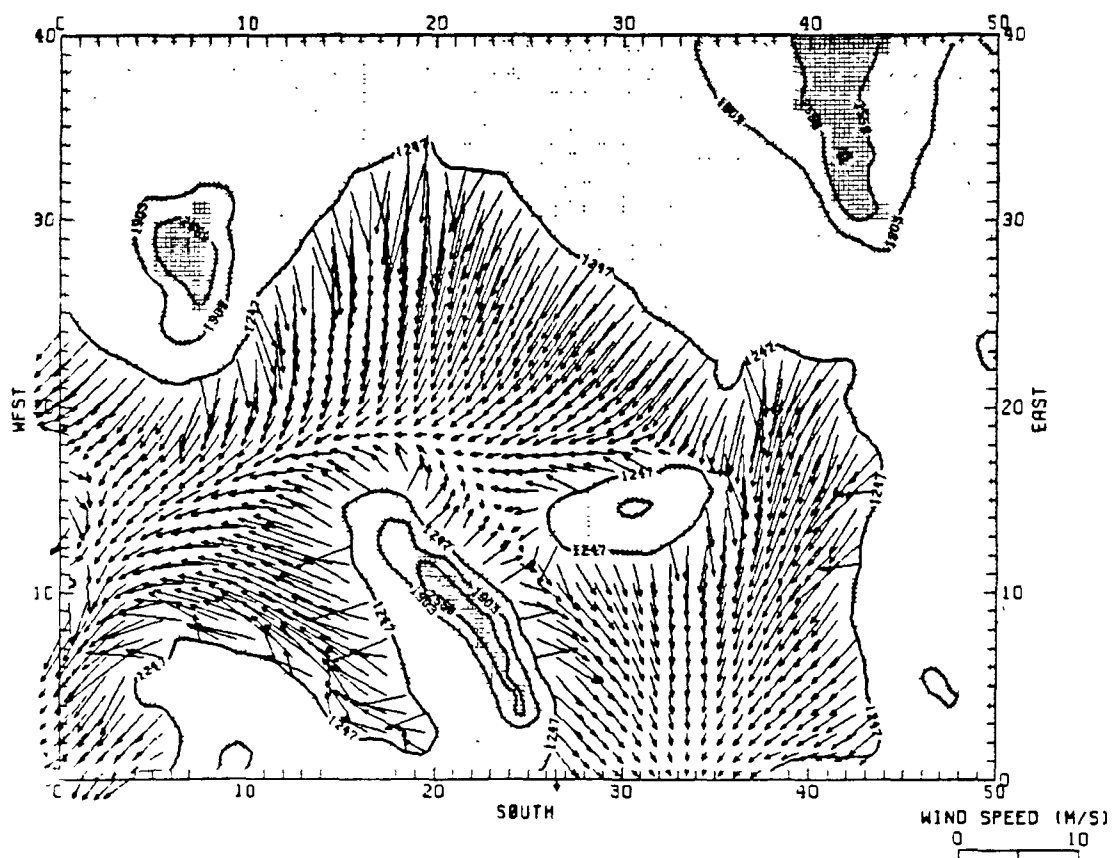


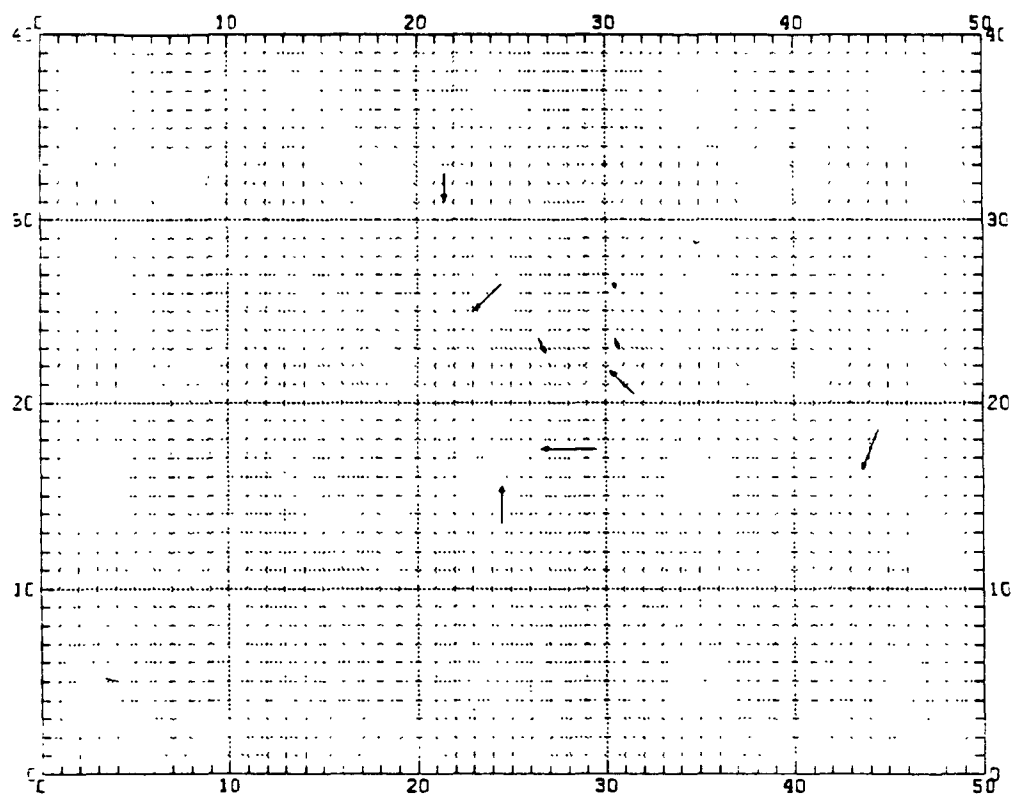
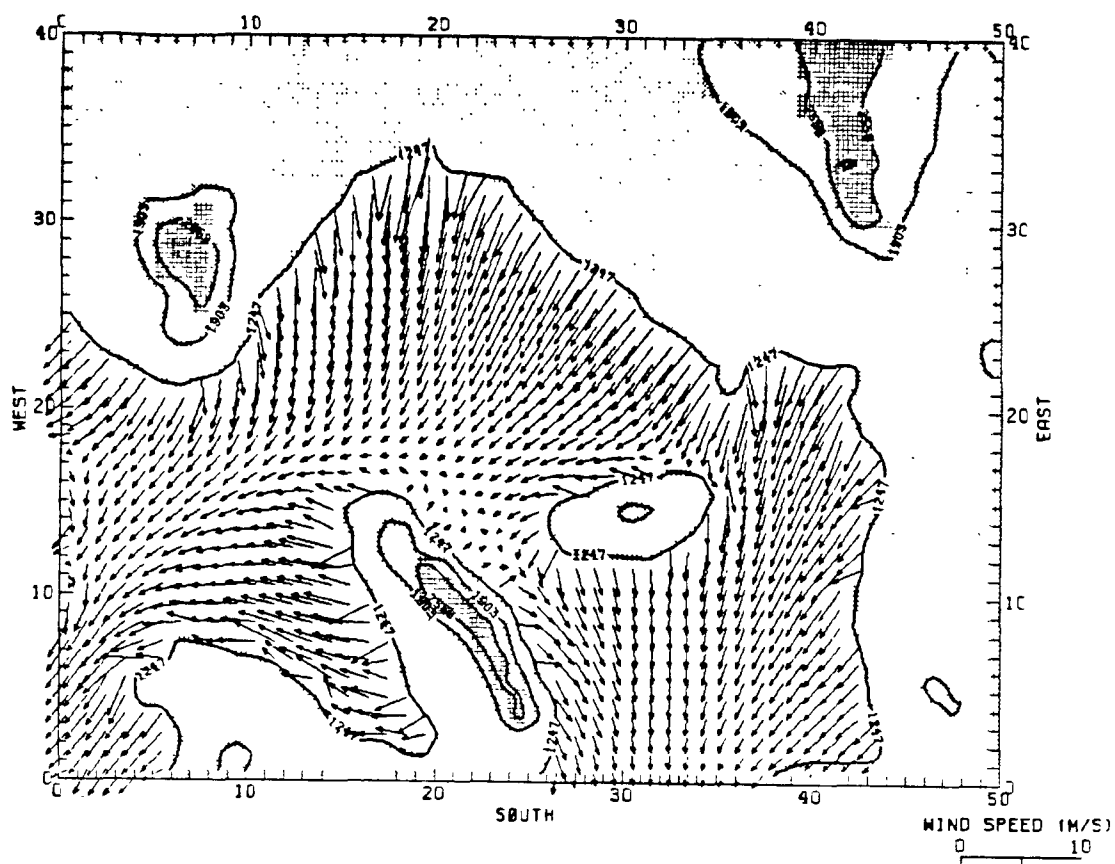
2200 MST

PART 3--7 MARCH 1977

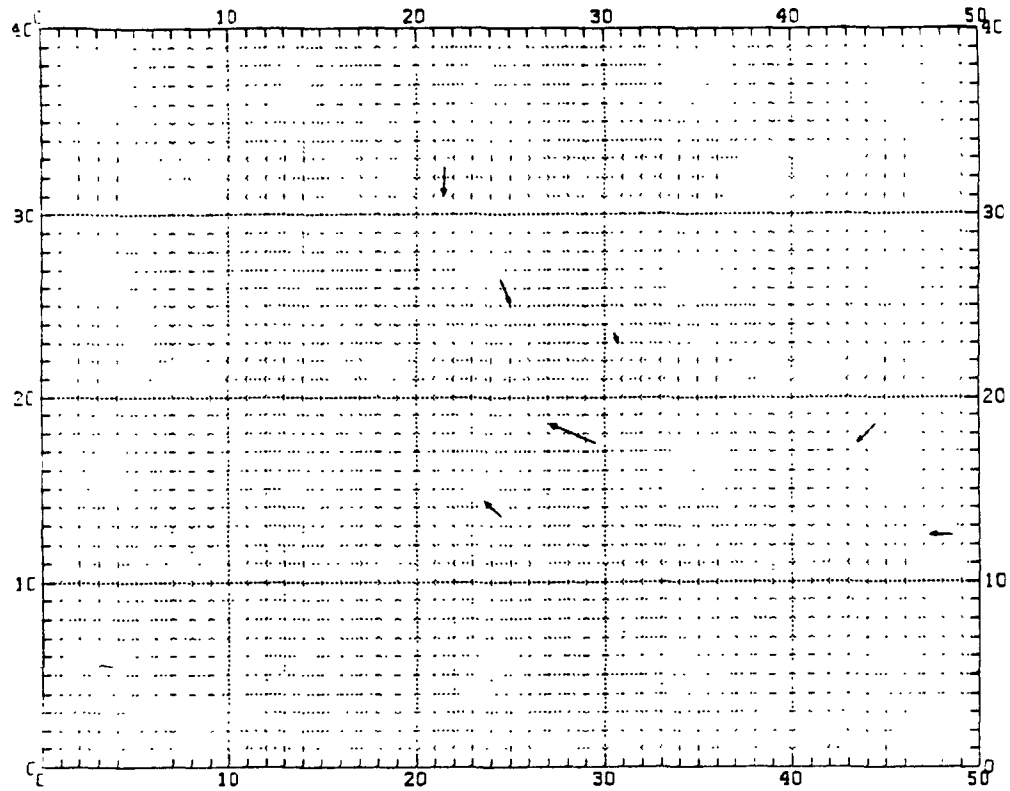
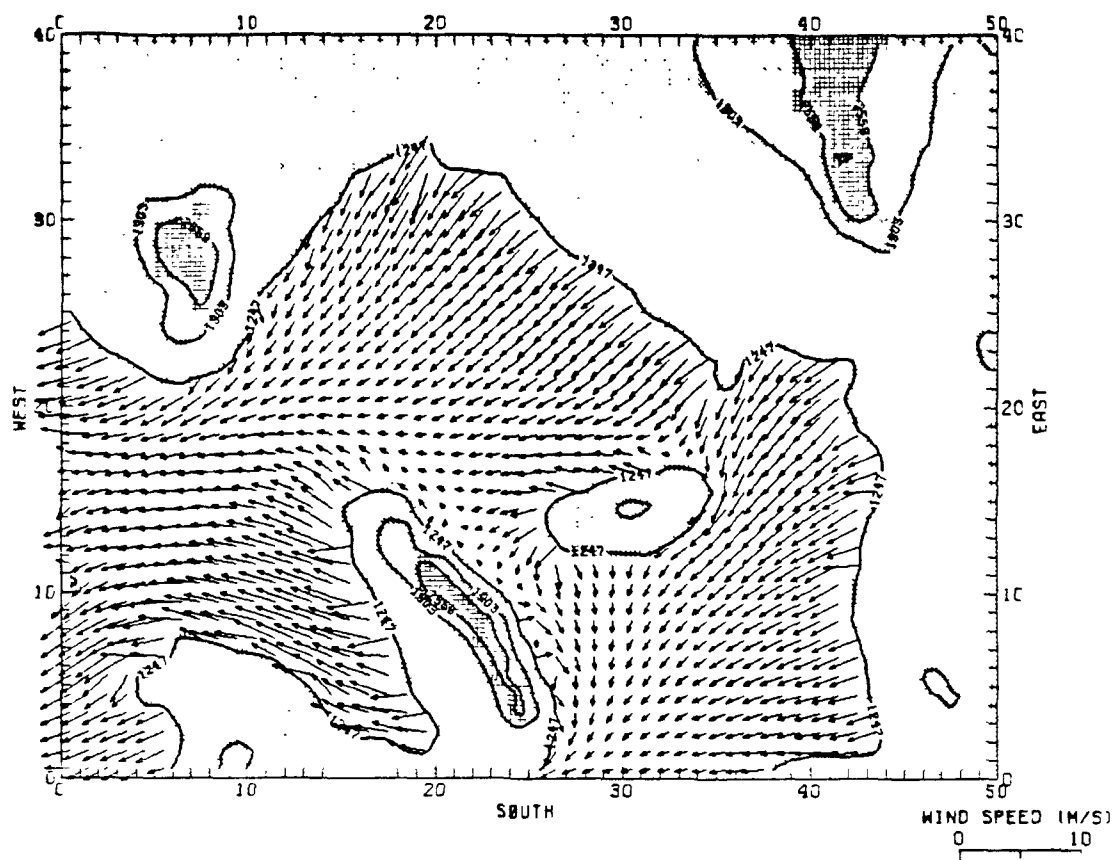


0000 MST



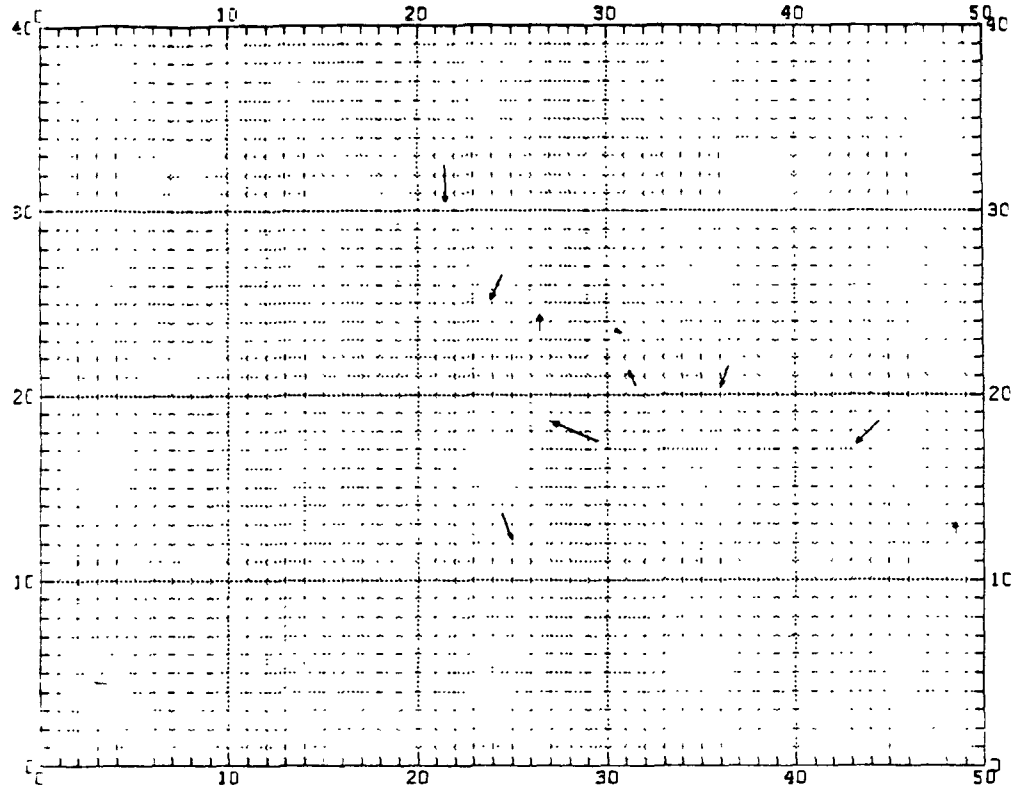
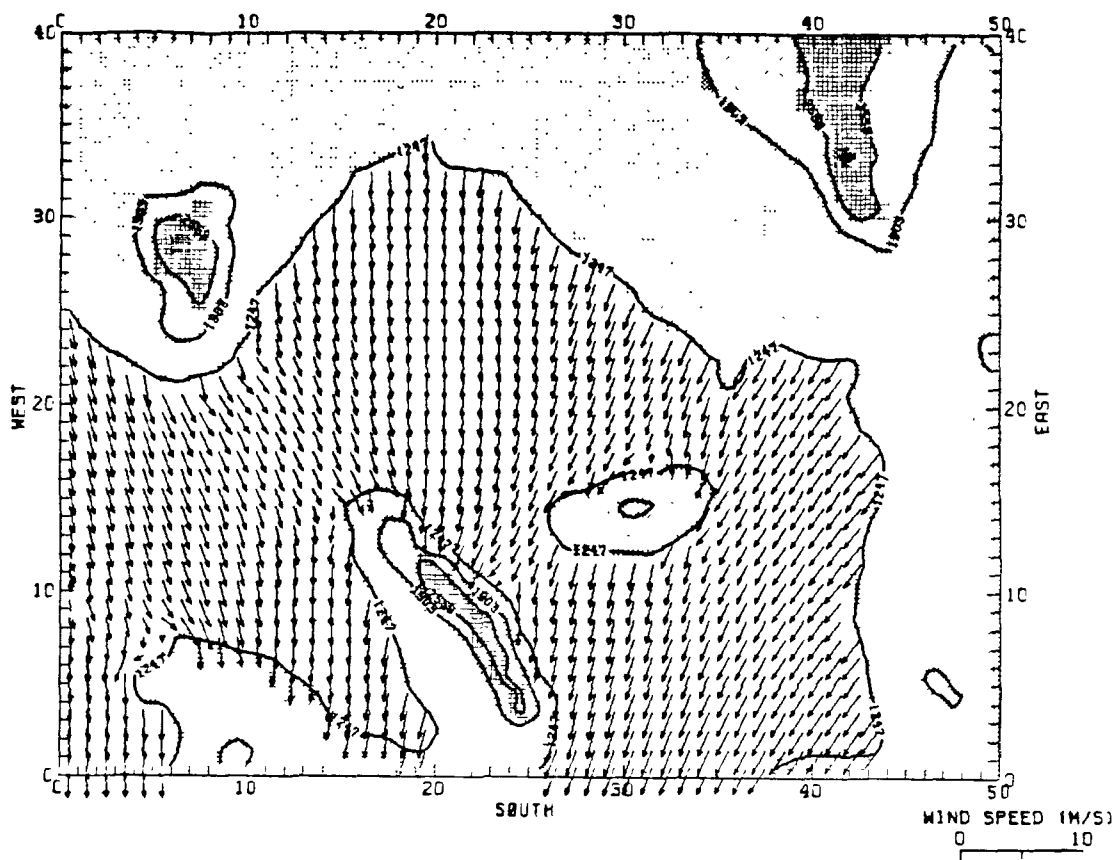


0400 MST

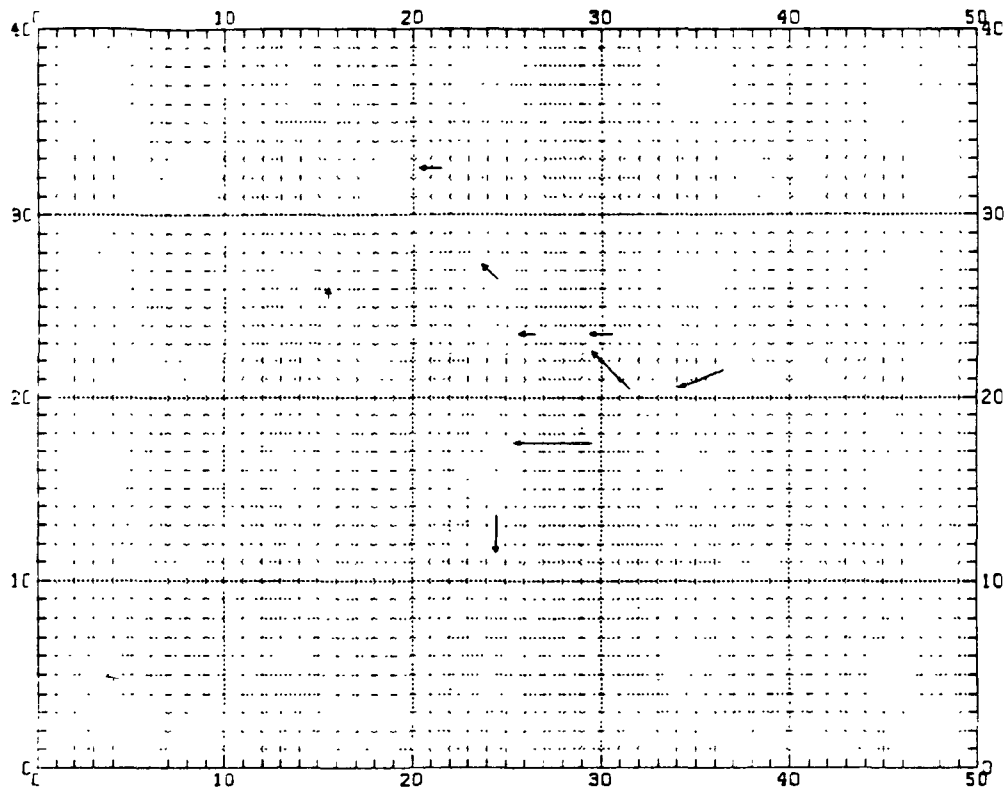
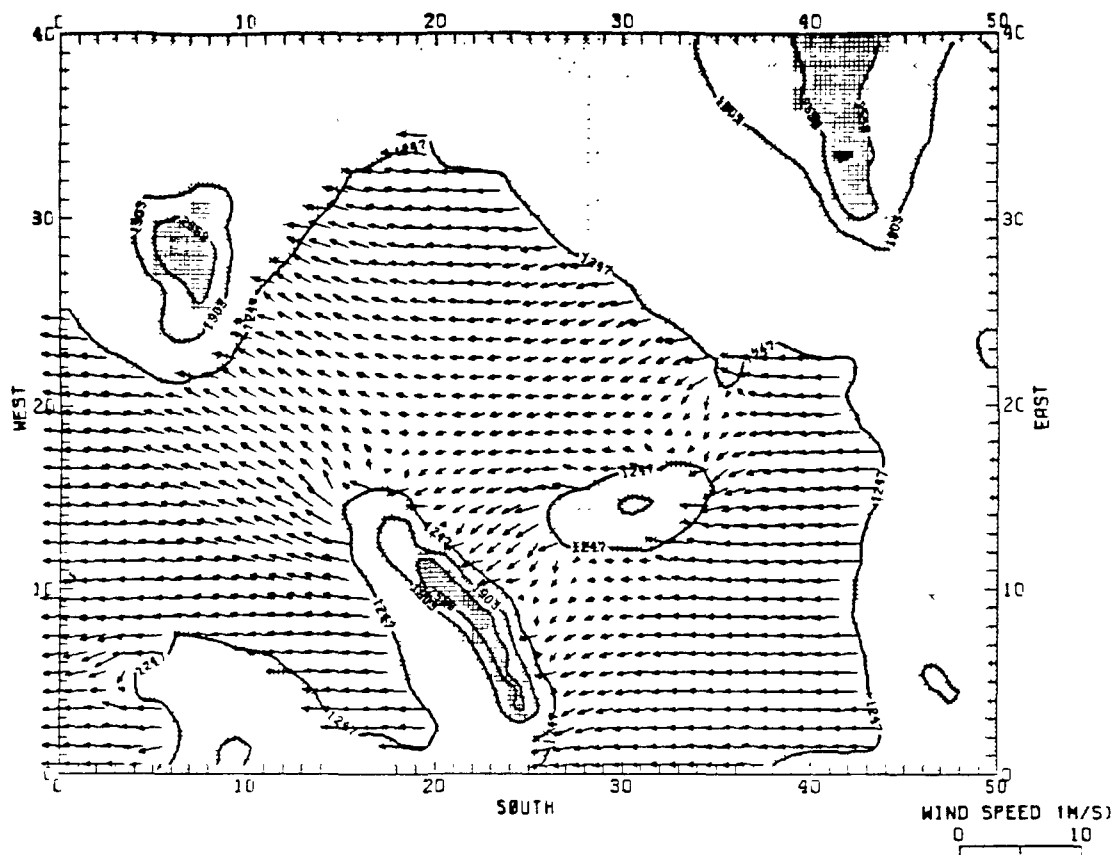


0600 MST

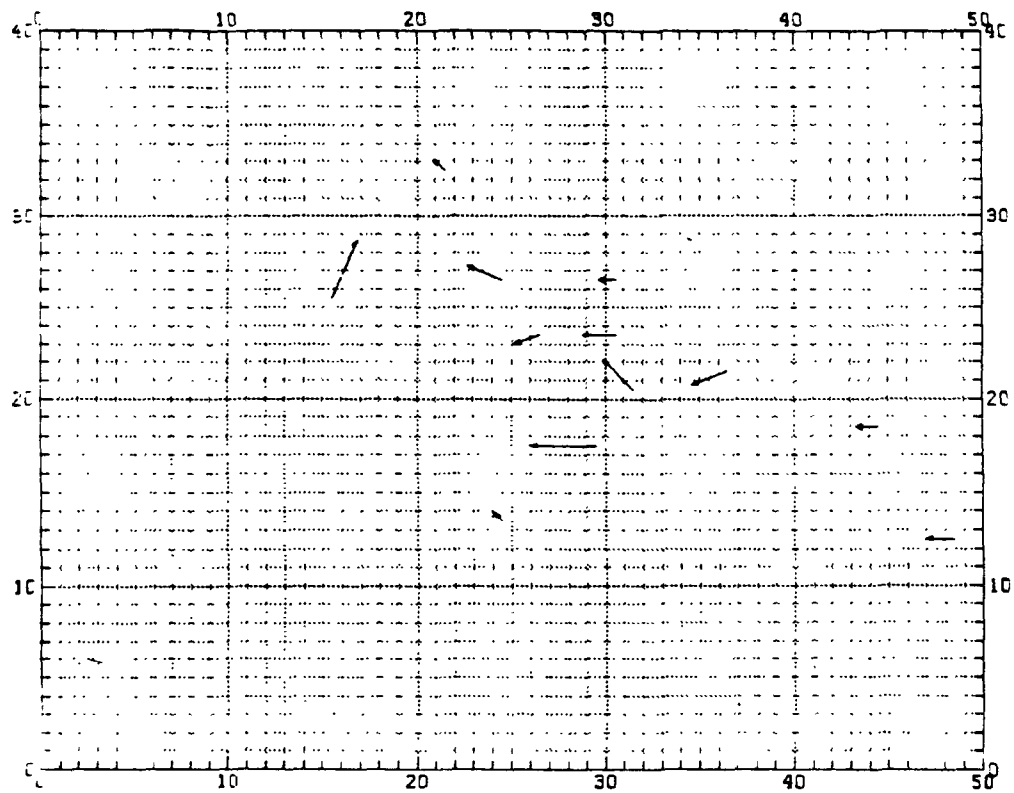
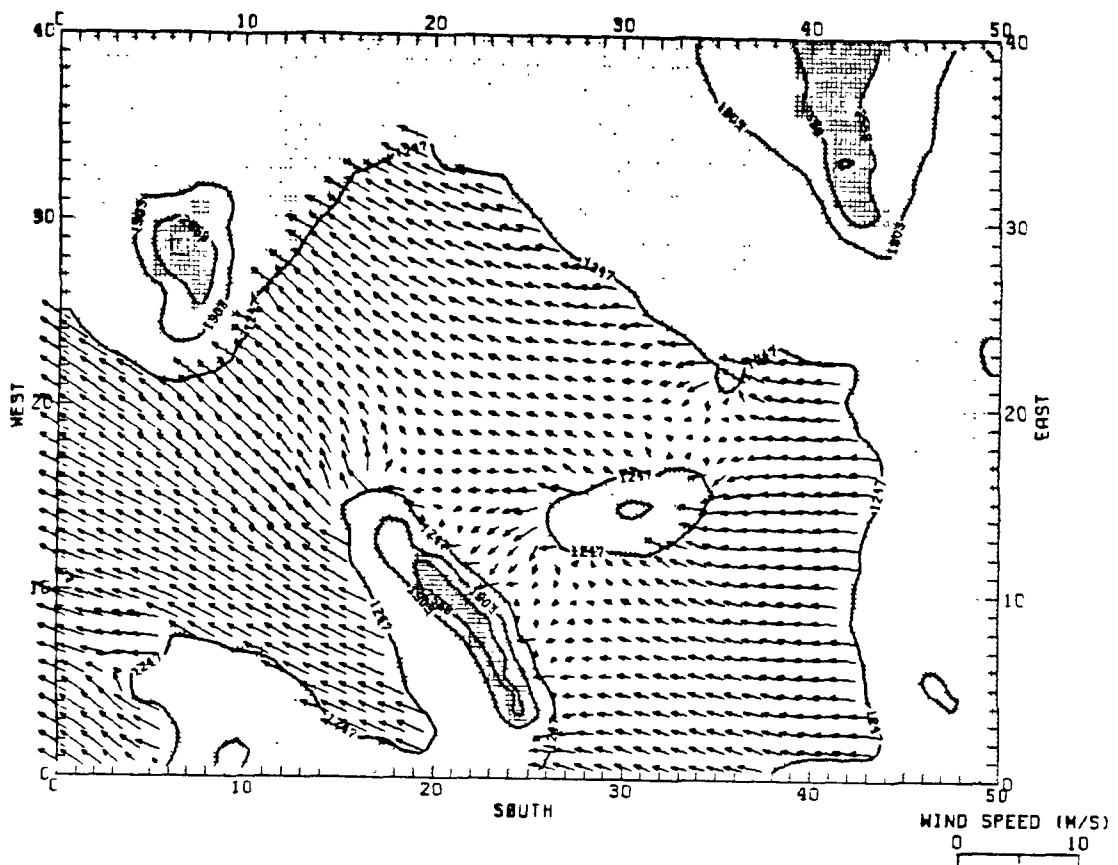




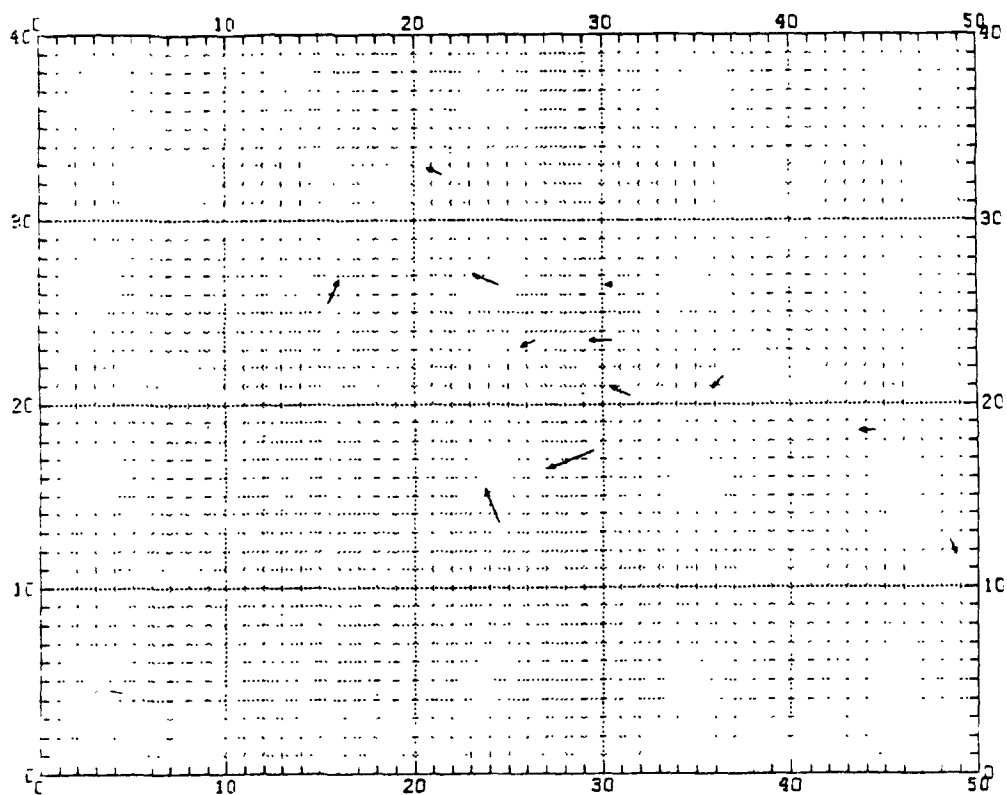
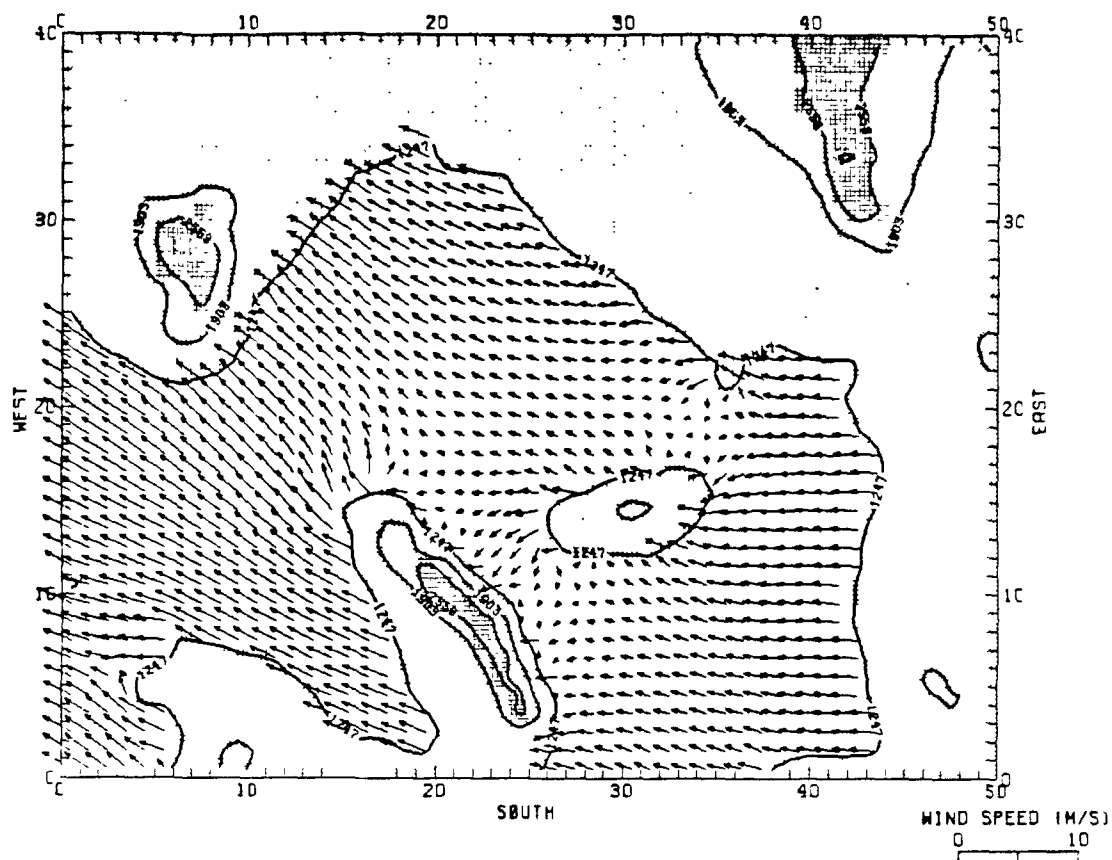
0800 MST



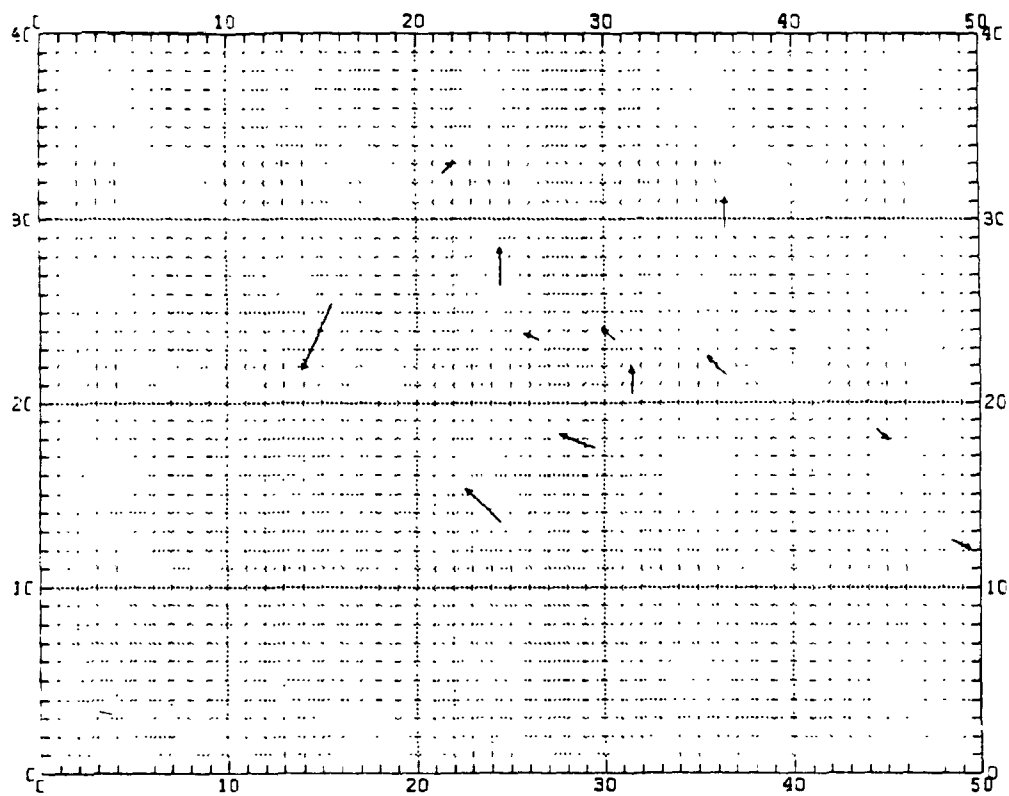
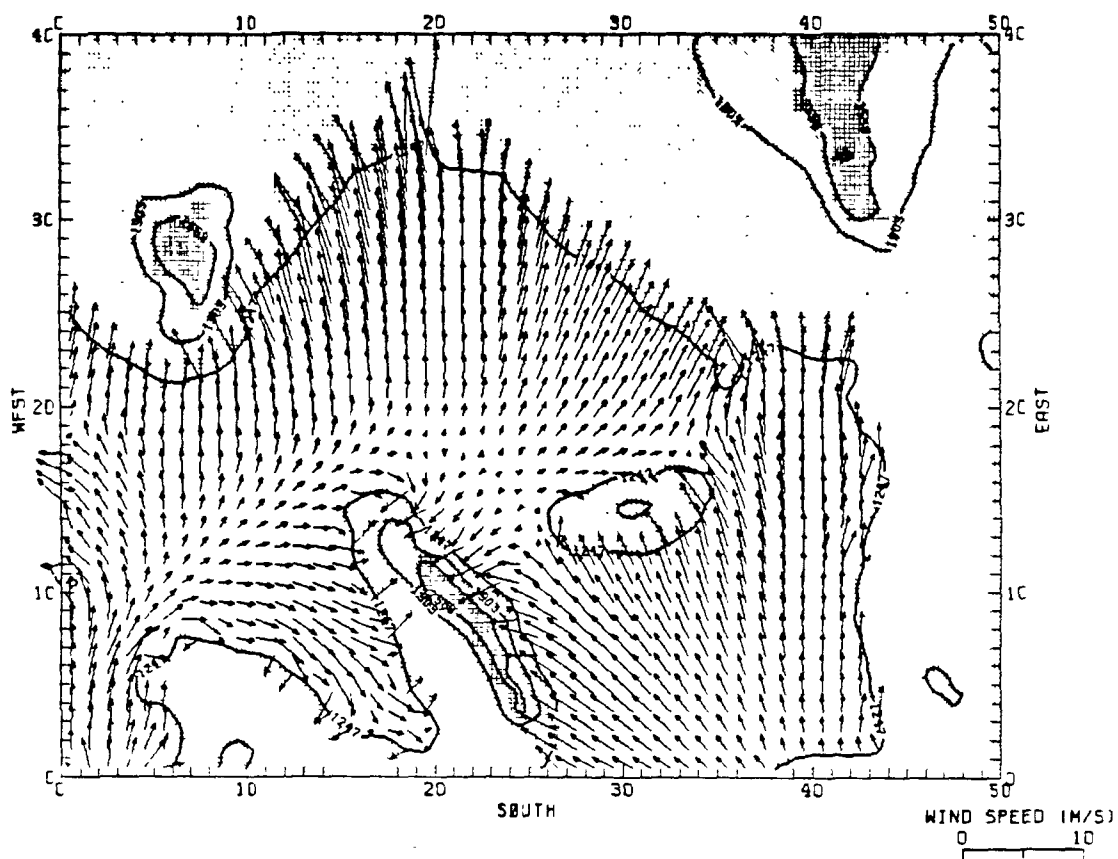
1000 MST



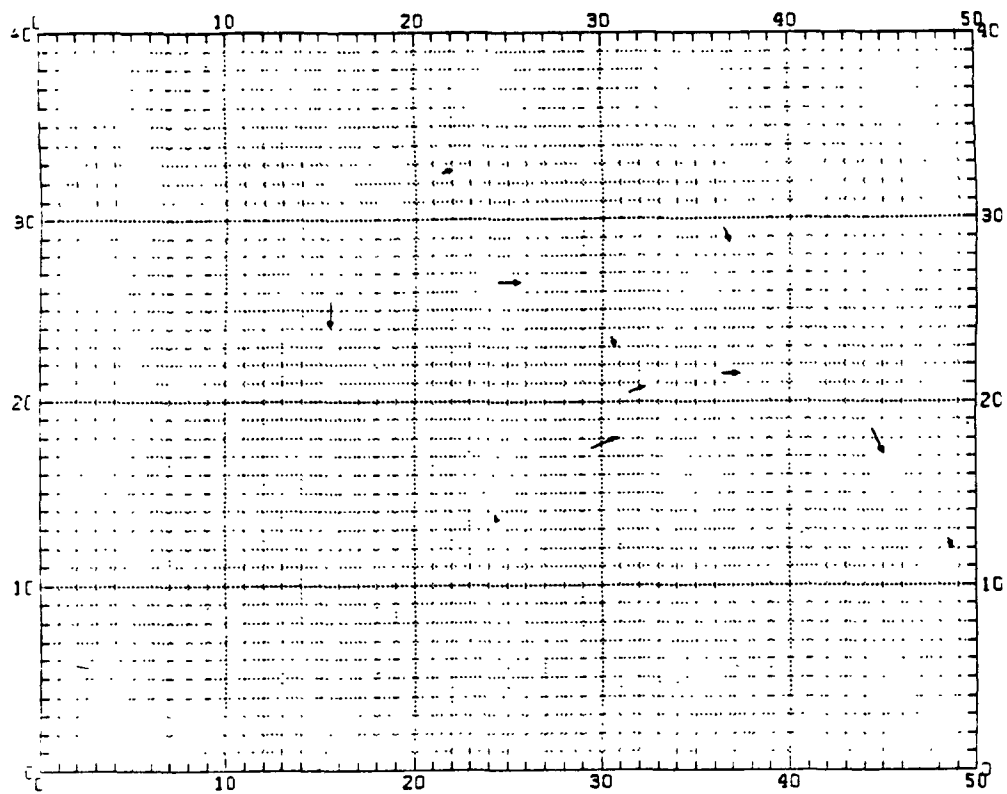
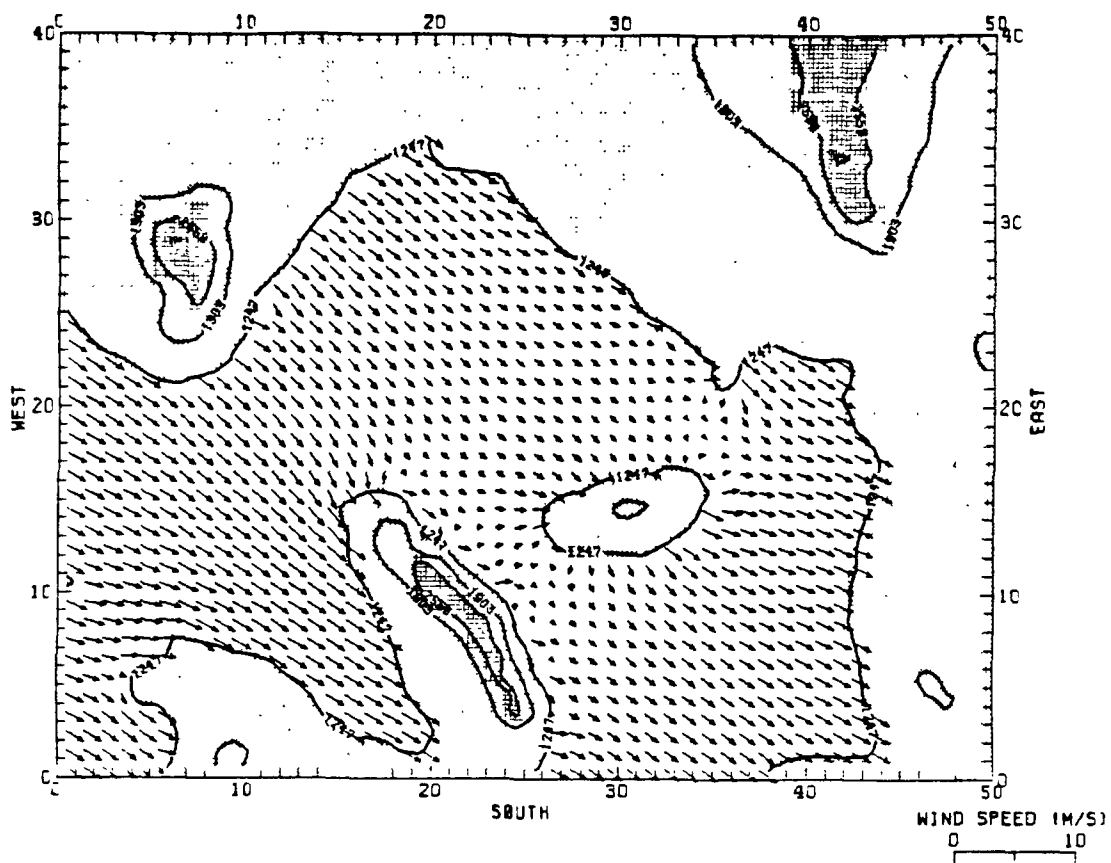
1200 MST



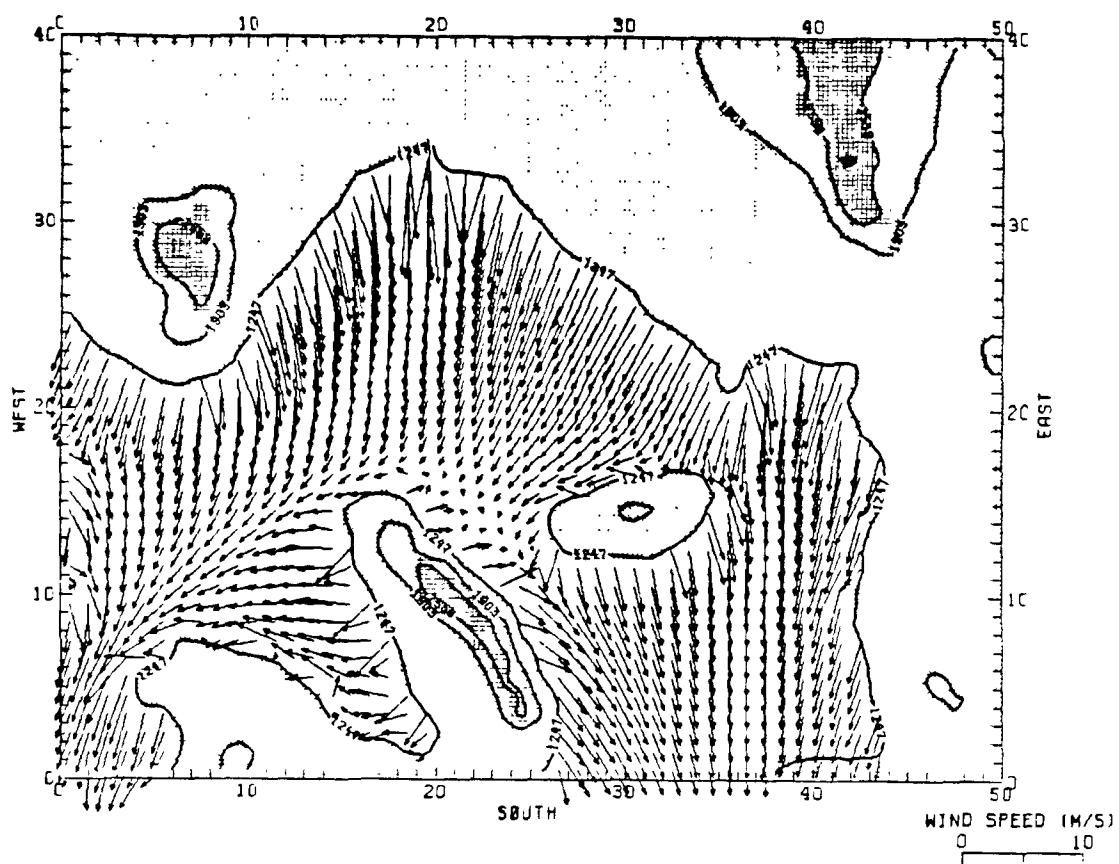
1400 MST

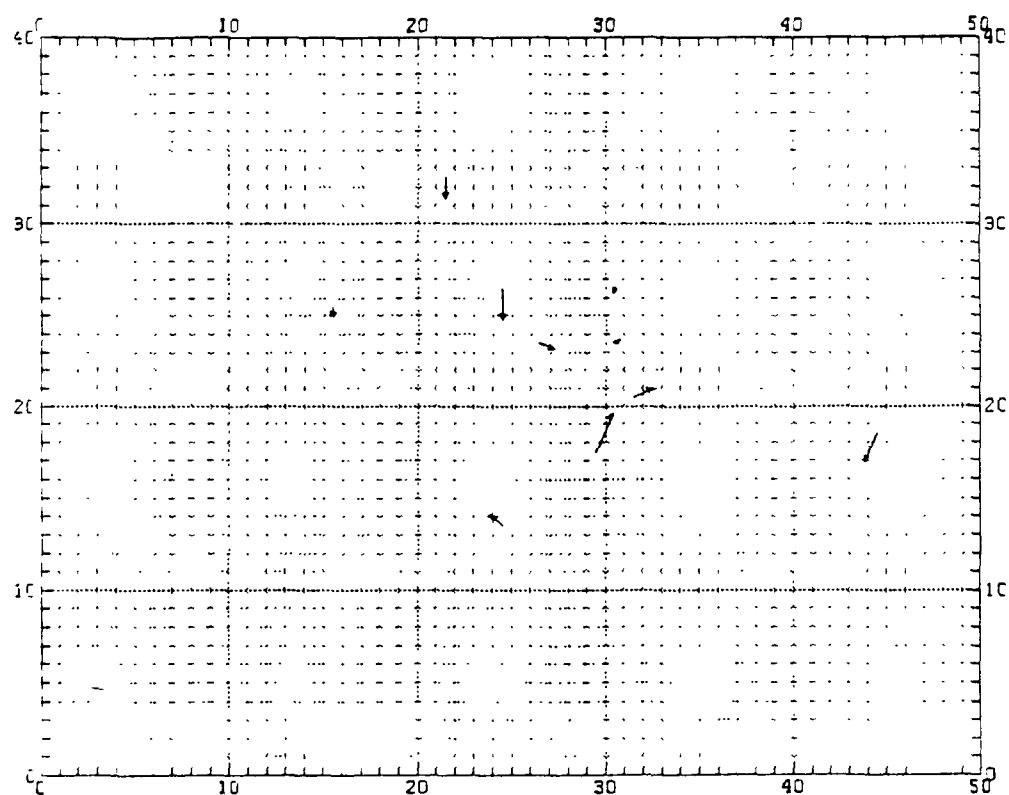
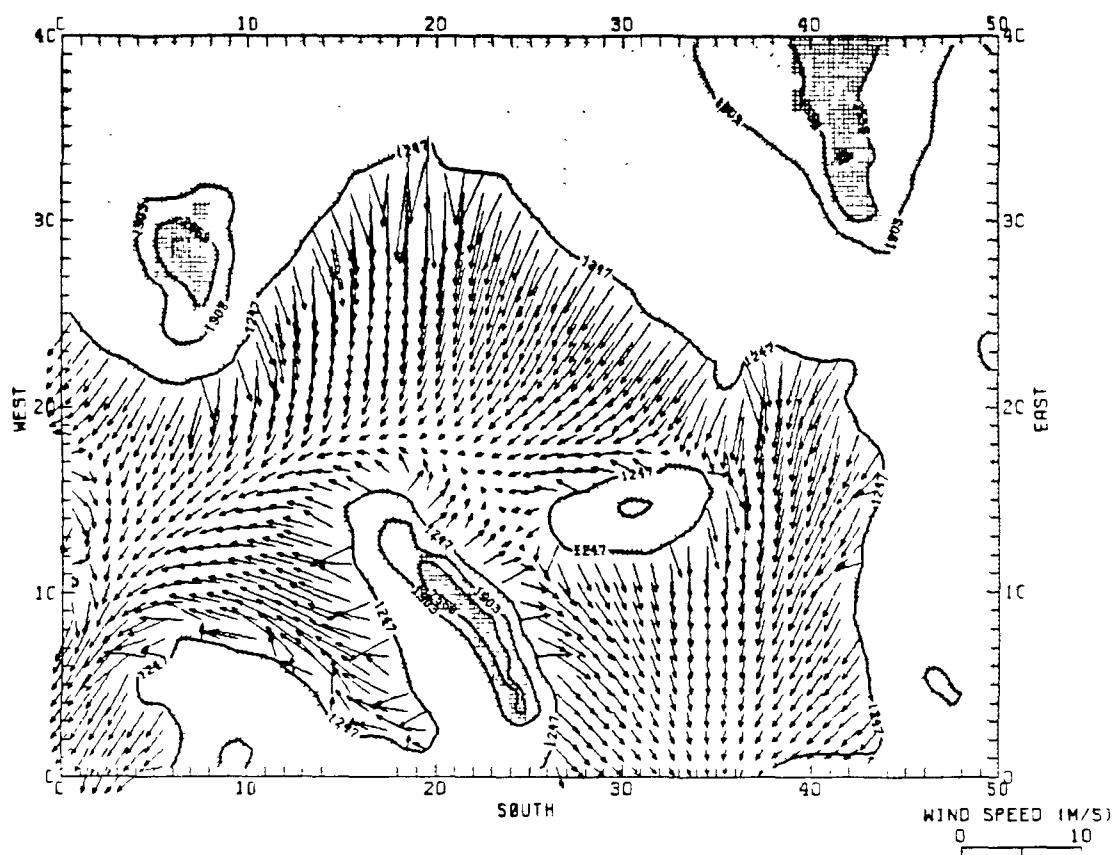


1600 MST



1800 MST

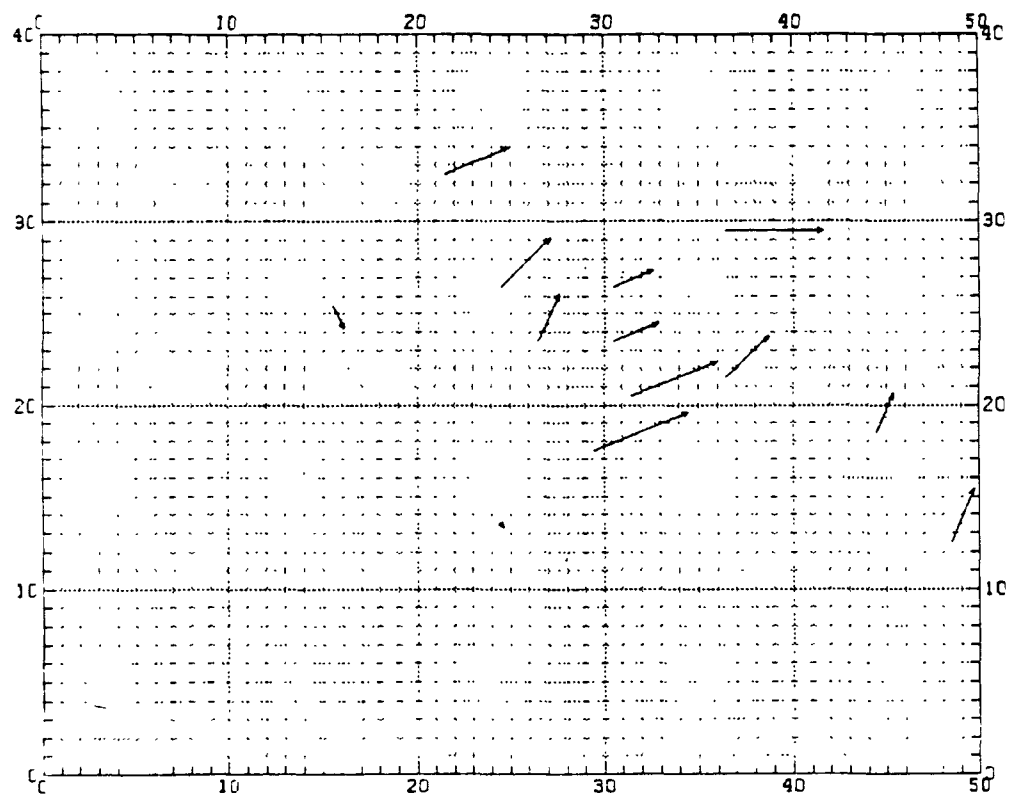
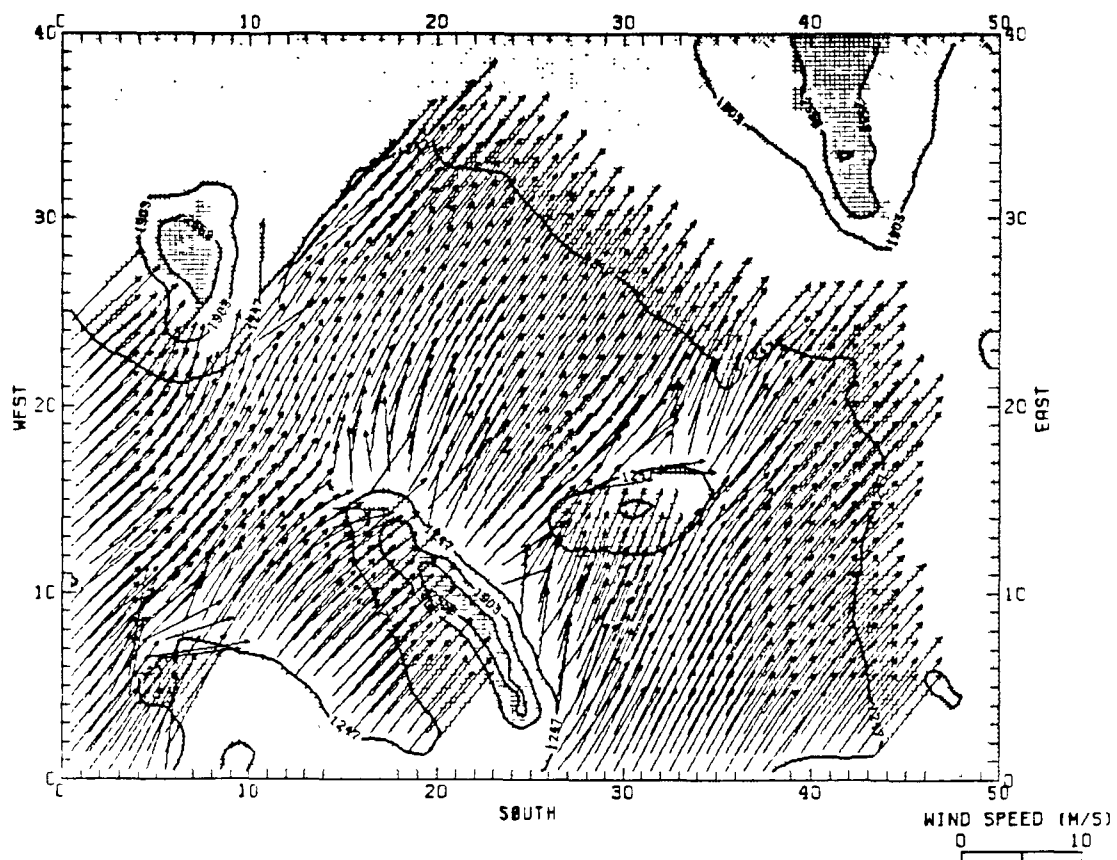




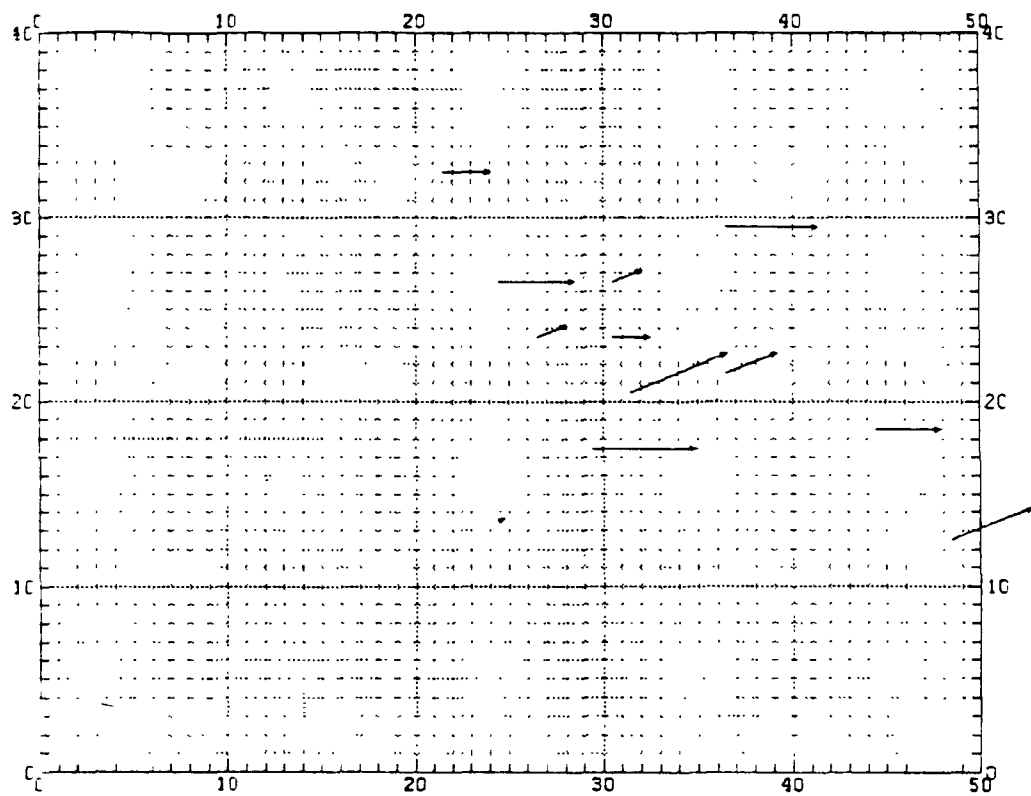
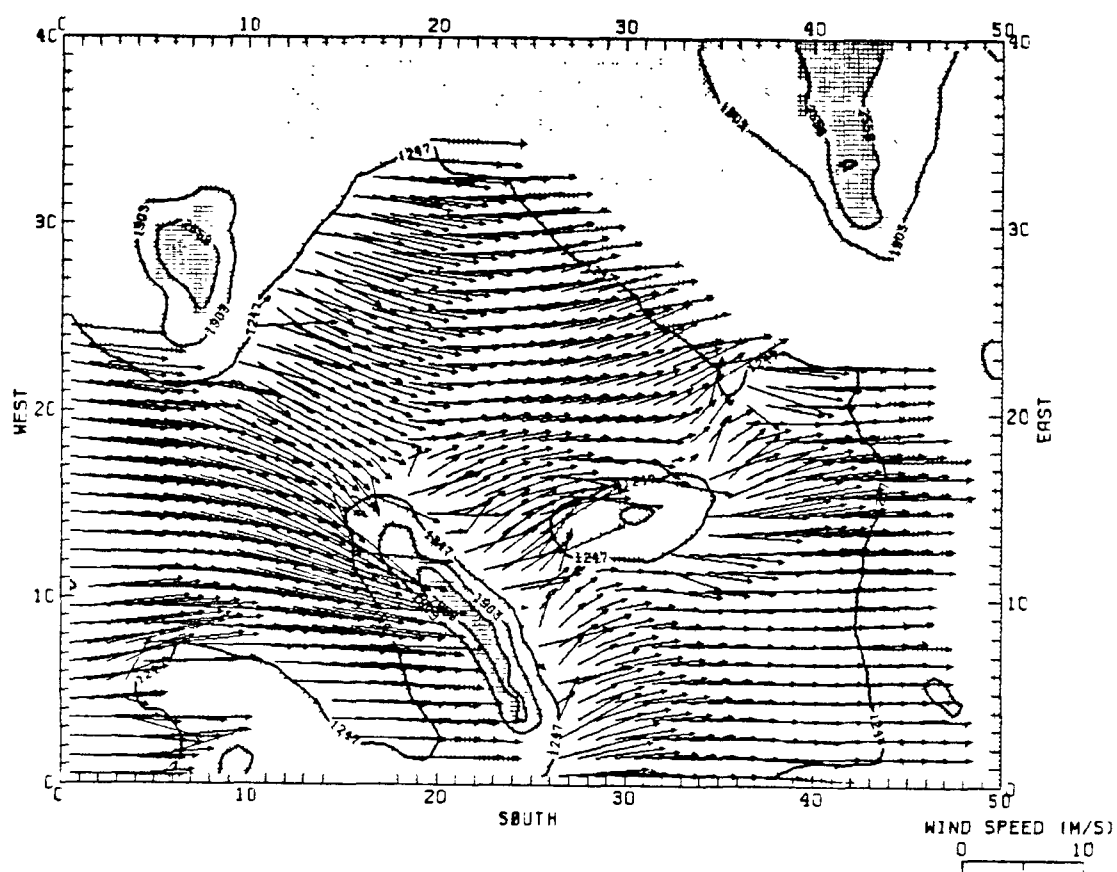
2200 MST



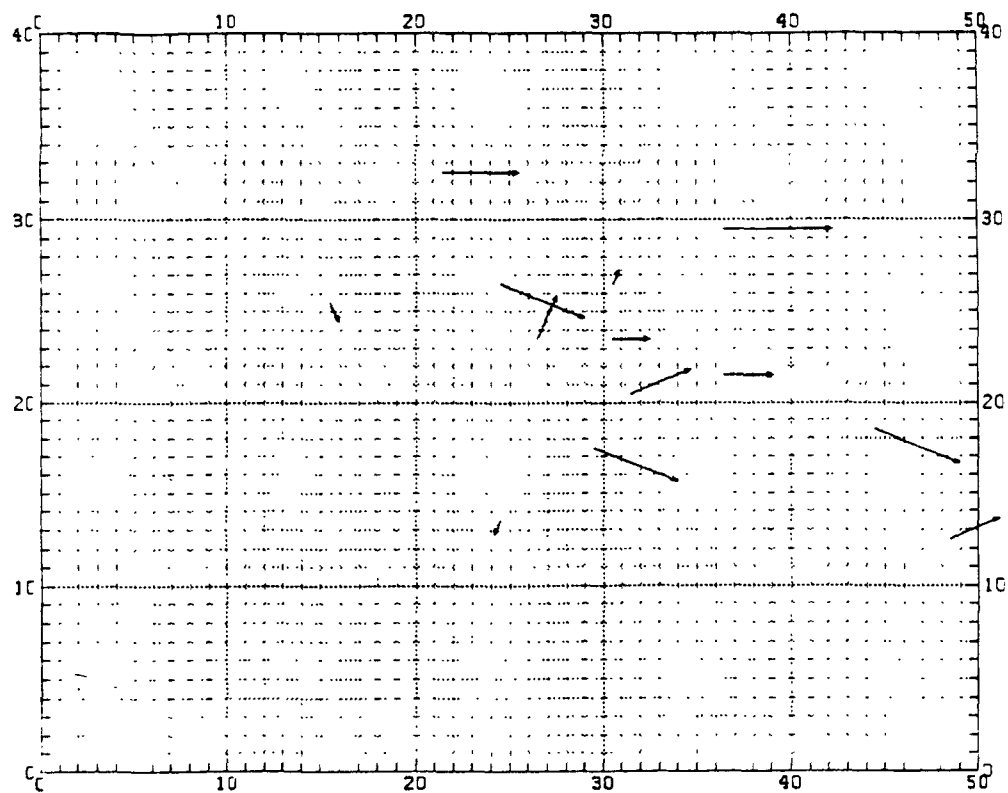
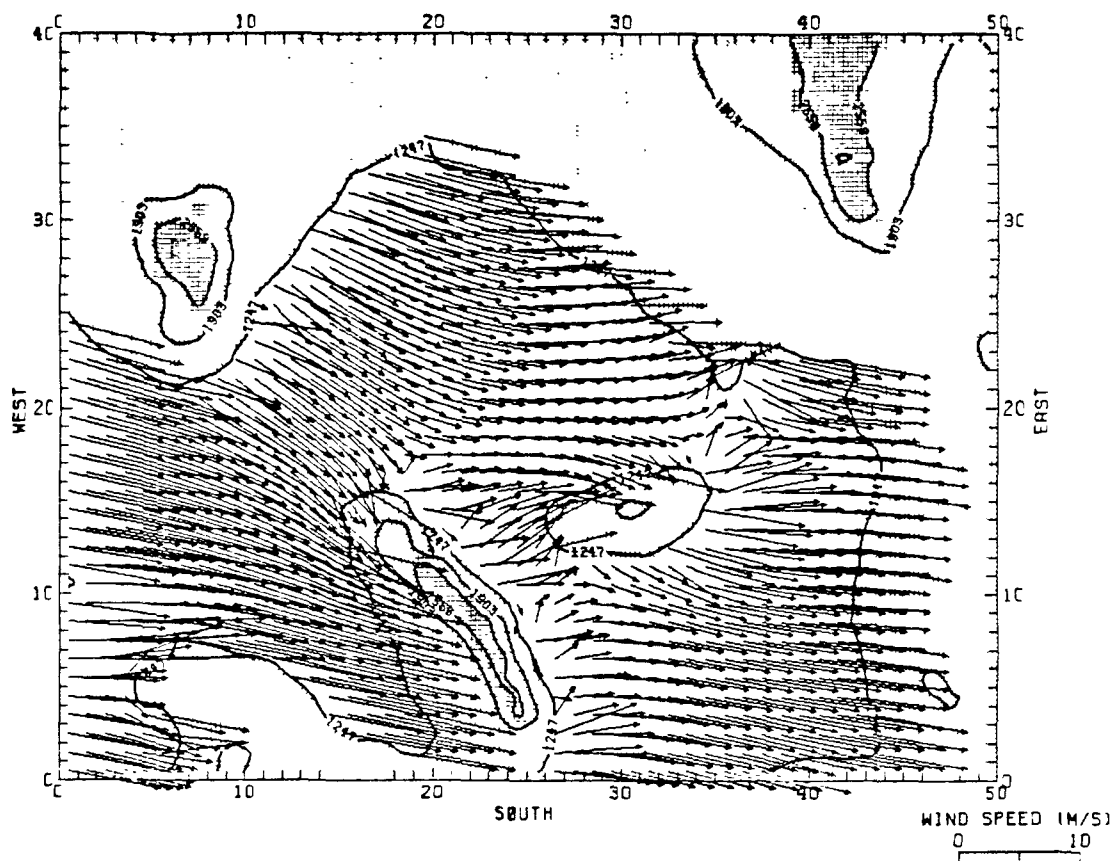
PART 4--10 MARCH 1977



0000 MST



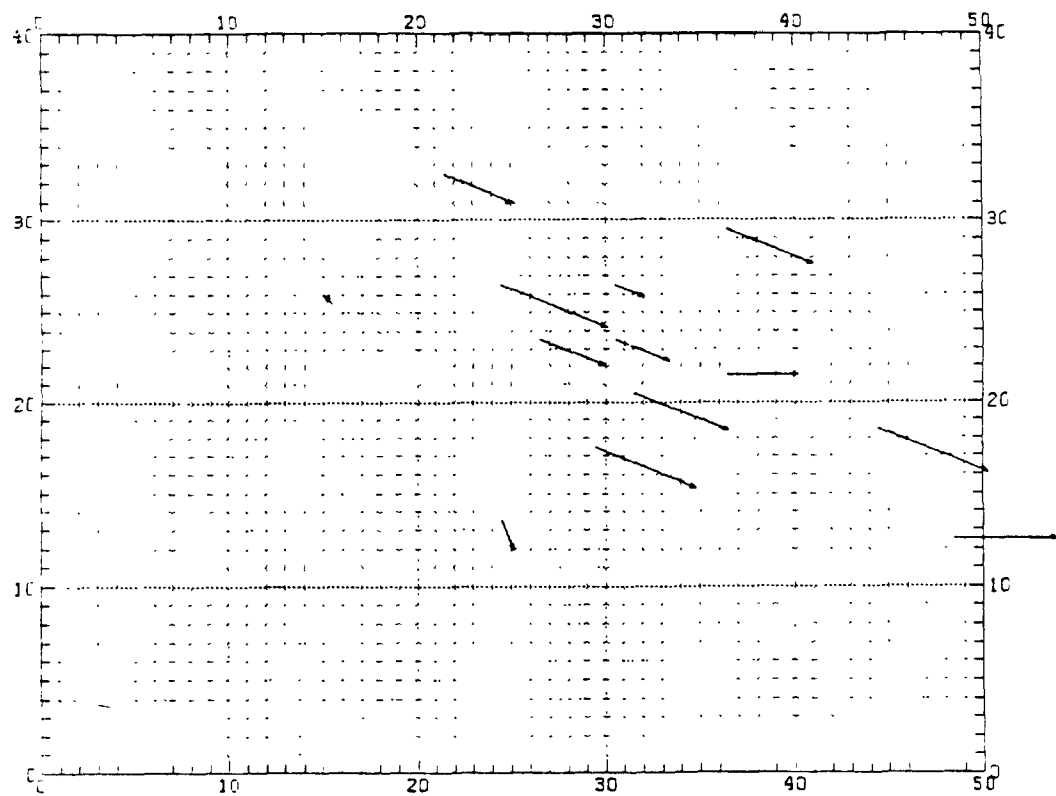
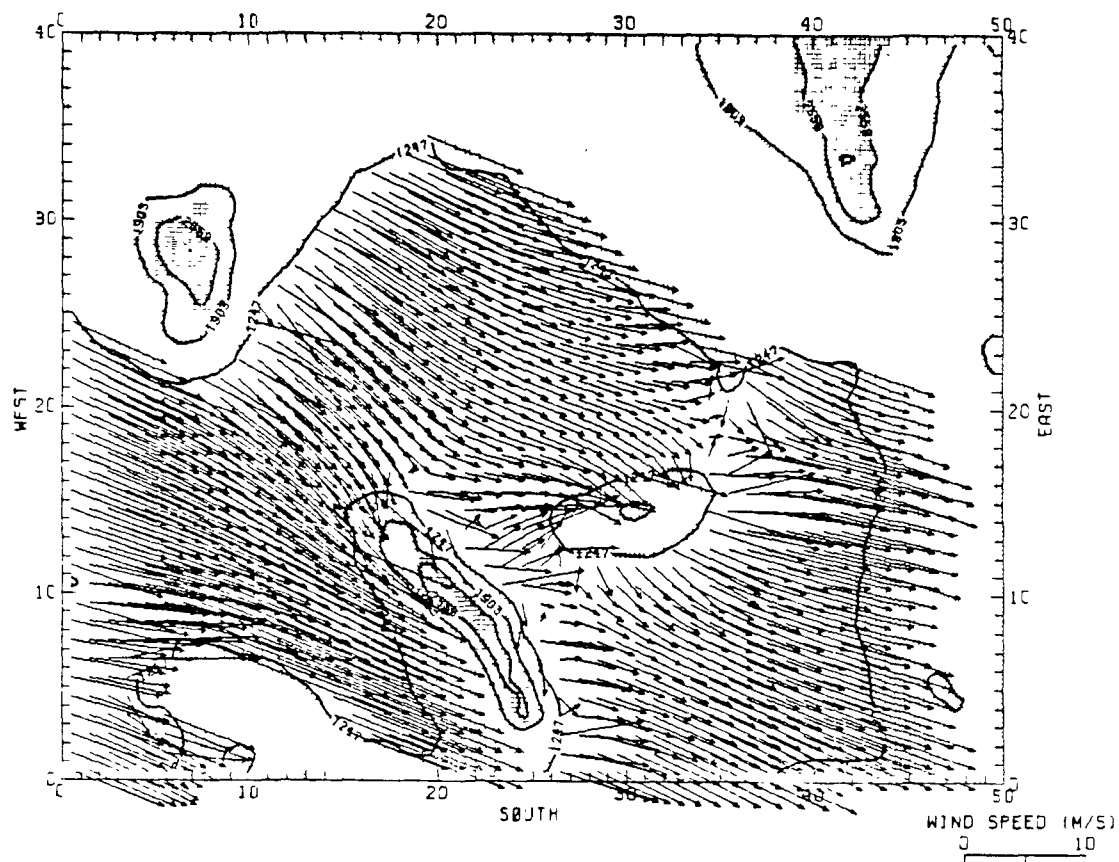
0200 MST



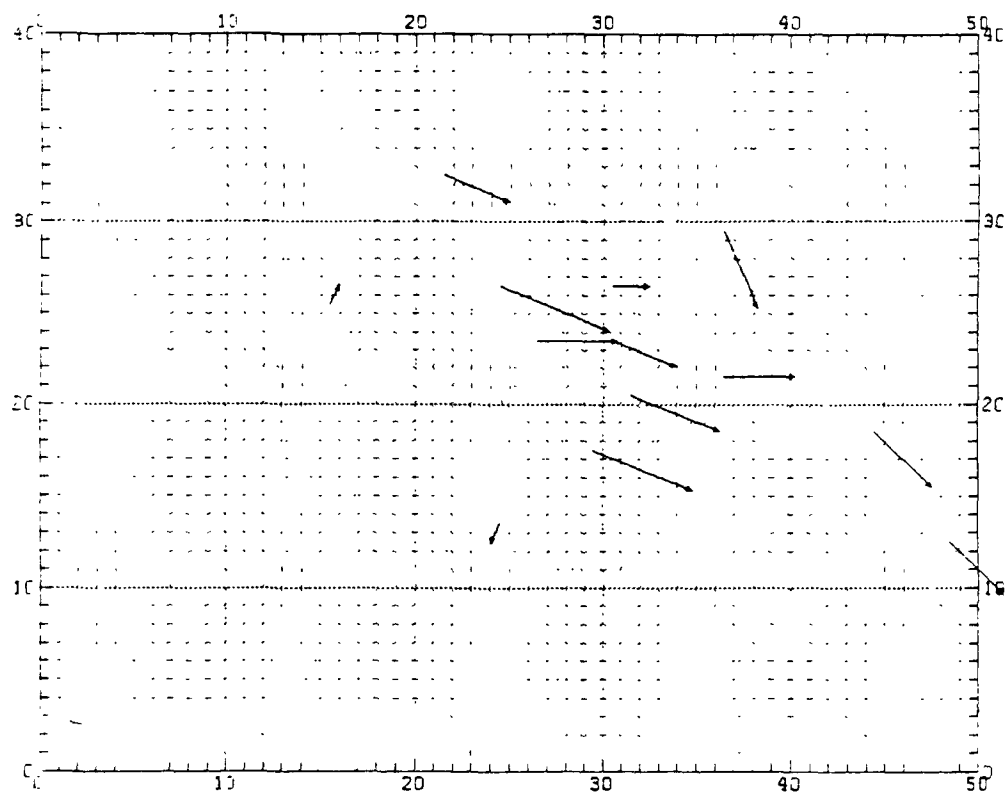
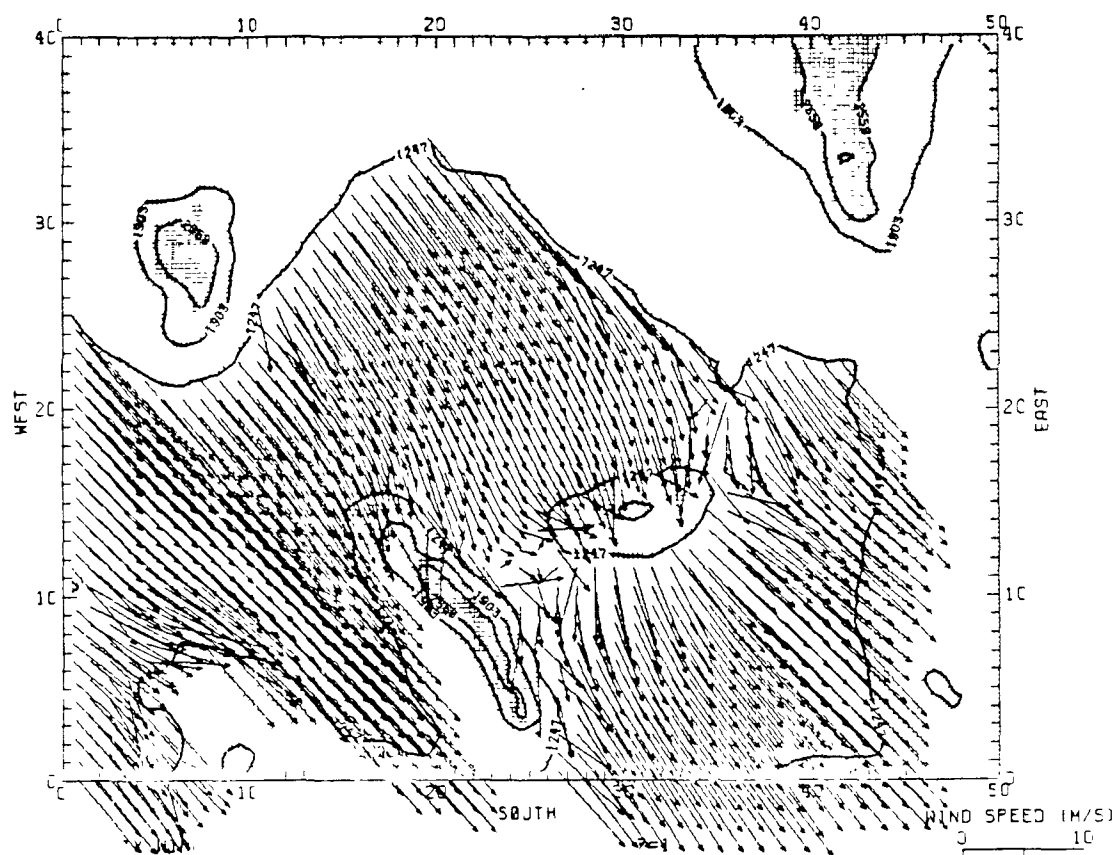
0400 MST





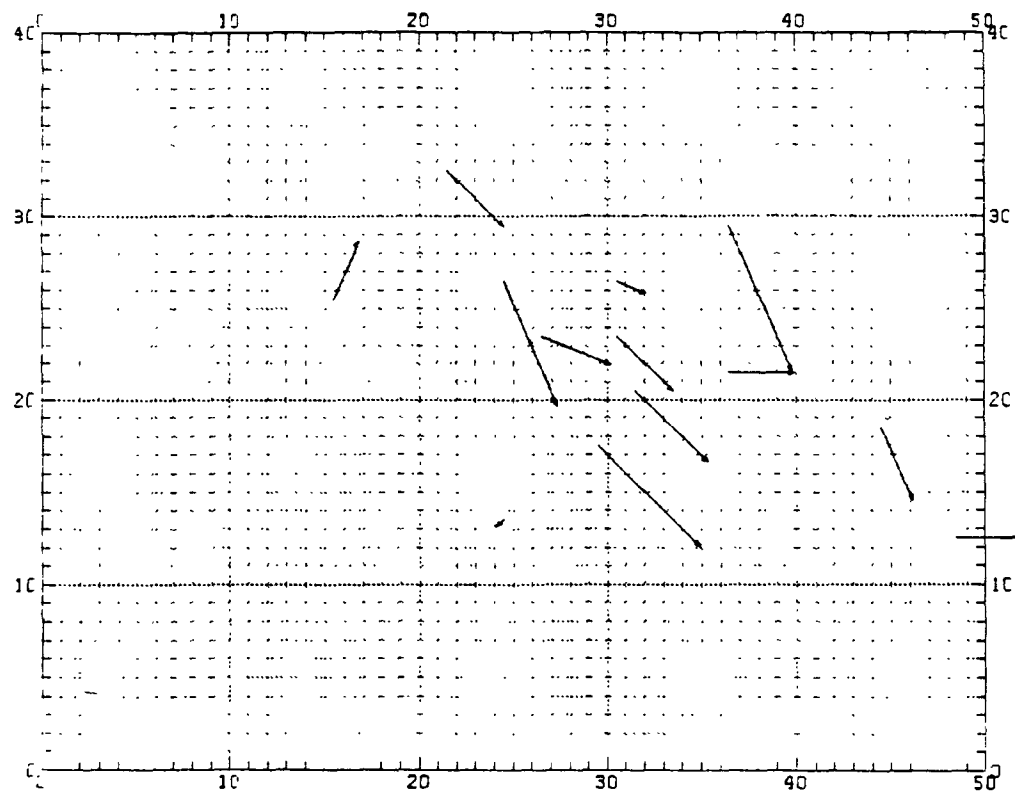
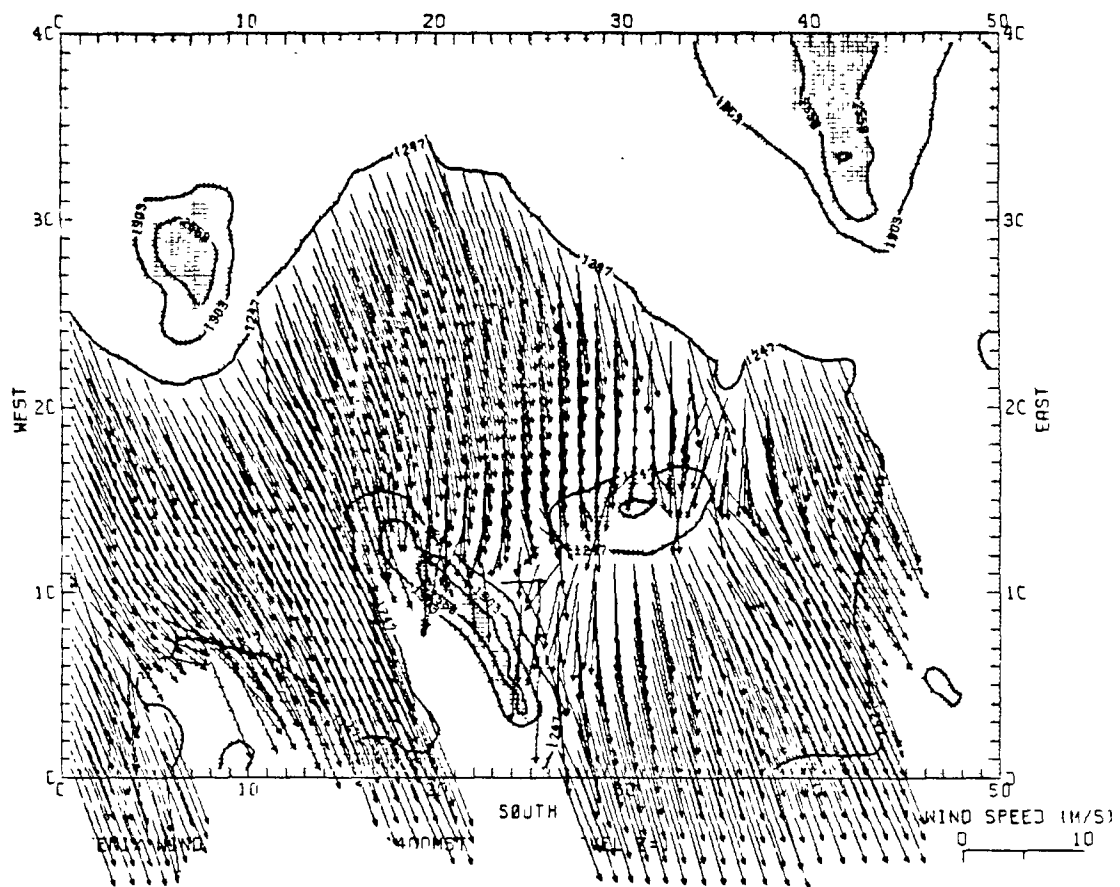


1000 MST

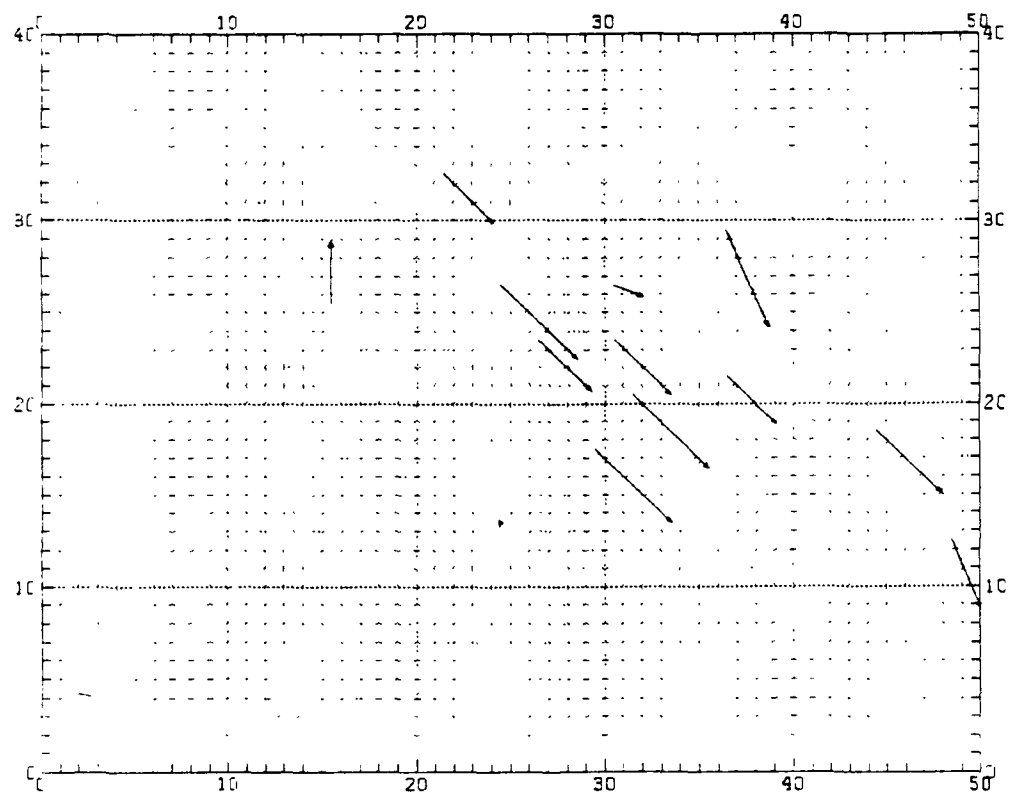
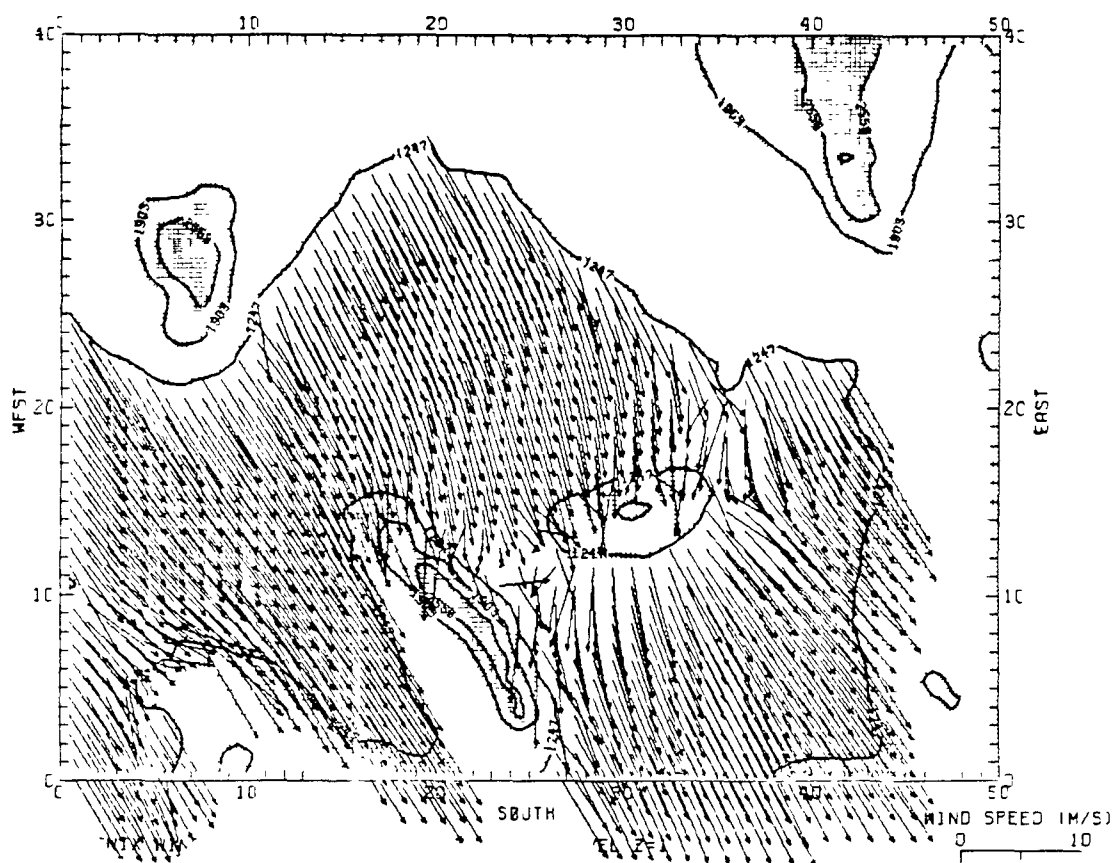


1200 MST

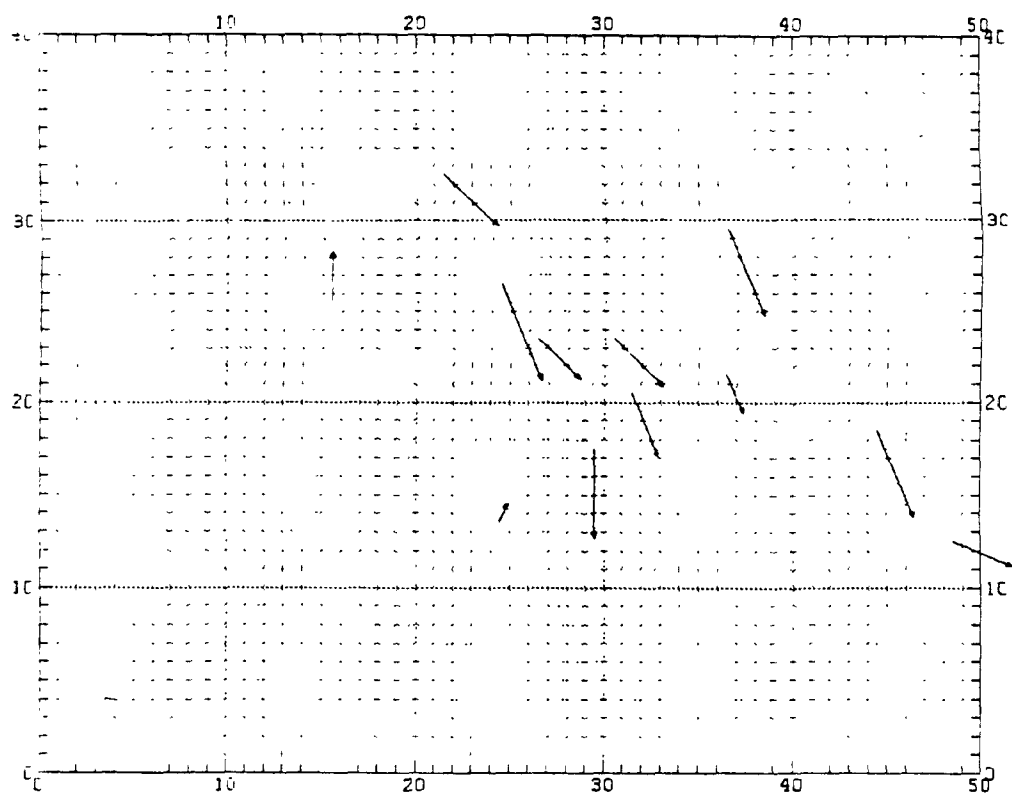
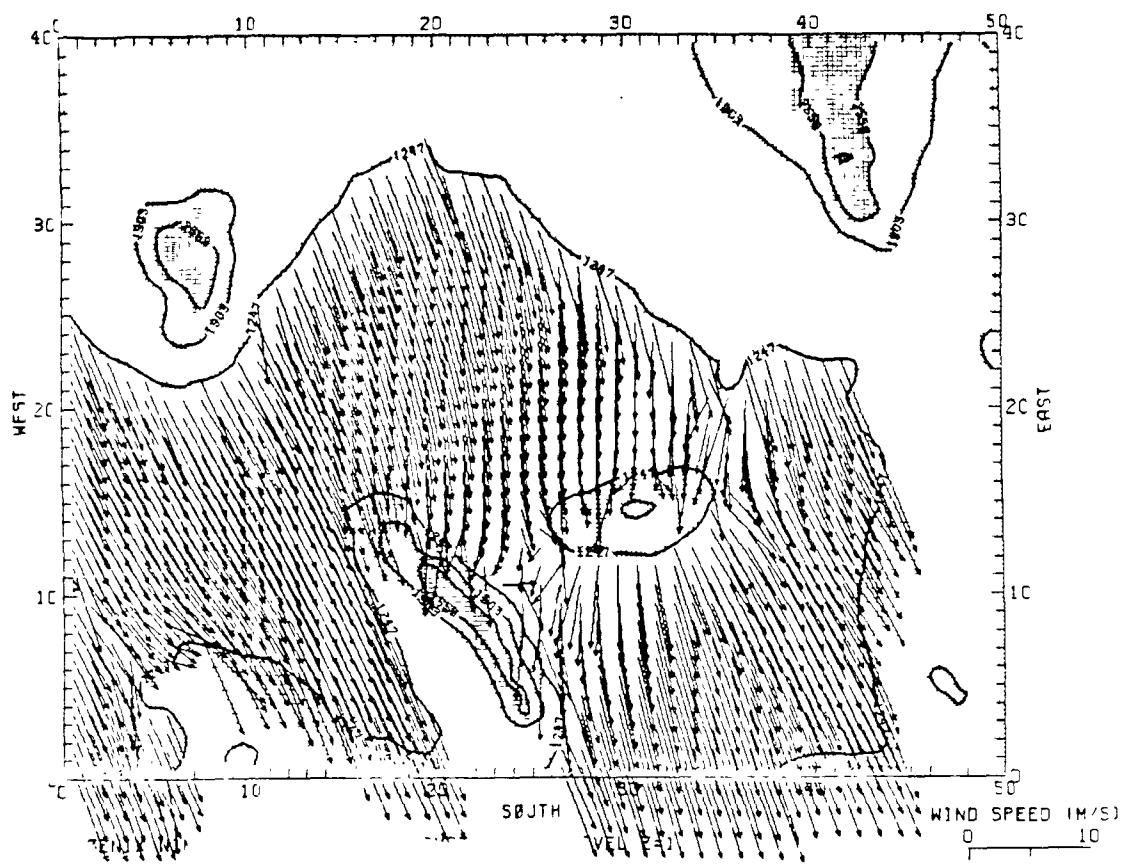


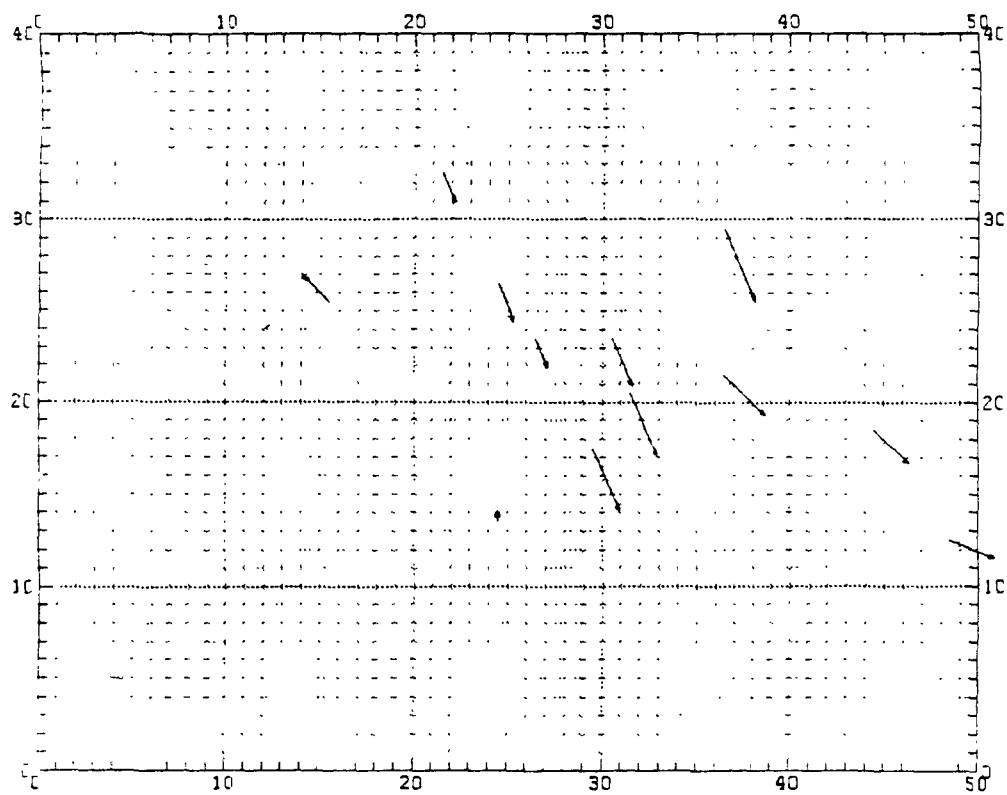
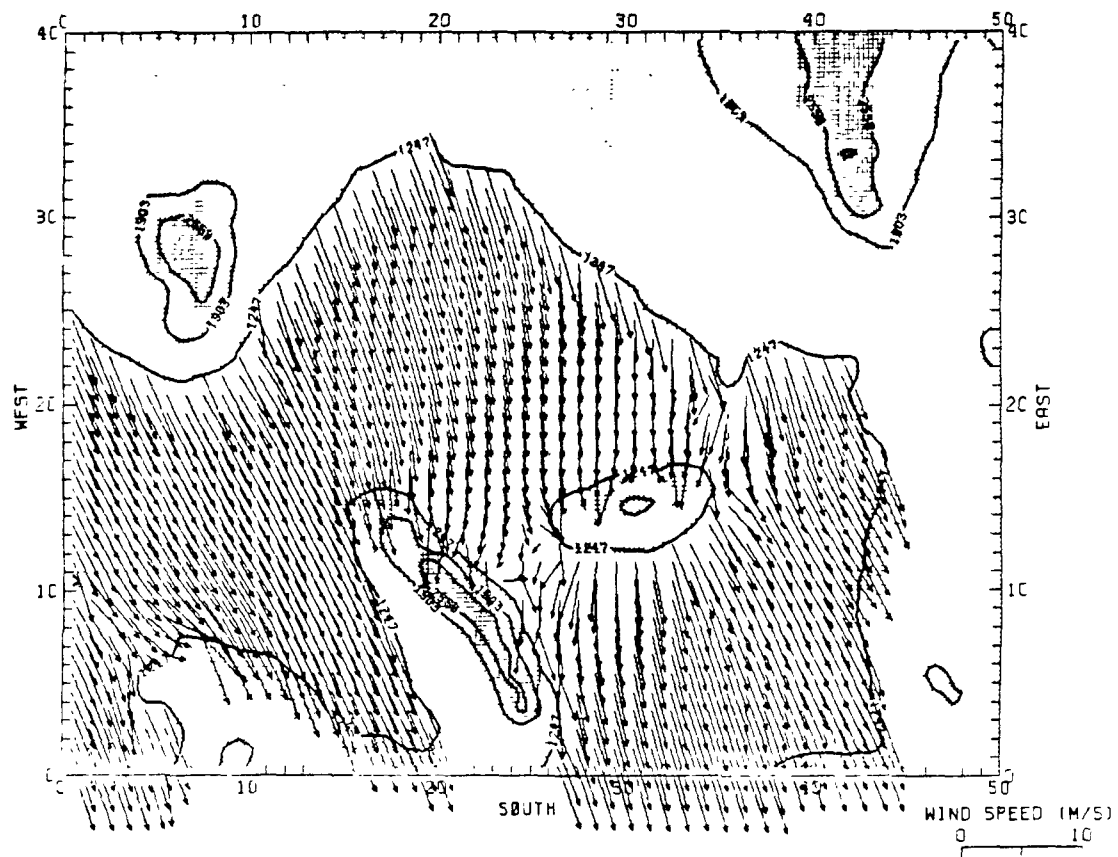


1400 MST

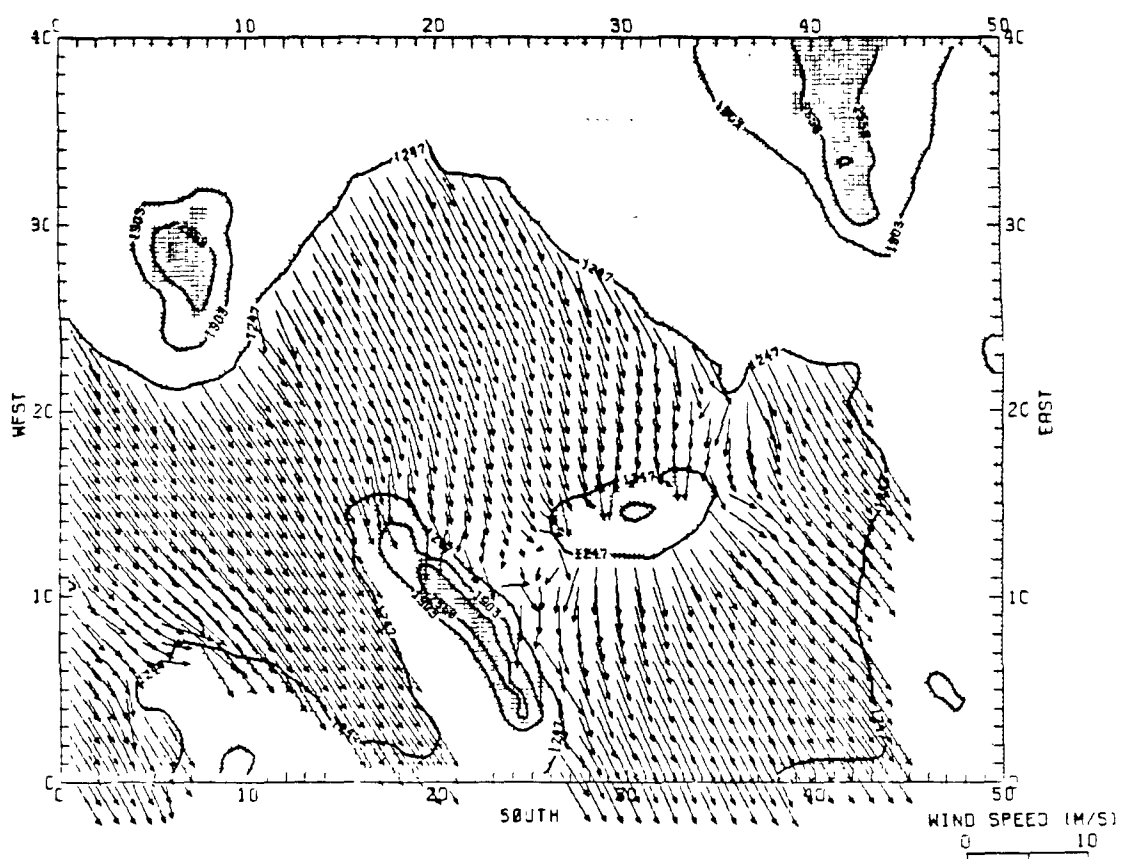


1600 MST





2000 MST



## REFERENCES

- Alaka, M. A. (1960), "The Airflow over Mountains," Technical Note No. 127, World Meteorological Organization, Geneva, Switzerland.
- Anderson, G. E. (1972), "A Mesoscale Wind Field Analysis of the Los Angeles Basin," The Center for the Environment and Man, Incorporated, Hartford, Connecticut.
- \_\_\_\_\_ (1971), "Mesoscale Influences on Wind Fields," J. Appl. Meteorol., Vol. 10, pp. 377-386.
- Aris, R. (1962), Vectors, Tensors, and the Basic Equations of Fluid Mechanics, Prentice-Hall, Incorporated, Englewood Cliffs, New Jersey.
- Berman, N. S. (1978), "Spatial and Temporal Resolutions of Urban Air Pollution Models for Evaluation of Transportation Strategies in Phoenix, Arizona," ERC-R-78010-1, Engineering Research Center, Arizona State University, Tempe, Arizona.
- Basso, M. J., L. H. Robinson, and R. G. Thuillier (1974), "The Analysis of Regional Air Flow Patterns and Their Use in Climatological and Episode Assessments of Air Quality," Proc. of the Symposium on Atmospheric Diffusion and Air Pollution, American Meteorological Society, Santa Barbara, California.
- Blasius, H. (1908), Z. Angew. Math. Phys., Vol. 56, pp. 1-37 (English translation, NACA Tech. Mem. 1256).
- Businger, J. A., et al. (1973), "Turbulent Transfer in the Atmospheric Surface Layer," D. A. Haugen, ed., Workshop on Micrometeorology, American Meteorological Society, Boston, Massachusetts.
- Buzbee, B. L., G. H. Golub, and C. W. Nielson (1970), "On Direct Methods for Solving Poisson's Equation," SAIM J. Num. Anal., Vol. 7, pp. 627-656.
- Dahlquist, G., and A. Björck (1974), Numerical Methods, Prentice-Hall, Incorporated, Englewood Cliffs, New Jersey.
- Deardorff, J. W. (1970), "A Three-Dimensional Numerical Investigation of the Idealized Planetary Boundary Layer," Geophys. Fluid Dyn., Vol. 1, pp. 377-410.
- Defant, A. (1951), "Local Winds," in Compendium of Meteorology, pp. 655-672, American Meteorological Society, Boston, Massachusetts.
- \_\_\_\_\_ (1933), "Der Abfluss Schwerer Luftmassen auf geneigtem Boden, nebst einigen Bemerkungen zu der Theorie stationärer Luftströme; Sitzungsberichte der Preuss. Akad. Wiss.," Phys. Math. Klassen.

- Dickerson, M. H. (1973), "A Mass-Consistent Wind Field Model for the San Francisco Bay Area," UCRL-74265, Lawrence Livermore Laboratory, Livermore, California.
- Eschenroeder, A., and J. R. Martinez (1972), "Evaluation of a Photochemical Pollution Simulation Model," General Research Corporation, Santa Barbara, California.
- Estoque, M. A., (1963), "A Numerical Model of the Atmospheric Boundary Layer," J. Geophys. Res., Vol. 68, pp. 1103-1113.
- Flohn, H. (1969), General Climatology, Elsevier Publishing Company, New York, New York.
- Förchtgott, J. (1949), "Wave Streaming in the Lee of Mountain Ridges," Bull. Met. Czech. Prague, Vol. 3, p. 49.
- Fosberg, M. A., W. E. Marlatt, and L. Krupnak (1976), "Estimating Airflow Patterns over Complex Terrain," USDA Forest Service Research Paper RM-162, Rocky Mountain Forest and Range Experiment Station, Fort Collins, Colorado.
- Gandin, L. S. (1965), "Objective Analysis of Meteorological Fields," Gidrometeorologicheskoe Izdatel'stvo, Leningrad (1963); translated from Russian by Isreal Program for Scientific Translations, Jerusalem.
- Grønskei, K. E. (1972), "A Three-Dimensional Transport Model for Air Pollution in an Urban Area with Application to SO<sub>2</sub> Concentration in Oslo," Proc. of the Third Meeting of the Expert Panel on Air Pollution Modeling, NATO, Paris, France.
- Hovermale, J. B. (1965), "A Non-Linear Treatment of the Problem of Airflow over Mountains," Ph.D Dissertation, Pennsylvania State University, University Park, Pennsylvania.
- Lettau, H. H. (1969), "Note on Aero-dynamic Roughness-Parameter Estimation on the Basis of Roughness-Element Description," J. Appl. Meteorol., Vol. 8, pp. 828-832.
- Lilly, D. K. (1973), "Calculation of Stably Stratified Flow Around Complex Terrain," Research Note No. 40, Flow Research, Incorporated, Kent, Washington.
- Liu, C. Y., and W. R. Goodin (1976), "An Iterative Algorithm for Objective Wind Field Analysis," Mon. Wea. Rev., Vol. 104, pp. 784-792.
- Liu, M. K., P. Mundkur, and M. A. Yocke (1974), "Assessment of the Feasibility of Modeling Wind Fields Relevant to the Spread of Brush Fires," R74-15, Systems Applications, Incorporated, San Rafael, California.

- Liu, M. K., et al. (1977), "Development of a Methodology for Designing Carbon Monoxide Monitoring Networks," EPA-600/4-77-019, Systems Applications, Incorporated, San Rafael, California.
- \_\_\_\_\_ (1973), "Automation of Meteorological and Air Quality Data for the SAI Urban Airshed Model," R73-SAI-32, Systems Applications, Incorporated, San Rafael, California.
- McElroy, J. L. (1971), "An Experimental and Numerical Investigation of the Nocturnal Heat-Island over Columbus, Ohio," Ph.D. Dissertation, Pennsylvania State University, University Park, Pennsylvania.
- McElroy, J. L., et al. (1978), "Carbon Monoxide Monitoring Network Design Methodology: Application to Las Vegas, Nevada," EPA-600/4-78-053, Environmental Monitoring and Support Laboratory, Environmental Protection Agency, Las Vegas, Nevada.
- Myrup, L. O. (1969), "A Numerical Model of the Urban Heat Island," J. Appl. Meteorol., Vol. 8, pp. 908-918.
- Nicholls, J. M. (1973), "The Airflow over Mountains, Research 1958-1972," Technical No. 127, World Meteorological Organization, Geneva, Switzerland.
- Orville, H. D. (1965), "A Numerical Study of the Initiation of Cumulus Clouds over Mountainous Terrain," J. Atmos. Sci., Vol. 22, pp. 684-699.
- Panofsky, H. A. (1949), "Objective Weather-Map Analysis," J. Meteorol., Vol. 6, pp. 386-392.
- Pielke, R. A. (1973), "A Three Dimensional Numerical Model of the Sea Breezes over South Florida," Ph.D Dissertation, Pennsylvania State University, University Park, Pennsylvania.
- Pitchford, A. M. (1976), Trip report on Phoenix to E. A. Schuck, Chief of Monitoring Systems Analysis Staff, Environmental Protection Agency, Las Vegas, Nevada.
- Reiter, E. R., and J. L. Rasmussen (1967), "Proceedings of the Symposium on Mountain Meteorology," Atmospheric Science Paper No. 122, Colorado State University, Fort Collins, Colorado.
- Sasaki, Y. (1970), "Some Basic Formalisms in Numerical Variational Analysis," Mon. Wea. Rev., Vol. 98, pp. 875-883.
- Sherman, C. A. (1975), "A Mass-Consistent Model for Wind Fields over Complex Terrain," UCRL-76171 (Rev. 1) Lawrence Livermore Laboratory, Livermore, California.



- \_\_\_\_\_ (1978), "A Mass-Consistent Model for Wind Fields over Complex Terrain," J. Appl. Meteorol., Vol. 17, No. 13.
- Stern, M. E., and J. S. Malkus (1953), "The Flow of a Stable Atmosphere over a Heated Island, Part II," J. Meteorol., Vol. 10, pp. 105-120.
- Swarztrauber, P., and R. Sweet (1975), "Efficient FORTRAN Subprograms for the Solution of Elliptic Partial Differential Equations," NCAR TN/1A-109, National Center for Atmospheric Research, Boulder, Colorado.
- Strand, J. N. (1971), "Airpol-Wind Trajectory Tracing for Air Pollution Studies," Jet Propulsion Laboratory, California Institute of Technology, Pasadena, California.
- Thyer, N. H. (1966), "A Theoretical Explanation of Mountain and Valley Winds by a Numerical Method," Arch. Meteorol. Geophys. Bioklim., Series A, Vol. 15, pp. 318-348.
- Truesdell, C. A. (1954), The Kinematics of Vorticity, Indiana University Press, Bloomington, Indiana.
- Weisburd, M. I., L. G. Wayne, and A. Kokin (1972), "Evaluation of the Reactive Environmental Simulation Model," Pacific Environmental Services, Incorporated, Santa Monica, California.
- Wendell, L. L. (1970), "A Preliminary Examination of Mesoscale Wind Fields and Transport Determined from a Network of Wind Towers," Technical Memo ERLTM-ARL 25, National Oceanic and Atmospheric Administration, Washington, D.C.

**TECHNICAL REPORT DATA**  
(Please read Instructions on the reverse before completing)

1. REPORT NO. EPA-600/4-79-066		2.		3. RECIPIENT'S ACCESSION NO.	
4. TITLE AND SUBTITLE  MODELING WIND DISTRIBUTIONS OVER COMPLEX TERRAIN				5. REPORT DATE October 1979	
				6. PERFORMING ORGANIZATION CODE	
7. AUTHOR(S) Mark A. Yocke and Mei-Kao Liu				8. PERFORMING ORGANIZATION REPORT NO.	
9. PERFORMING ORGANIZATION NAME AND ADDRESS Systems Applications, Incorporated 950 Northgate Drive San Rafael, California 94903				10. PROGRAM ELEMENT NO. 1HE775	
				11. CONTRACT/GRANT NO. 68-03-2446	
12. SPONSORING AGENCY NAME AND ADDRESS U.S. Environmental Protection Agency-Las Vegas, NV Office of Research and Development Environmental Monitoring Systems Laboratory Las Vegas, NV 89114				13. TYPE OF REPORT AND PERIOD COVERED	
				14. SPONSORING AGENCY CODE EPA/600/7	
15. SUPPLEMENTARY NOTES This report is the first in a series. For further information, contact J.L. McElroy, Project Officer, (702) 736-2969 X241, Las Vegas, NV					
16. ABSTRACT  Accurate determination of wind fields is a prerequisite for successful air quality modeling. Thus, there is an increasing demand for objective techniques for analyzing and predicting wind distribution, particularly over rugged terrain, where the wind patterns are not only more complex, but also more difficult to characterize experimentally. This report describes the development of a three-dimensional wind model for rugged terrain based on mass continuity. The model is composed of several horizontal layers of variable thicknesses. For each layer, a Poisson equation is written with the wind convergence as the forcing function. Many types of wind perturbations over rugged terrain are considered in this model, including diversion of the flow due to topographical effects, modification of wind profiles due to boundary layer frictional effects, convergence of the flow due to urban heat island effects, and mountain and valley winds due to thermal effects. Wind data collected during a comprehensive field measurement program at Phoenix, Arizona, were used to test the model.					
17. KEY WORDS AND DOCUMENT ANALYSIS					
a. DESCRIPTORS		b. IDENTIFIERS/OPEN ENDED TERMS		c. COSATI Field/Group	
Mathematical models		Wind fields		14B	
Environmental models		Predicting wind distribution		55A	
Atmospheric models		Complex terrain		68A	
		Three-dimensional wind model			
		Wind perturbations			
		Testing mathematical model			
		Phoenix, Arizona			
18. DISTRIBUTION STATEMENT  RELEASE TO PUBLIC		19. SECURITY CLASS (This Report) UNCLASSIFIED		21 NO. OF PAGES 122	
		20. SECURITY CLASS (This page) UNCLASSIFIED		22. PRICE	

---

United States  
Environmental Protection  
Agency

Environmental Research  
Information Center  
Cincinnati OH 45268

---

Official Business  
Penalty for Private Use  
\$300

Postage and  
Fees Paid  
Environmental  
Protection  
Agency  
EPA 335



Special Fourth  
Class Rate  
Book

If your address is incorrect, please change on the above label,  
tear off, and return to the above address  
If you do not desire to continue receiving this technical report  
series CHECK HERE ☐ tear off label, and return it to the  
above address

---

EPA-600/4-79-066